UNIVERSITÀ DEGLI STUDI DI MILANO

PhD School in Molecular and Cellular Biology

Department of Biosciences

XXXV cycle

Two novel genes downstream of the florigenic and the photoperiodic induction control rice plant development in the reproductive stage

PhD Candidate:
Lorenzo MINERI

Scientific supervisor: Prof. Fabio FORNARA
PhD school coordinator: Prof. Roberto MANTOVANI

A.Y. 2021/2022

Abstract

Rice (*Oryza sativa L.*) is a facultative short-day plant belonging to the *Poaceae* family. It is a model species for grasses, and its relatively small genome and easiness of handling makes it a good model to study complicated genetic network such as flowering. Flowering is fundamental for higher plants since it leads to the generation of the offspring to perpetuate the species. Florigens are essential components in flowering, and they are produced in the leaf blades before being transported to the shoot apical meristem, where they activate the transcription of floral identity genes. In rice Hd3a and RFT1 are the florigens, which form a complex with OsFD1 and a 14-3-3 protein to activate the transcription of target genes: worth mentioning are *OsMADS14*, *OsMADS15*, *OsMADS18* and *OsMADS34/PAP2*. My PhD project aimed to discover new genes involved in the flowering process downstream of the florigens and to compare the promotion-specificity of *Hd3a* and *RFT1*. RNA-seq experiments were conducted on transgenic lines expressing either *Hd3a* or *RFT1* when induced with exogenous dexamethasone, and wild type, short-day (SD)-induced plants to identify differentially expressed genes. Crossing the three datasets 15 genes emerged as strongly regulated by all three inductive conditions. Among them were floral identity genes and ten uncharacterized genes. Expression analysis along reproductive transition revealed that the florigens are necessary for the regulation of eight of them, and *RFT1* is a stronger activator/repressor than *Hd3a*. Spatial expression of three genes unveiled a similar pattern: low expression in the SAM and a marked expression at the primary and secondary branches meristems. The attention was then focused on two of the uncharacterized genes, an F-BOX containing protein and a MAIN-like protein, by generating knock-out lines using CRISPR/Cas9 technology. Phenotypic analysis of homozygous plants has shown that the genes are involved in collateral processes, rather than flowering itself: the F-BOX protein, encoded by *Broader Tillering1* (*BRT1*), regulates tiller angle during short induction, besides suppressing bract-like structures in the panicle; the MAIN-like gene, *OsMAIL1*, is involved in the activation of genes that specify carpel identity.

Riassunto

Il riso (*Oryza sativa L.*) è una pianta a giorno corto facoltativa appartenente alla famiglia delle Poaceae. È una specie modello per le piante erbacee a causa del genoma relativamente piccolo e la facilità di gestione, in particolare quando si tratta di studiare network genetici complessi come quello riguardante la fioritura. Fiorire è un processo fondamentale per le piante superiori, dato che ha come fine ultimo la generazione di progenie per garantire la sopravvivenza della specie. I florigeni sono componenti essenziali nella fioritura: vengono prodotti nelle lamine fogliari per poi essere trasportati al meristema apicale del germoglio, dove attivano la trascrizione dei geni di identità fiorale. In riso i florigeni sono Hd3a e RFT1, i quali formano un complesso con OsFD1 mediato da proteine 14-3-3 che attiva la trascrizione di geni target: *OsMADS14, OsMADS15, OsMADS18* and *OsMADS34/PAP2*. Poco è noto di altri target. Lo scopo del progetto è quello di scoprire nuovi geni coinvolti nel processo di fioritura a valle dei florigeni, oltre che di comparare la specificità di attivazione data da *Hd3a* e *RFT1*. Tre esperimenti di RNA-seq sono stati condotti su piante che esprimevano solo *Hd3a*, piante che esprimevano solo *RFT1*, e piante indotte da condizioni di giorno corto per identificare i geni differenzialmente espressi. Dall'incrocio delle tre collezioni di dati sono emersi 15 geni come fortemente regolati in tutte e tre lo condizioni di induzione. Tra di loro, si ritrovano i geni di identità fiorale oltre a dieci geni non caratterizzati. L'analisi di espressione durante la transizione riproduttiva ha mostrato che i florigeni sono necessari per la regolazione di otto di essi, oltre al fatto che *RFT1* è un attivatore/repressore più forte rispetto ad *Hd3a*. La localizzazione spaziali di tre geni esemplificativi è simile: poco espressi nel meristema vegetativo, ed un'espressione più accentuata nei meristemi dei rami primari e secondari della pannocchia. L'attenzione si è poi spostata su due fra i geni non caratterizzati, codificanti per una proteina F-BOX ed un MAIN-like, sfruttando la tecnologia CRISPR/Cas9 per generare mutanti non funzionali. L'analisi fenotipica di piante omozigoti per l'allele non funzionale ha rivelato che questi geni sono coinvolti in processi collaterali alla fioritura: la proteina F-BOX, *BRT1*, regola l'angolo dei culmi durante l'induzione da giorno corto, oltre a sopprimere la formazione di brattee nella pannocchia; il gene MAIN-like, *OsMAIL1*, è coinvolto nell'attivazione di geni che specificano l'identità del carpello.

Summary

1. Introduction

1.1 Rice overview

Rice (*Oryza sativa* L.) is a staple crop that feeds billions of people around the world. It is thus a major interest of scientists to research on it, on its fundamental genetic networks, with the ultimate goal of food security and adapting it to stresses, allowing its cultivation in new areas and improving yield. It is a good model species for cereals since it has a rather small genome (around 400Mb) and it is a diploid organism, making it an easy plant to work with. Its domestication began more than 10000 years ago in the Hunan and Hubei region, in the basin of the Yangtze River (Nornile, 1997) from the ancestor *Oryza rufipogon* (Londo *et al.*, 2006). There are two main subspecies that are *japonica*, which comprises also *javanica* (or *tropical japonica*), *temperate japonica* and aromatic, and *indica*, that encompasses also *aus*. *Temperate japonica* rice is mainly grown in temperate areas such as northern China, Japan but also in the western world, and the majority of the Italian elite varieties belong to this subspecies. The *indica* varieties, as the name suggests, are mainly grown in the Indian subcontinent and southeast Asia. It was suggested that the two subspecies derived from two independent domestication events from two subpopulation of *O. rufipogon* (Londo *et al.*, 2006). (Huang *et al.*, 2012) generated a map of rice genome variation by sequencing hundreds of accessions of *O. rufipogon*, *japonica* and *indica*. *O. rufipogon* was classified into three types based on population structure, namely Or-I, Or-II and Or-III which correlated with geographical position. Their results suggested that japonica was domesticated from Or-III in the south of China, while *indica* emerged as a crossing of early *japonica* with local (Sout-east Asia and Indian subcontinent) wild rice, although *indica* underwent a higher amount of gene flow, and its weak population structure makes it difficult to reconstruct its dispersal path (Gutaker *et al.*, 2020). Though, the domestication genes are present with the same alleles in both *japonica* and *indica*, a further proof for the post-domestication hybridaziotion between *japonica* and *proto-indica* (Choi *et al.*, 2017).

1.2 Rice morphology

Rice is an annual monocot grass belonging to the *Poaceae* family. It is up to 150cm tall, 90 cm on average. The leaves are flat, long, and rich in silicate, and are constituted of two parts: the sheath, wrapping the culm, and the blade, extending from the top of the sheath with a fixed angle; the two are joined by the auricle. The

shoot is made of a sequence of empty internodes and full nodes. The root apparatus is quite broad, rather than deep (Fig. 1A). The inflorescence is an apical panicle and is made of a rachis from which primary branches (and often from them secondary branches) start (Fig. 1B): the branches bear the spikelets, each bearing a floret that contains the male and female organs (it is a hermaphrodite flower, Fig. 1C). The flower possesses six anthers, and a single pistil with two styluses and stigmas (Fig. 1C). While *O. rufipogon* was both autogamous (~50%) and allogamous (~50%), cultivated rice is an autogamous plant, the pollination occurs when the anthers are still enclosed in the glumes, so cross pollination usually occurs with a frequency of 1 to 5%, depending on the variety (Hoshikawa, 1989).

Its life cycle lasts 4-5 months on average, and is divided in embryogenesis,

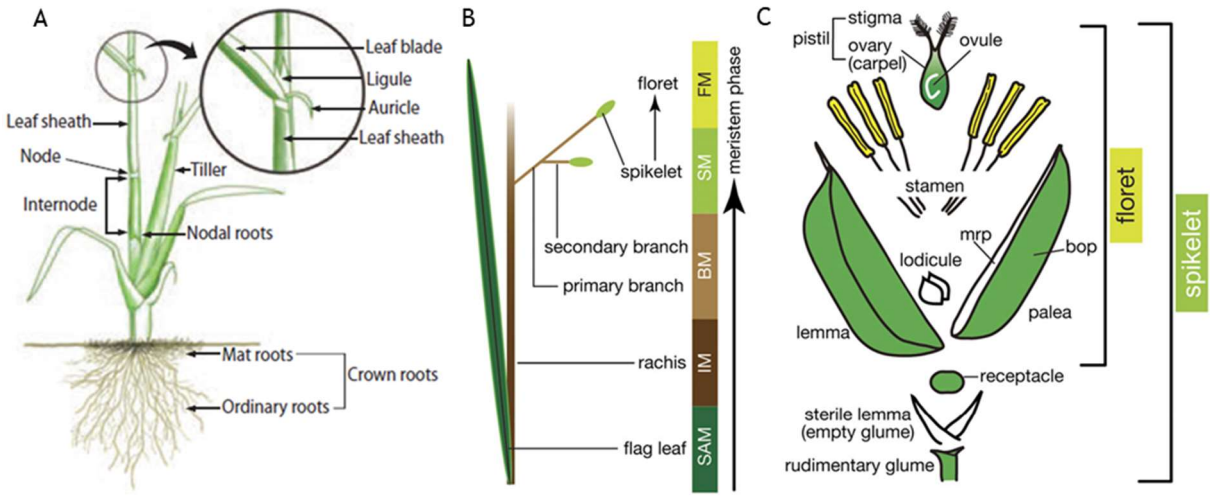

Figure 1. ***Rice plant and panicle morphologies*** *A) Morphology of a vegetative phase plant. In the circle, a magnification of the leaf junction. B) schematic representation of a panicle and its components and stages of development of the shoot apex during the reproductive phase. SAM: shoot apical meristem; IM: inflorescence meristem; BM: branches meristem; SM: spikelet meristem; FM: floret meristem. C) Scheme of a spikelet with all the components.*

vegetative, reproductive, and ripening stage (Fig. 2). The vegetative phase is usually two months long and goes from sprouting to flowering: during this type of growth the plant produces most of its biomass in the form of leaves and tillers. The tillering stage is part of the vegetative growth, and the first tiller is usually produced from the bud of the second leaf, when the fifth leaf emerges. The tillers develop from the axillary meristems at the base of the plant, inside the leaves. The leaves are named as Ln (where n is a progressive number), starting after the coleoptile. When L5 emerges from the sheath of L4, a tiller emergers from the axis of L2, when L6

emerges so does a tiller from L3, and so on. The leaves and the tillers are arranged as a distichous pattern.

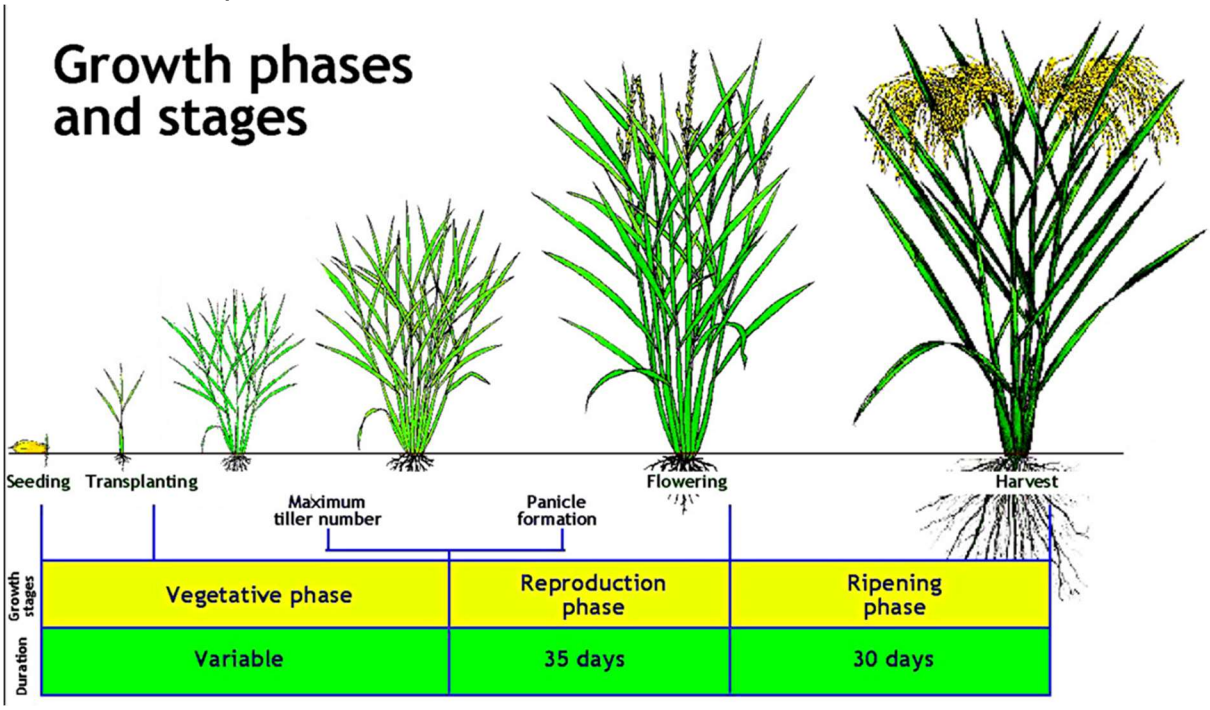

Figure 2. ***Stages of the life of a rice plant***

The reproductive stage starts when the right internal and external conditions are favourable, that is the warm climate, the right photoperiod, the maturity of the plant, and it takes 30-35 days typically. The vegetative meristem begins its development into a panicle, going through changes, elongating to create an inflorescence meristem first, and then the primary, secondary branches, and lastly the spikelets. At the same time the internodes elongate to bring the panicle at the top of the plant. The panicle is enveloped in the sheath of the flag leaf, the last leaf produced by the plant and the one that is mostly responsible to feed the panicle by photosynthesizing. The swollen sheath of the flag leaf that contains the panicle is called a boot. When the first spikelet emerges from the boot, heading begins, and it is completed once the entire panicle is out. Then the anthesis occurs and the plant self-pollinates. The fruit starts to develop and later to harden, during the last stage, the ripening.

1.3 Development of the shoot apical meristem during reproductive growth

When the florigens arrive at the SAM and their targets are expressed, the meristem undergoes changes that ultimately will lead to flowering. From vegetative meristem

(VM, Fig. 3A), with its typical dome shape, it starts to elongate to become an inflorescence meristem (IM, Fig. 3B,C) after around 7 days of induction. Then, the primordia of the primary branches start to form on the side of the cylinder, together with a bract that is soon suppressed and remains undeveloped (Fig. 3D). Soon after, at around 15SDs, it is the time of the secondary branches to form, and at the same time we can see the presence of bract hairs, that forms from the degenerated bracts (Fig. 3E,F). After 20 SDs, the glumous flowers start to develop (Fig. 3G). The young inflorescence is shown in Fig. 3H. It already possess all the organs that will develop into the mature panicle that will be brought at the top of the plant by the elongating internodes.

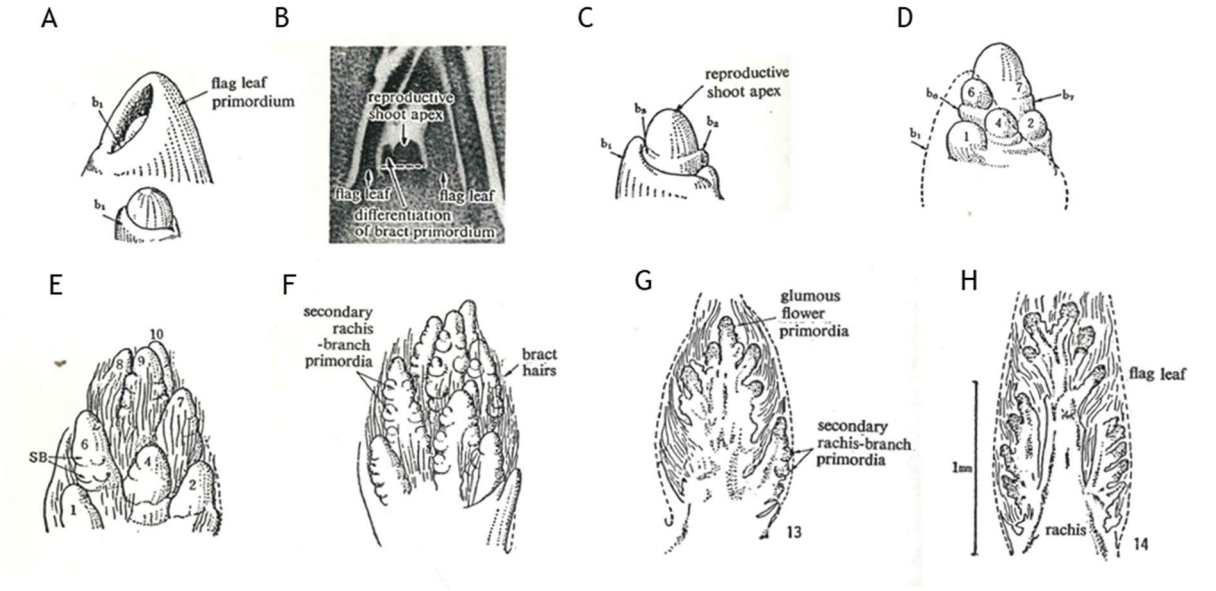

Figure 3. ***Development of the shoot apex*** *A) Microscope image of a shoot apex in the first stages of development into a reproductive one; we can see it has already started elongating. B) Vegetative meristem with its peculiar dome shape; b1: bract primordium. C) inflorescence meristem with three bract primordia (b) D) shoot apex in the primary branches meristem (PBM, which are indicated by the numbers) phase; flag leaf is represented by the dotted line. E) secondary branches (SB) meristem phase; the bracts have degenerated into hairs F) later stage of SBM. G) Spikelet meristem (SM) stage, the primordia of the flowers are developing. H) Young inflorescence, the dotted line represets the flag leaf.*

1.4 Photoperiodism and flowering

The main purpose of living organisms is to reproduce and create progeny, and plants are not exempt: they need to flower when the internal and environmental conditions are the best to produce viable seeds. Flowering initiation is a fundamental process reprogramming the plant to enter the reproductive stage of its life. One of the most important environmental cues indicating that the time is right is the photoperiod (or day length). Photoperiodism is the ability of living organisms, animals, plants, and

even bacteria to perceive the length of dark and light phases during a period of 24h and respond to it physiologically. Plants especially heavily rely on this mechanism for their development. They can be divided in three groups based on the relative day-length they respond to by flowering: short-day plants, that flower only when day-length falls under a certain threshold, long-day plants, that flower only when day-length is above a certain threshold, and day-neutral plants, which flower independently of day length (GARNER & ALLARD, 1920). Understanding the basis of this phenomenon could help adapting the plant to higher latitudes, covering areas that are now inaccessible.

The perception of the light conditions is controlled by photoreceptors, the phytochromes (Kendrick & Spruit, 1977). Phytochromes exist in two interconvertible forms, which are distinguished by the wavelength they absorb: P_r form (non-active, red-absorbing form) and P_{fr} form (active, far-red-absorbing form). The first type of light is present during the day, while the latter is more abundant at dusk or under the shade of other plants. When phytochromes absorbs red light they undergo a conformational change, converting from their P_r form to its P_{fr} form. This conversion is reversible, and when P_{fr} absorbs far-red light it converts back to P_r. Not only, but P_{fr} spontaneously decay to P_r form during the night. The two forms of phytochrome have different biological activities, and the ratio of P_{fr} to P_r in the plant determines how the plant responds to light (Smith, 2000; Quail, 2002). For example, high levels of P_{fr} promote flowering in long-day plants, while low levels of P_{fr} inhibit it, and vice versa for short-day plants (Izawa *et al.*, 2002).

Rice is a short-day plant, and that means that it commits to flower when the daylight hours fall under a certain threshold, in this case 13.5 hours of light per day (Itoh *et al.*, 2010). To be more precise, rice is considered a facultative short-day plant since it can also flower under longer photoperiods, but it will take more time to do so in such conditions.

1.5 Florigens and PEBPs

Phosphatidylethanolamine-binding proteins (PEBPs) are small globular proteins found in any eukaryotic kingdom, from plants to animals (Schoentgen & Jollès, 1995; Gopi & Arambakkam Janardhanam, 2017; Dong *et al.*, 2017; Shenouda *et al.*, 2020). The

first one was isolated from bovine brain in the '80s (Bernier & Jollés, 1984).The name comes from the fact that they have been found to bind phosphatidylethanolamine (Bernier *et al.*, 1986). The function its very diversified in every organism, and more so between plants and animals, but they are often related to developmental processes.

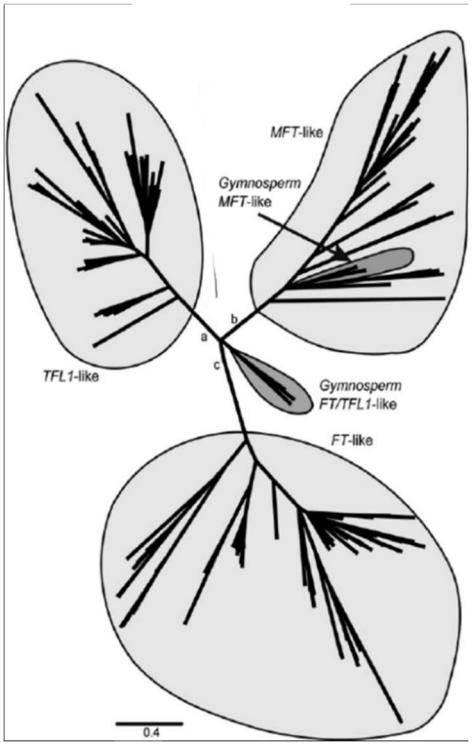

Figure 4. ***Phylogenetic tree of plant PEBPs***

In plants, they have been demonstrated to shape plant and inflorescence architecture and act as both promoters and repressors of flowering (Bradley *et al.*, 1996; Kardailsky *et al.*, 1999; Kobayashi *et al.*, 1999). In higher plants we can divide PEBPs into three families: Flowering locus T (FT)-like, Terminal Flower 1 (TFL1)-like, and MOTHER of FT (MFT)-like (Fig. 4); these are all Arabidopsis genes, but they are not the only PEBPS, there are also Twin sister of FT and TFL1 (TSF), Arabidopsis Thaliana Centroradialis homologue (ATC) and Brother of FT and TFL1 (BFT) with minor, and non-essential to flowering, roles.

FT is the main florigen, that is a protein responsible to carry the florigenic signal that ultimately leads to flowering. It is produced in specialized companion cells of the leaves when the right photoperiodic and seasonal conditions are met (Chen *et al.*, 2018), and then migrates through the phloem to reach the shoot apex, where it starts the flowering cascade. On the other hand, TFL1 has the exact opposite effect of FT, repressing flowering (Shannon & Ry Meeks-Wagner', 1991). Contrary to FT, TFL1 is also expressed during the vegetative stage, contributing in keeping the meristem in its indeterminate state (Bradley *et al.*, 1997). The divergent function may seem surprising, since they share a high identity percentage. One molecular basis for this depends on a single residue, Y85, that can convert FT to TFL1 and vice versa (Hanzawa *et al.*, 2005). (Ahn *et al.*, 2006a) discovered that another reason of this divergent function partially lies in the fourth exon of the genes, encoding for what was called the segment B: the chimeric FT protein with the TFL1 segment B had a late flowering phenotype. Segment B is highly conserved in FT orthologs, but not in

TFL1 orthologs. TFL1 is a mobile signal as well, but its movement is more restricted than FT: it is produced in the inner cells of the meristem but then translocates to the outer cells as well (Conti & Bradley, 2007). Given its supposed capability to bind to 14-3-3 and FD proteins, much like FT, TFL1 has been proposed to form an alternative complex, the Florigen Repressor Complex (FRC), thus competing with FT in the bond (Pnueli *et al.*, 2001a). Thus, flowering is a delicate process involving multiple players and the result is given by a fine balance of activators and repressors. Being a PEBP, FT was supposed to bind PE, and the putative binding site for PE was an anion pocket (Serre *et al.*, 1998). However, recent findings have shown that FT binds phosphatidylcholine (PC) rather than PE; besides, the proposed anion binding pocket is unlikely to be able to accommodate the big hydrophilic head of PC (Nakamura *et al.*, 2019a).This bond is a flowering accelerator. The binding site has been found, and mutations in it causes a loss of binding properties to PC and a delay in flowering (Nakamura *et al.*, 2019a). Furthermore, PC has another layer of control on flowering time since when the temperatures are cold it gets sequestered in the plasma membrane, and this causes a late flowering, while warmer temperatures catalyze its release and thus accelerate flowering (Susila *et al.*, 2021). In rice there are thirteen PEBPs, of which the two florigens are *Heading date 3a* (*Hd3a*) and *Rice flowering locus T 1* (*RFT1*), and they have been demonstrated to be essential for flowering (Komiya *et al.*, 2008a). They are both located on chromosome 6 at 11kb distance. Like Arabidopsis FT they are produced in the companion cells in the leaves when both internal and external favourable conditions are met. Absolute *Hd3a* transcript amount gradually increases in SDs, but does not in LDs (Kojima *et al.*, 2002). In SDs, the expression follows a circadian rhythm with a peak right before dawn (Fig. 5). The temporal expression pattern of *RFT1* is similar to that of *Hd3a* (Fig. 5), and both transcripts have been detected only in leaf blades, but not in the sheaths nor in the roots (Komiya *et al.*, 2008a). GUS assay reported that *Hd3a* is specifically expressed in the companion cells of the leaves, while the transcripts of *Hd3a* and *RFT1* has not been detected in the SAM; thus, it is the protein products of both Hd3a and RFT1 that are translocated to the SAM, and not the mRNA, as also demonstrated by the signals coming from GFP-fused florigens (Fig. 6A-G and Fig. H,I respectively, Tamaki *et al.*, 2007a; Komiya *et al.*, 2009). The movement of Hd3a once it reaches the SAM has been investigated by Tamaki *et al.* (2015). The florigen

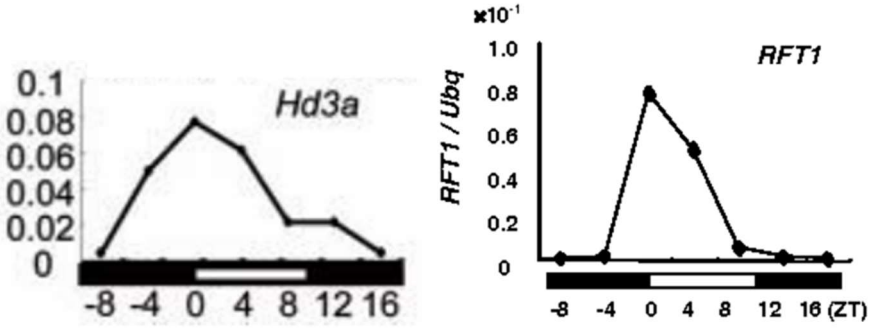

Figure 5. ***Expression pattern of Hd3a and RFT1 in SDs*** *Black and white bars under the graphs represents the photoperiod. ZT: zeitberger time.*

was tagged with GFP and driven by its own promoter. The fluorescent signal was analysed in developing meristems whose identity was assigned by morphology. GFP signal was absent from the vegetative meristem (VM, Fig. 6A,B) but was detected

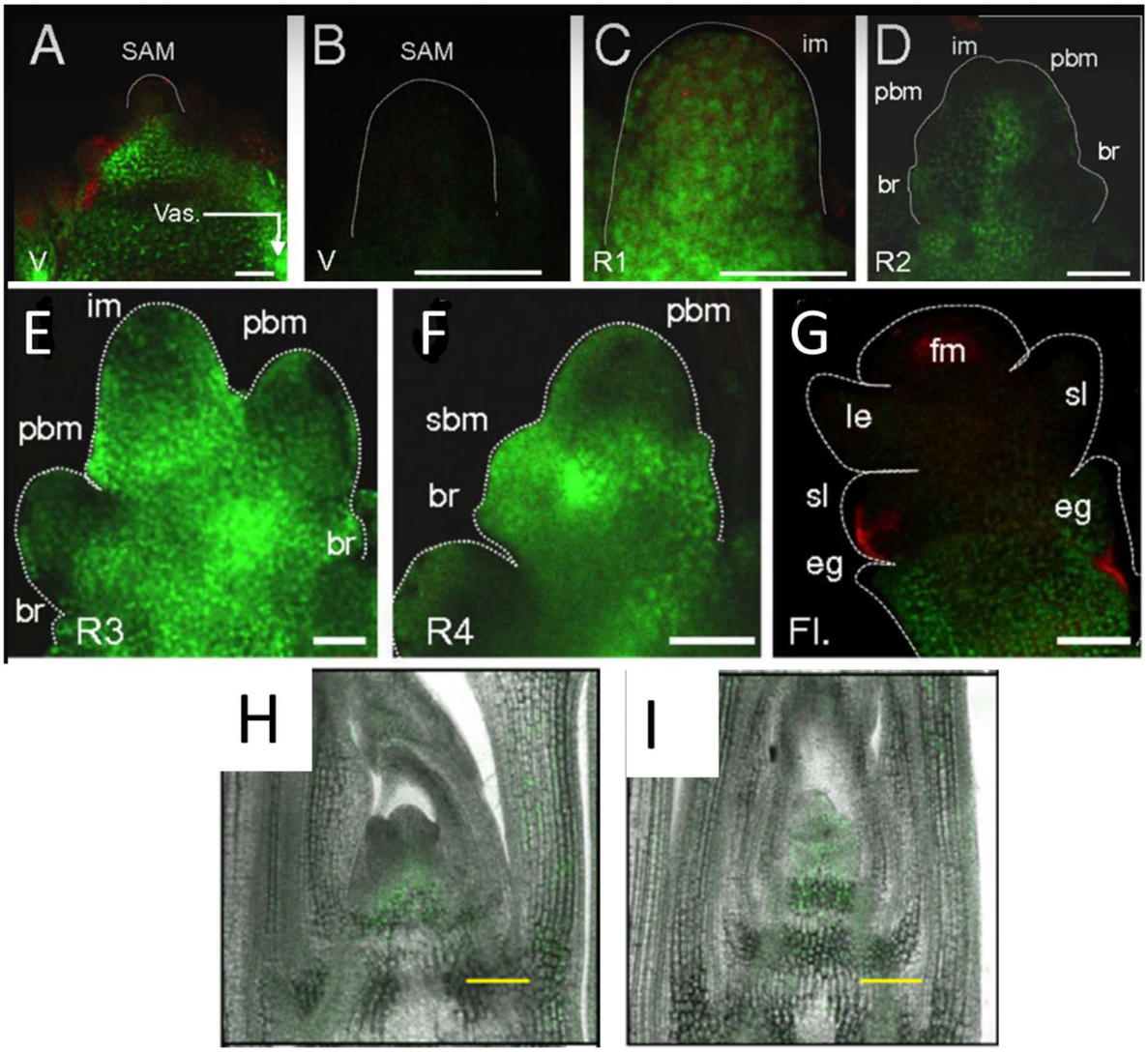

Figure 6. ***Localization of Hd3a and RFT1 during floral commitment of the SAM*** *A-G) Signal of Hd3a-GFP (under the control of pHd3a) in various developmental stages of the shoot apex, vegetative (A), with a magnification of the shoot apical meristem (SAM, in B), inflorescence meristem (im, C), primary branch meristem (pbm, D), later development of primary branches (E), secondary branches meristem (sbm, F) and floret (G). Br: bract; fm: floret meristem; le: lemma; eg: empty glume; sl: sterile lemma. H,I localization of RFT1 in the vegetative meristem (H) and infloresence meristem (I). Scale bars: 50um*

underneath it, at the upper part of the shoot vasculature. As the meristem developed into inflorescence meristem (IM) the signal became strong in it (Fig. 6C), but it was weak in newly forming branch primordia (Fig. 6D). Hd3a-GFP was still clearly detectable in the shoot apex of later stages of development (Fig. 6E), but was weak in the PBM and SBM (Fig. 6F), and also completely absent from the floral organs (Fig. 6G). Transgenic lines that suppressed *RFT1*, *Hd3a*, or both using RNAi were generated. The RNAs were designed on the 5' UTR of *RFT1* and 3' UTR of *Hd3a* to achieve a specific silencing, given the high sequence identity between the two florigens. Flowering time of these lines were evaluated: what was found is that in SDs, *RFT1* RNAi flower at the same time as wild type plants, while *Hd3a* RNAi plants have a 30 days delayed heading date (Fig. 7A). In LDs, *Hd3a* RNAi plants flowers at

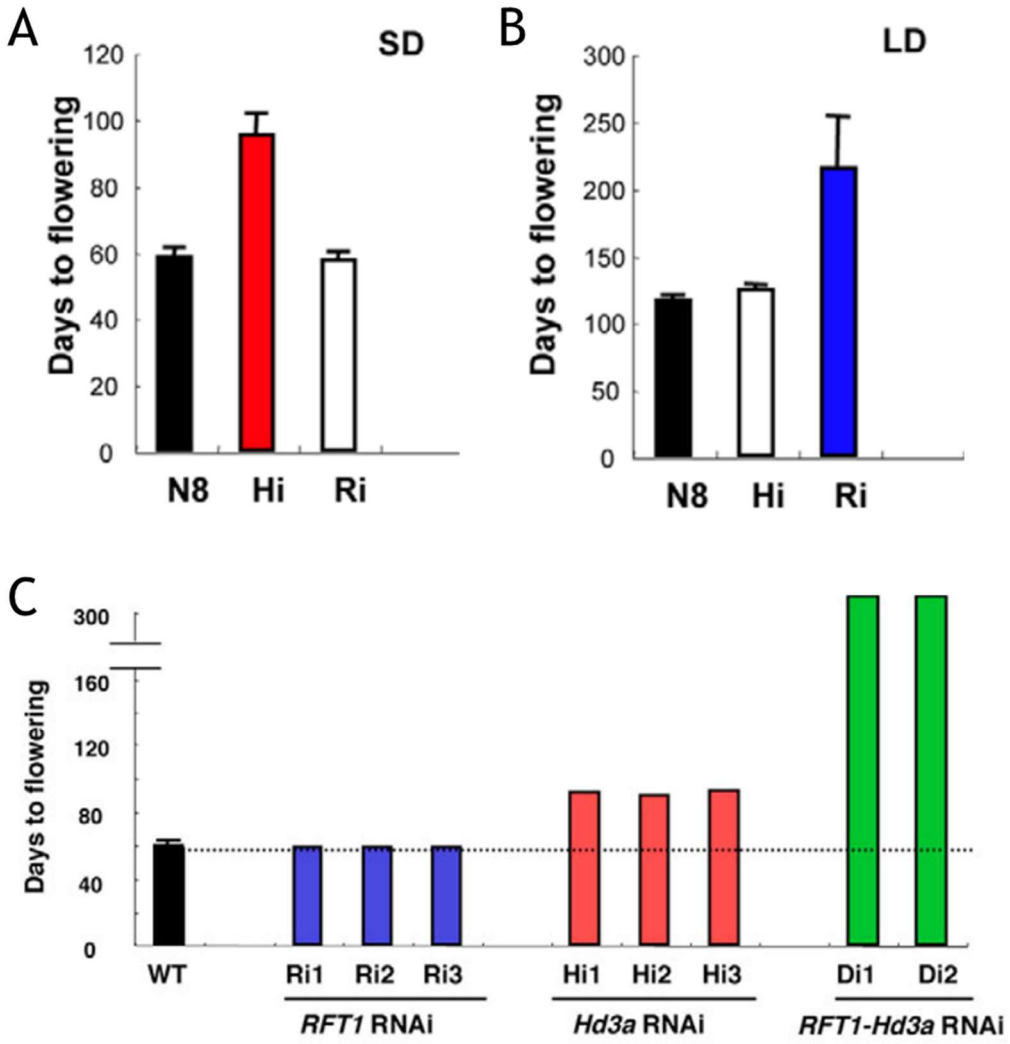

Figure 7. ***Flowering time of florigens RNAi lines*** *Flowering time of Hd3a RNAi line (Hi) and RFT1 RNAi line (Ri) in SDs (A) and LDs (B). C) Flowering time of Hi, Ri and the double knock-down Hd3a RFT1 RNAi lines Di. Dotted line represents the flowering time of the control.*

the same time as the wild type, while heading date is 100 days delayed in *RFT1* RNAi plants (Fig. 7B). *RFT1-Hd3a* RNAi plants could not flower even after 300 SDs, but rather continued their vegetative growth producing leaves (Fig. 7C, Komiya *et al.*, 2008). Hd3a acts only in SDs, while *RFT1* is expressed and functional in both photoperiods, although its action is more prominent in LDs. The gene *OsFTIP1,* which causes a delay in flowering only in LDs when knocked down, can interact with RFT1 both *in vitro* and *in vivo,* and is supposedly involved in loading RFT1 in the phloem (Song *et al.*, 2017). This specific interaction can also explain the different photoperiod-related actions of the two florigens.

Analogously to Arabidopsis, rice possess anti-florigens homologous of TFL1, called Rice CENTRORADIALIS1 (RCN1), RCN2, RCN3 and RCN4. Overexpression of *RCN1* and *RCN2,* besides delaying flowering, also generates denser panicle with more branches, since the commitment to floral identity is retarded (Nakagawa *et al.*, 2002). During the early stages of primary rachis branch development, *RCN1* expression can be observed in the inflorescence meristem (IM). After the late secondary rachis branch differentiation, *RCN1* was no longer expressed there, but becomes limited to the uppermost internodes before elongation, whereas it continues to be expressed in the vascular bundles of leaves and stems during later stages of development, such as floret primordia initiation and stamen and carpel primordia differentiation. *RCN3* could not be detected by *in situ* hybridization (Zhang *et al.*, 2005). Compared to a wild type plant, a rice plant with knocked-down *RCN* genes exhibits a smaller panicle with fewer branches (Liu *et al.*, 2013). All *RCN* genes are expressed in stem and roots for all the stages of plant life, regardless of photoperiod when tested with qRT-PCR. Interestingly, they are not expressed in the SAM. GUS essay confirmed that all four *RCNs* are expressed in the vasculature underneath the SAM, but not the SAM itself: fusing them with GFP proteins revealed that they are translocated to the meristem, both vegetative and reproductive, where the act (Kaneko-Suzuki *et al.*, 2018). Here, Kaneko-Suzuki at al. also demonstrated that RCNs bind to 14-3-3 competing with Hd3a, creating a repressor complex like TFL1 does. *RCN4* is also repressed by *OsMADS34/PAP2,* a transcription factor activated by the FAC (Zhu *et al.*, 2022b). This creates a further level of regulation between florigens and antiflorigens.

1.6 Florigens act as parts of multimeric complexes

As mentioned, FT enters the SAM from the phloem and induce the shift to the reproductive stage. In doing so it does not work alone, but as part of a multimeric complex, the Florigen Activating Complex (FAC). It was first proposed that FT required FD, a bZIP transcription factor, to be able to bind the DNA (Abe *et al.*, 2005). FD expression does not depend on circadian clock, and its only expressed in the SAM, so it gives FT a spatial regulation, that sums with the temporal regulation given by the CO network in the leaves (Wigge *et al.*, 2005). The FAC binds the DNA activating the transcription of floral identity genes *APETALA1* (*AP1*), *LEAFY (LFY)* and *FRUITFUL* (*FUL*). At the same manner of *FT*, *Hd3a* and *RFT1* are produced in the sieve elements of the leaves and are then translocated to the shoot apical meristem (SAM) (Tamaki *et al.*, 2007b). Rice florigens need a bridge protein, Gf14c from the 14-3-3 family, to bind OsFD1 (homologues to FD), the bZIP protein which binds the promoters of floral identity genes, and there is a pair of each of these components in the final complex (Fig. 8). The florigens bind the 14-3-3 in the cytoplasm, and then enter the nucleus where they bind the *OsFD1* components, forming an heterohexamer (Taoka *et al.*, 2011a). More recently, through a yeast-two-hybrid essay, Ho & Weigel, 2014 demonstrated that a 14-3-3 protein is involved in FAC assembly also for the FT complex. The most well-known genes which are activated by the FAC in rice are: *OsMADS14* and *OsMADS15*, orthologs of *AP1*, *OsMADS18*, and *OsMADS34* (also known as *PAP2*, ortholog of *SEPALLATA*). They act concertedly catalyzing the switch to inflorescence meristem of the vegetative SAM. The quadruple mutant *MADS14;15;18i pap2* is unable to produce a panicle but continues to generate leaves (Kobayashi *et al.*, 2012). Overexpression of *OsMADS14* causes a very strong phenotype in which the transformed calli generates flower-like structures already in the regeneration plate (Jeon *et al.*, 2000). Overexpressing *OsMADS18* causes an early-flowering in the plant (Fornara *et al.*, 2004), but silencing it through RNAi does not cause any evident phenotype, that is probably masked by the redundancy with *OsMADS14* and *15*. *OsMADS34*/*PAP2* shapes panicle architecture: when knocked out, the resultant panicle is shorter, since the node do not properly elongate, and denser, because of the delay in these mutants in the transition from branches to spikelets.

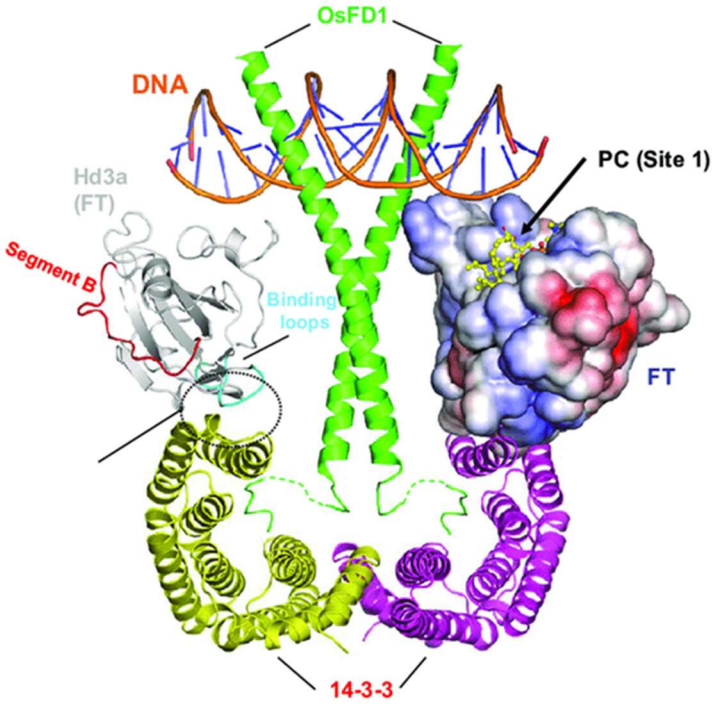

Figure 8. ***Model of the FAC*** *The florigen is represented in gray, ribbon view on the left, where the segment B is highlighted in red and the binding site to the 14-3-3 is highlighted in blue, and with surface potential on the right, where the PC binding site is shown. 14-3-3 bridge proteins are represented in yellow and magenta, bZIPs OsFD1 in green bound to the DNA.*

The Florigen-Gf14c-OsFD1 is not the only complex that can be formed. Already in 2001, Pnueli shown that florigens could bind different proteins belonging to the 14-3-3 family, suggesting the existence of combinatorial possibilities giving rise to different activating complexes, possibly with different targets. Furthermore, also the existence of alternative FD proteins bound by the florigens was demonstrated (Tsuji *et al.*, 2013). In particular, in their work Tsuji et al. discovered that the FAC comprising *OsFD2* is involved in leaf development: its overexpression produces smaller leaves and a shorter plastochron, and the interaction with Gf14b and Hd3a was demonstrated with both yeast-two-hybrid-assay (Y2H). It was later demonstrated that Hd3a and RFT1 are able to form a complex in the leaves that serves as the effector of a feedback loop that represses florigens themselves (Brambilla *et al.*, 2017). The bZIPs involved are Hd3a BINDING REPRESSOR FACTOR1 (HBF1) and HBF2, assessed with Y2H and BiFC. Expression analysis found that in SD-induced *GVG:RFT1* and *GVG:Hd3a* plants sprayed with dexamethasone (DEX, see results for a description of these lines) the amount of endogenous *Hd3a* and *RFT1* was lowered. This effect is reached via Ehd1, whose promoter is bound by HBFs. Also, *hbf1 hbf2* mutant plants head earlier than the wild type counterpart. Lastly, these alternative FACs act in the SAM as well repressing the transcription of

OsMADS14 and *OsMADS15*. Recently, another minor bZIP was identified as a floral promoter, *OsFD4* (Cerise *et al.*, 2021). The expression of floral marker was assessed in *osfd4* plants after the SD induction, and their expression was lower than it was in the wild type, although not as low as in *osfd1* mutants. A DAP-seq experiment found that there are specific subsets of genes preferentially bound by OsFD1, OsFD4 and HBF1. Interestingly, OsMADS14 and OsMADS15 promoters were not found to be bound by either bZIPs, suggesting an indirect regulation or the need for other stabilizing proteins not present in the experimental conditions.

1.7 Other effects of the PEBPs in plants

The effect of the florigens transcend that of mere flowering. In fact, PEBP proteins have been found also in ancient plants, like gymnosperms and bryophytes, and in particular *MFT*-like genes (Karlgren *et al.*, 2011), which act, respectively, as promoters of bud set in a photoperiod-responsive manner (Gyllenstrand *et al.*, 2007) and promoters of the development of the sporophytes (Hedman *et al.*, 2009). This suggested that the FT family evolved to allow angiosperm to carry on their distinctive process, which is flowering (Karlgren *et al.*, 2011; Pin & Nilsson, 2012). It has been shown that *Hd3a* can promote branching in rice plants (Tsuji *et al.*, 2015a). Transgenic plants overexpressing *Hd3a* (*pRPP16:Hd3a-GFP,* where pRPP16 is phloem-specific promoter) had more branches than the wild type, contrarily to *Hd3a* RNAi plants, which had less. Tsuji *et al.* also observed that the axillary buds are produced as much as in the wild type, but in *Hd3a-OE* they are prompted to grow instead of staying dormant. Similarly to what happens at SAM level, Hd3a is translocated form the phloem to the axillary buds: GFP-fused Hd3a was clearly visible in this organ. Hd3a was also fused with Kaede, a fluorescent protein forming a high molecular weight complex, and in *Hd3a-Kaede* plants the fluorescent signal was only present in the phloem, and the number of branches was comparable to that of wild type plants, meaning that Hd3a needs to be unloaded to the lateral bud in order to promote its outgrowth. This complex is different from the one found in the SAM since *OsFD1* is not involved, suggesting that there are multiple florigen-containing complexes that can be formed, allowing for a certain plasticity to the function of the florigen.

StSP6A, a potato paralogue of *FT* is not only responsible for flowering, but also tuberization (Navarro *et al.*, 2011). Overexpression of *Hd3a-GFP* in a strictly SD flowering and tuberizing cultivar, *Andigena*, allowed it to tuberize and flower even in LD non-inductive conditions. Grafting *Hd3a-GFP* shoot on wild type stolons caused formation of both flowers and tubers, but only the protein, and not the mRNA, was found in the stolons, confirming the mobile nature of the tuberigen that are produced in the leaves and then translocated to the stolons. Overexpressing *StSP6A* causes tuberization in LDs, while silencing it triples the days needed to tuberize in inductive SDs. StSP6A is also expressed in the stolons themselves, even if with a delay respect to the leaf expression; in fact, in Hd3aox potato plants, an increase in the stolon-expressed *StSP6A* is observed. *StCO* is the paralogue of rice *Hd1*, with the same dual function based on the photoperiod. Grafting *StSP6Aox* on *StCOox* stocks heavily represses *StSP6A* expression. Thus, *StSP6A* is controlled by the CO potato homologue, which is under photoperiodic control.

Another alternative function have been seen in poplar . Böhlenius *et al.*, 2006 isolated *PtFT1* from–*Populus trichocarpa,* an orthologous of *FT*. Its overexpression in *Populus tremula x tremuloides* caused the formation of flower-like structures already in the regeneration plate, meaning that Pt*FT1* is a powerful floral inducer. Trees usually undergo a juvenile phase that lasts years, before entering the adult stage in which they cycle between vegetative and reproductive phases yearly. Pt*FT1* expression in poplar shoot tips collected from 2 to 6 years old plants has shown that the level gradually increases until a threshold that is critical for flowering. Poplars cessate growth and set their buds in a photoperiod-dependent way, when the day length shortens, which in temperate regions coincide with autumn. *35S::FT1*, though, kept growing well after SD induction. Contemporarily similar conclusions were drawn for *PtFT2* as well (Hsu *et al.*, 2006). Later it was demonstrated that during cold and short days during winter, *PtFT1* transcripts were plentiful in all the tissues examined, while during warm and long days in springtime, *PtFT2* transcripts were abundant mainly in the leaves and developing reproductive buds (Hsu *et al.*, 2011). What was suggested in this work is that the progressive increase in spring temperatures causes a decline in *PtFT1* transcription, which marks the end of the reproductive onset and signals the initiation of reproductive bud development during the growth season. Our data demonstrates that the expression of *FT1* during the

growth season impedes the formation of genuine vegetative shoots and buds, and all buds tend to be reproductive. In contrast, during early spring, the gradual increase in temprature and longer daylight hours induces *PtFT2* signaling, which stimulates the reprise vegetative growth. To add on that, an FD-like gene has been characterized (Tylewicz *et al.*, 2015); the interaction between FTs and PtFDL1 is essential for the maintenance of *Like-APETALA1* (*LAP1*) expression, a gene that prevents growth cessation (Azeez *et al.*, 2014). By grafting poplar genotypes with different resposnses to seasonal cues, it has been demonstrated that PtFT is a mobile signal expressed in the leaves and then translocated to the meristems (Miskolczi *et al.*, 2019). Another process worth mentioning is interonode elongation in rice. The gene responsible for the process is *PREMATURE INTERNODE ELONGATION1* (*PINE1*), a zinc-finger transcription factor which is downregulated by the arrival of the florigens at the base of the SAM as soon as flowering starts (Gómez-Ariza *et al.*, 2019). The CRISPR *pine1* mutant have a prostrate growth already two weeks after germination, while *PINE1ox* (under the control of a meristem-specific promoter) have shorter internodes making it hard for the panicle to fully emerge form the flag leaf sheath. Interestingly, neither mutant altered flowering time nor panicle morphology or fertily, clearly demonstrating that flowering and internode elongation can be genetically uncoupled.

1.8 The flowering gene network

As said, rice can flower both in SDs and LDs. The external coincidence model proposed that photoperiodic measurement is done by the interaction of exogenous light signals with circadian regulated genes. Circadian regulated genes have a regular expression pattern that lasts 24 hours, after which it is resetted and starts again. In this scenario, whether the expression peak of the gene falls in day-time or night-time depends on the photoperiod. In rice there are two different, although interconnected, pathways that lead to the production of the florigens in the two different conditions and are also tightly linked to the circadian clock though the clock component *GIGANTEA* (*OsGI*). One is conserved among plants, while the other, involving *Ehd1*, is specific to rice. An important player of the first one is *Hd1*, an ortholog of Arabidopsis *CONSTANS* (*CO*). It is a B-box zinc-finger protein with CCT domain(Yano *et al.*, 2000). Unlike A. thaliana CO, that is not stabilized in SDs since

the gene expression peaks at night, and therefore cannot activate *FT* in such condition, rice Hd1 protein accumulation does not depend on the photoperiod, as it follows the mRNA abundance under any condition (Valverde *et al.*, 2004; Ishikawa *et al.*, 2011). According to Zong *et al.*, (2021), Hd1 promotes the expression of florigens under SD conditions, while it inhibits them under LD conditions. This change in function of Hd1 based on photoperiod can be explained by its interactions with Ghd7 or Ghd8 (Du *et al.*, 2017; Sun *et al.*, 2022). Under LD conditions, they fully can form complexes that repress the transcription of *Ehd1*, *Hd3a*, and *RFT1*. However, under SDs, the complexes lack the necessary components due to reduced expression of *Ghd8* and instability of Ghd7 protein, which leads to the conversion of Hd1 into a transcriptional activator. This explanation is also genetically supported, as the *Hd1 ghd7 ghd8* mutants flower earlier than the *hd1 ghd7 ghd8* mutants regardless of the photoperiod. *Ghd7* is promoted by red light ,and a gate is present in the morning allowing for accumulation of the protein in LDs. In SDs, in turn, the expression is lower as the gate shift into the night, and the protein in also degraded through *OsGI*

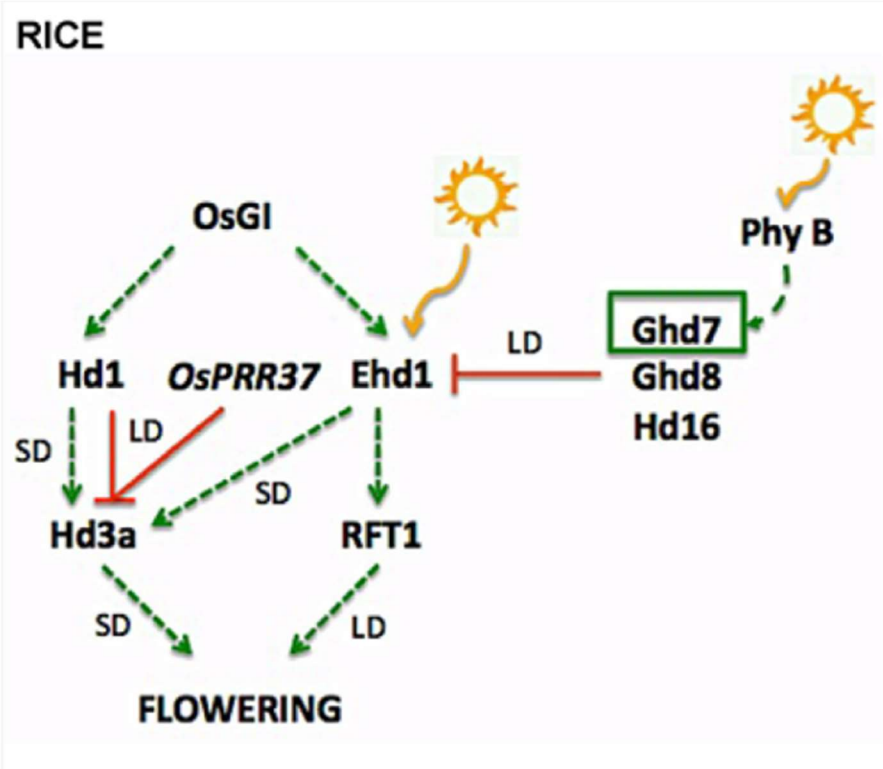

Figure 9. ***Genetic control of rice flowering in SDs and LDs*** *Dotted green arrow indicates activation, red line repression. The sun stands for photoperiodic control.*

(Itoh *et al.*, 2010). Another core regulator is *PRR37* (PSEUDO-RESPONSE REGULATOR 37), a flowering repressor that acts both on the florigens themselves and *Ehd1* (*Early heading date 1*) in long day conditions. *Ehd1* is the hub of the second pathway that

is specific to rice (Doi *et al.*, 2004). It is a B-type response regulator that in short days it promotes flowering, while in long days its expression is lowered by several repressors and cannot therefore carry out its function (Peng *et al.*, 2007; Ryu *et al.*, 2009; Lee *et al.*, 2010). Both *Ehd1* and *Hd1* are direct activators of the transcription of the florigens *Hd3a* and *RFT1* (Izawa *et al.*, 2002; Doi *et al.*, 2004) (Fig. 9).

1.9 Molecular control of tiller angle in rice

Tiller angle is a trait critical for optimizing plant architecture and maximize yield. It has been a major character interested during rice domestication .The gene responsible for the switch to erect growth, *PROSTRATE GROWTH1* (*PROG1*) has been identified in common wild rice, which is prostrate, by creating NILs using *Teqing* (a cultivated and erect, variety) as a recipient (Tan *et al.*, 2008; Jin *et al.*, 2008). It encodes for a C_2H_2 zinc-finger transcription factor. 182 modern rice varieties, both *indica* and *japonica*, possess the same loss of function *prog1* allele that causes the erect habit, a hint that this trait was fixed early during domestication. Currently, tiller angle is a target for improvement in many breeding programs. The normal behaviour of a cultivated plant is to open its tillers during the tillering phase to better compete with other plants, shading them and capturing more light. After flowering, the angle starts to decrease so that the canopy takes up less space and the leaves can maximize photosynthesis in a crucial step of the life cycle (Wang *et al.*, 2022). Columnar plants are more likely to produce bigger and stronger panicles due to an efficient photosynthesis (Wang & Li, 2008). Breeders have been searching for the perfect angle for plants, that balances planting density and yield: larger plants are more efficient in the competition against weeds, and a better air and humidity flow which lead to less pests susceptibility, but this comes at the expenses of planting density; compact plants are more susceptible to pests since they are sown very close to one another and there is little to no air-flow, but this method allows for a higher planting density (and that translates to more yield), and also can maximize photosynthesis (Wang *et al.*, 2022).

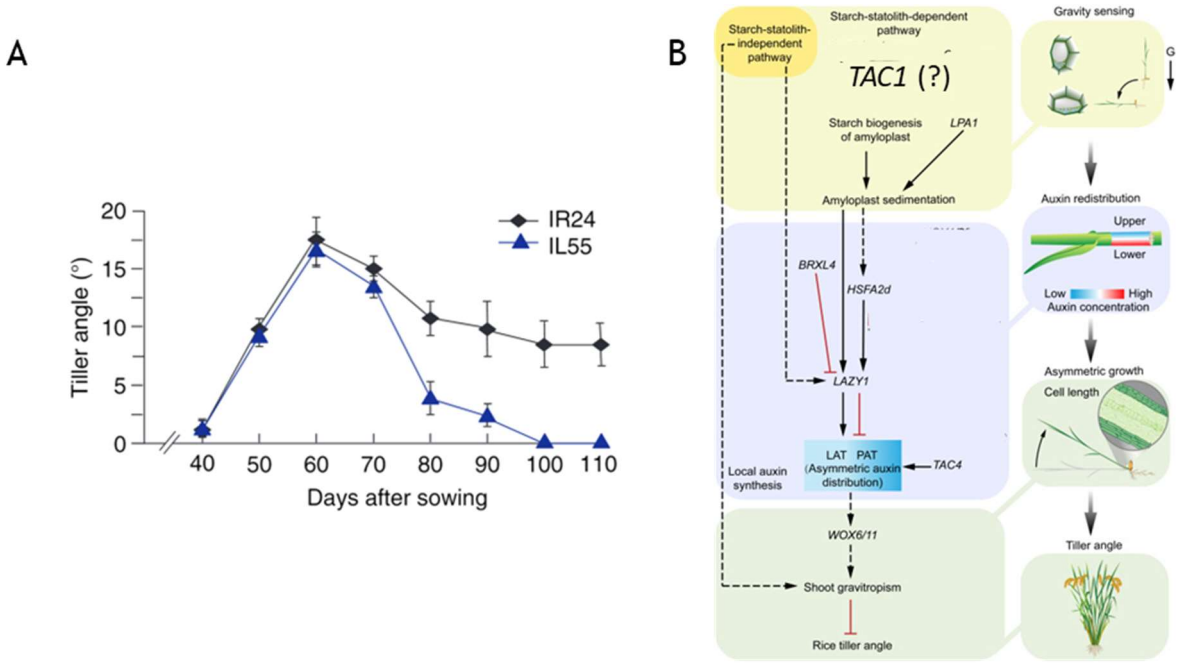

Figure 10. ***Tiller angle control in rice*** *A) Changes in the tiller angle during the life of the plant. IR24 possess the functional TAC1 allele, IL55 the non-functional tac1. Error bars represent standard deviation. B) gene network with the major players involved in the control of tiller angle, together with the specific pathway in which they act. Black arrows mean activation, red lines means repression, and dotted arrows mean an indirect, or not well defined, activation. G: gravity.*

Tiller angle control depends on many factors, such as the auxin pathway (and also other hormones even if to a lesser extent), gravitropism, light perception and others. Besides *PROG1*, many genetic players have also been discovered up to now. *Tiller angle control 1* (*TAC1*) was retrieved as a QTL from the comparison of representative *indica* and *japonica* cultivars (IR64 and IL55), the first having a wider tiller angle and the latter a more compact one (Fig. 10A, Yu *et al.*, 2007). IR64 possess the *tac1* allele, where a 'AGGA' to 'GGGA' mutation causes the loss of a splicing site in the 3'UTR, leading to a shorter transcript with a lower expression than its wild type, longer counterpart. Overexpression of *TAC1* produces plants with a wider tiller angle, while silencing it with RNAi causes erect plants. GUS-assay revela that it is expressed at the base of tillers, as well as in nodes. The differences in the architectures of IR64 and IL55 reflect the different approach in the domestication in the two cultivation areas, because japonica rice was grown in harsher environments than indica, at both higher latitudes and altitudes, and the denser planting allowed by the narrower angle, together with less susceptibility to pests and efficient photosynthesis, helped improve the yield (Jiang *et al.*, 2012). Later on also another gene, *TAC3*, was found to contribute to tiller angle control, especially in *indica* (Dong *et al.*, 2016).Tiller angle control is tightly linked with gravitropism and auxin distribution. The gravitropic growth of the plant is mediated by the asymmetric distribution of the

auxins: through organelles called statoliths the plant can sense the direction of gravity, and with a mechanical signal transmitted by the cytoskeleton redirects the auxin flux towards the bottom side of the root/shoot; this asymmetric distribution causes a curvature, that is positively gravitropic in the roots (they grow towards gravity) and negatively gravitropic in the shoots (they grow on the opposite direction of gravity)(Chen *et al.*, 1999). A "lazy" mutation, responsible for prostrate growth in rice and due to a recessive factor, has been known for almost a century (Jones & Adair, 1938). Although numerous studies suggested that the prostrate habit was due to a poor gravitropic response, and in particular an impaired lateral auxin transport that would normally follow statolith-dependent gravity perception (Abe & Suge, 1993; Abe *et al.*, 1994; Godbolé *et al.*, 1999), it was only in 2007 that the genetic basis of the lazy phenotype were discovered by fine mapping of an F_2 population generated by the crossing of prostrate *la1-ZF802* and three erect Chinese cultivars, and the gene has been called *LAZY1* (*LA1*) (Li *et al.*, 2007; Yoshihara & Iino, 2007). *la1* knock-out mutants has a very wide tiller angle. Expression analysis reveals that *LA1* is only expressed in the stem and coleoptile, but not in the roots, making it a shoot-gravitropism-specific gene. *In situ* hybridization demonstrated that its transcript is present at the leaf-stem junction, and also in the vascular bundles of unelongated nodes. Furthermore, auxin transport was assessed using a reporter line: *la1* has an enhanced polar auxin transport (PAT) and impaired lateral auxin transport (LAT), which cause an auxin disbalance leading to the abnormal tiller phenotype (Li *et al.*, 2007). . *LAZY1* is positively regulated by *Heat stress transcription factor 2D* (*HSFA2D*): *hsfa2d* plants have a wider tiller angle, and are less responsive to gravity; to add on that, *LAZY1* is underexpressed in the tiller base.(Zhang *et al.*, 2018). Furthermore, Zhang and his group found two redundant Wuschel homeobox genes, *WOX6* and *WOX11*, through an RNA-seq comparing gravistimulated plants and non-gravistimulated plants (the same RNA-seq from which *HSFA2D* was retrieved) which are highly responsive to gravity. To put these three genes (*HSFA2D*, *WOX6* and *WOX11*) in the auxin signalling pathway, their expression levels were assessed in naphthaleneacetic acid (NAA, a synthetic auxin analog)-treated plants: the expression of both WOX genes was higher than in mock-treated plants, while no changes were detected in the expression of *HSFA2D*, situating the formers downstream of the auxin signalling, and the latter upstream of it. Besides, the

expression pattern of *WOX6* and *WOX11* is very different between the two sides of gravistimutlated shoots, being significantly more expressed in the lower side. Where the single mutants *wox6* and *wox11* had a wild type-like growth habit, the double *wox6 wox11* mutant had a substantially wider tiller angle; also, their expression is lowered both in *hsfa2d* and *la1* plants. This suggest that *HSFA2D* and *LAZY1* control tiller angle by regulating the expression of the redundant genes *WOX6* and *WOX11* in an auxin-distribution-dependent fashion. *LAZY1* is also under the control of *Brevis Radix Like 4* (*OsBRXL4*). It affects the cellular localization of LA1, misplacing it form the nucleus to the cytoplasm. In fact, transforming protoplasts with fluorescent-tagged LA1 and increasing plasmid concentration of OsBRXL4, an increasing amount of LA1 is detected in the cytoplasm. The overexpression of *OsBRLX4* leads to prostrate plants, while RNAi *OsBRXL4* plants are more erect, supporting the hypothesis that LAZY1 must be in the nucleus to affect tiller angle by narrowing it, and also OsBRXL4 acts upstream of it in the gravitropic response by misplacing it in a different cellular compartment (Li *et al.*, 2019)., Recently, a link between *PROG1* and *LAZY1* has been found. *LA1* transcript amount is lowered in plants carrying the wild rice *PROG1* allele (called *prog1-D*), and luciferase-activity assay confirmed that in the presence of a functional *PROG1*, *LA1* transcription is inhibited. Overexpression of *LA1* in *prog1-D* plants can partially rescue the impinged gravitropism phenotype. Interestingly, this mechanism only works in the light, because dark-grown *prog1-D* plants have a regular response to gravity, and *LA1* expression is comparable to that of wild type plants (Zhang *et al.*, 2022). A gene working in the first phases of gravity perception is *LOOSE PLANT ARCHITECTURE1* (*LPA1*). *lpa1* plants have a wider tiller angle, and microscope inspection has shown that the issue lies in the sedimentation of amyloplasts in the pulvinus, whose rate is reduced respect to *LPA1* plants causing a delay in gravity perception (Wu *et al.*, 2013). *TAC4* is another gene acting on auxin distribution. *tac4* show a wider tiller angle and poor response to gravity in every stage of the life cycle, and analysis with DR5:GUS reporter indicates that in *tac4* mutants the endogenous content of auxins is not only reduced, but the asymmetrical distribution is perturbed leading to the architectural phenotype. A scheme of the mechanism of tiller angle control together with the genes I mentioned in the paragraph is shown in Fig. 10B.

1.10 Regulation of gene expression by F-BOX proteins

F-BOX containing proteins are widespread throughout the eukaryotic organisms. The F-BOX motif was given its name when discovered as part of a Cyclin (Chang *et al.*, 1996), and thus being part of the ubiquitination process. The domain itself is made of about 50 aminoacids and works through protein-protein interaction. The ubiquitination process, composed of three steps involving the E1 E2 and E3 enzymes (or complexes), is just as important as the pre- and post-transcriptional regulation of genes functions, as it is responsible for protein turnover. E1 is the ubiquitin-activating enzyme, it binds with ubiquitin spending an ATP molecule; the activated ubiquitin is then passed to E2, the ubiquitin-conjugating enzyme and, finally, to the target protein that has been recruited by E3. The high target specificity is given by the combinatorial effect, because where there are only few E1 enzymes, there are

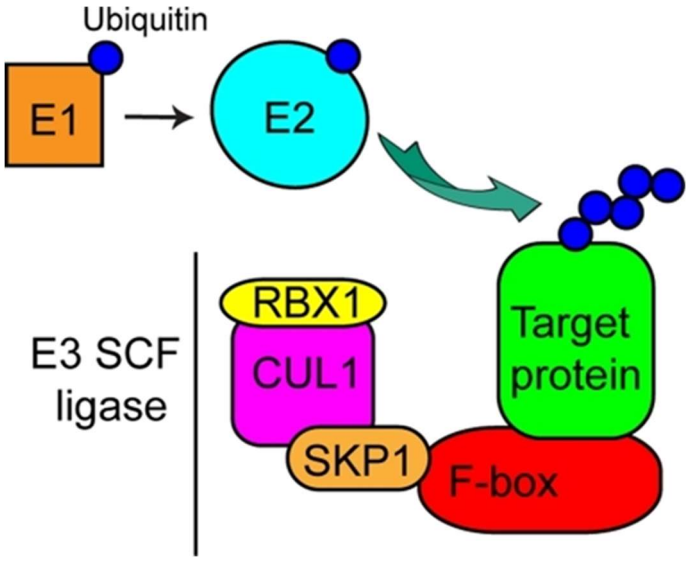

Figure 11. ***Schematic structure of the SCF ligase in the context of the ubiquitination process***

many different E2 and even more E3 complexes, allowing for thousands of different possible cascades recruiting as many targets. Besides, the fate of the target is decided by the kind of ubiquitin chain with which it is tagged, ranging from the most common protein degradation through the proteasome, to signalling, regulation of the cell cycle, and autophagy (Hershko & Ciechanover, 1998; Geng *et al.*, 2012; Komander & Rape, 2012).

In detail, F-BOX proteins are usually part of the SCF (Skp, Cullin and F-BOX) complex (Fig. 11), a particular type of the E3 ligase complex (Lechner *et al.*, 2006). This complex is the one responsible for proper target recognition, which occurs by

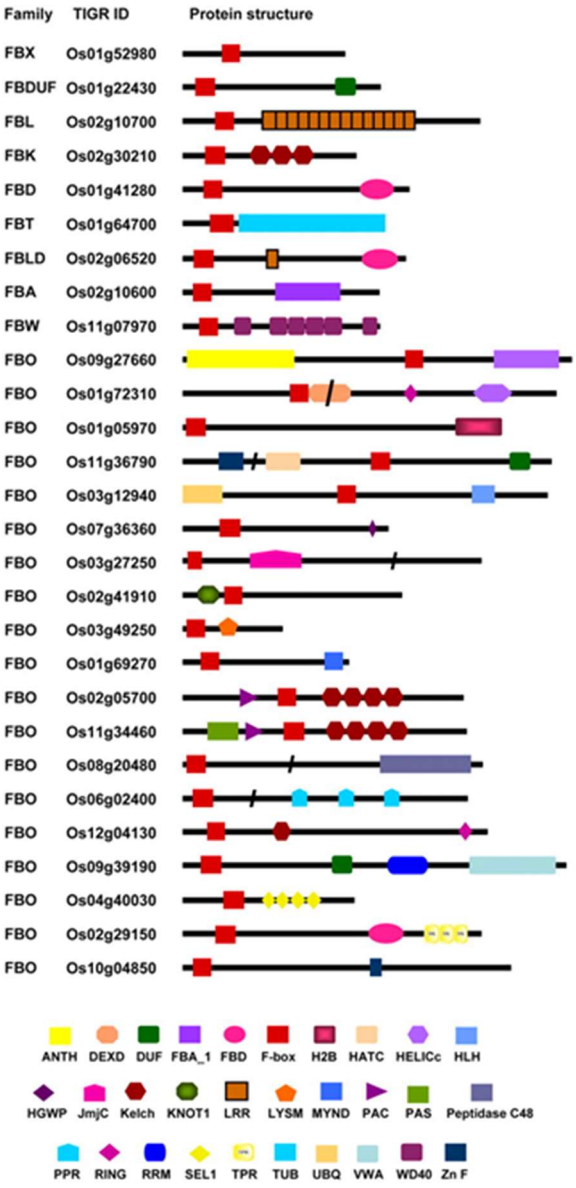

Figure 12. Different F-BOX families in rice *Organization of the domains of representative F-box proteins from each family. ANTH, ANTH domain; DEXD, DEAD-like helicase domain; FBA_1, F-box associated domain; FBD, domain present in F-box and BRCT domain containing proteins; H2B, histone H2B; HATC, hAT family dimerization domain; HELICc, helicase superfamily C-terminal domain; HLH, helix-loop-helix domain; HGWP, HGWP motif; JmjC, Jumonji; Kelch, kelch repeats; KNOT1, knottins; LysM, Lys motif; MYND, MYND finger; PAC, motif C terminal to PAS motifs; PAS, PAS domain; Peptidase C48, Ulp1 protease family C-terminal catalytic domain; PPR, pentatricopeptide repeats; RING, ring finger; RRM, RNA recognition motif; SEL1, sel1-like repeats; UBQ, Ub domain; VWA, von Willebrand factor type A domain; WD40, WD40 repeats; ZnF, zinc finger.*

interaction with the F-Box protein and therefore there are many different, and specific, E3 complexes (Hershko *et al.*, 2000).

The F-Box containing proteins are much more represented in plants than in the animal and fungi kingdoms, with *A. thaliana* possessing 694 genes and rice 678 (Xiao & Jang, 2000; Jain *et al.*, 2007). The F-BOX motif is almost always at the N-term of the protein, and it is accompanied by another protein-protein interaction domain at the C-term: it is the latter that confers target-specificity to the complex. Given the high number of genes, they can be divided into subfamilies based on the C-term (Fig. 12): FBX, that only possess the F-BOX domain and represent almost half of the pool; FBDUF containing the domain of unknown function (DUF); FBL containing LRR motifs; FBK containing Kelch repeats; FBD; FBT containing TUB domains; FBLD that possess both LRR and FBD; FBA with an F-BOX-associated domain; FBW with WD40 domains; FBO that groups all the other domains (Jain *et al.*, 2007).

The first F-BOX protein discovered in plants has been called Unusual floral organs (UFO) (Levin & Meyerowitz', 1995), even if only recently it has been discovered that it works as a transcription factor (Rieu *et al.*, 2023). The mutants produce aberrant flowers in *Arabidopsis*. Other relevant F-BOXes, which are well characterized and

are known to be involved in flowering are Flavin-rich, kelch repeats, FBOX1 (FKF1) and Zeitlupe (ZTL) (Somers *et al.*, 2000; Imaizumi *et al.*, 2005; Song *et al.*, 2014). FKF1 induces expression of *CO* by degrading a repressor of its transcription CDF1 (Imaizumi *et al.*, 2005). ZTL, in turns, acts on the regulation of the circadian clock by degrading a central component, TOC1 (Más *et al.*, 2003).

In this thesis, I will later describe the functional analysis of *OsFBX125*, that besides the F-BOX domain in the N-term, it also has an FBA at the C-term, making it one of the four FBA F-BOX proteins we can find in rice (Jain *et al.*, 2007).

1.11 MAIN-like genes

A second gene that I will later present (*LOC_Os07g32406*) was at first annotated as a generic expressed protein. After a domain family search, it scored a high similarity with the *A. thaliana* gene *MAINTENANCE OF MERISTEM* (*MAIN*). *MAIN* was first discovered through in a *pSUC2::GFP* population (that produces GFP at the level of the companion cells, which move to the sieve elements and is then unloaded from the phloem) that had been mutagenized through T-tagging: some of the plants were unable to unload the GFP from the vasculature and had developmental defects in the SAM and RAM (Wenig *et al.*, 2013). *MAIN* belongs to a new class of proteins that is specific of plants. It is a nuclear protein that is mainly, but not only, expressed in the meristem. *main* mutants show developmental defects in many tissues, such as roots, which are shorter, leaves, that are smaller, and the meristem, and later on in the inflorescence that is fasciated and presents organs that have lost their identity. Furthermore, Wenig *et al*. (2013 observed an accumulation of dead cells due to damaged DNA, as if the mutants had an impaired DNA-repairing activity.

MAIN has three paralogous in A. thaliana: *MAIN-like1* (*MAIL1*), *MAIL2* and *MAIL3*. It was suggested that *MAIL1* and *MAIN* are part of the same pathway, and together contribute to maintain a correct genome stability (Ühlken *et al.*, 2014). *mail1* mutants also show developmental defects, in the roots especially, and even more so when combined with *main* mutations. It was later demonstrated that *MAIN* and *MAIL1*, possess a transposon-related plant mobile domain, and constitute a novel and alternative way of silencing transposons by regulation of chromatin condensation (Ikeda *et al.*, 2017). Recently, a third player in this pathway was characterized:

PROTEIN PHOSPHATASE 7 LIKE (*PP7L*). It is part of a complex together with *MAIN* and *MAIL1*, as demonstrated by Co-IP, Y2H and colocalization. Its mutants are a phenocopy of the other two mutants (de Luxán-Hernández *et al.*, 2020).

2. Aim

Reproduction is a fundamental step for every living organism to ensure species survival. Thus, the switch to vegetative phase to reproductive is in plants is a delicate and finely regulated process, both by genetics and the environment. The florigens play a pivotal role in higher plants flowering, as they are the final output of an intricated genetic network encompassing sensing of internal and external cues so that the phase shift happens at the right time of the plant life. In rice (*Oryza sativa L.*), *Hd3a* and *RFT1* have been indicated as the florigens, without which the plant cannot flower even in the inductive short-day (SD) photoperiod. They are produced in the leaf blades and then migrates via phloem to reach the shoot apical meristem (SAM), behaving like protein phytohormones. Their function is partially redundant. Here, they form a heterohexameric complex with a bZIP factor OsFD1 and bridged by a 14-3-3 protein, called florigen activation complex (FAC): it binds the promoter of floral identity genes activating their transcription and starting the floral commitment. Besides the well characterized OsMADS14, OsMADS15, OsMADS18 and OsMADS34/PAP2 little is known about other genes under the control of the florigens.

Our interest was directed to the discovery of novel genes involved in the flowering process downstream of the florigens, but also highlighting the differences, if any, in target promotion between Hd3a and RFT1, since the dissimilarities in their activation have already been elucidated. We started from three RNA-seq experiments in which i) only Hd3a was induced with dexamethasone, ii) only RFT1 was induced with dexamethasone and iii) natural induction was simulated shifting the plants to SDs. The obtained differentially expressed genes (DEGs) were filtered with stringent conditions, and 15 emerged as strongly regulated by all three inductive conditions. Among them we found floral identity genes together with ten uncharacterized genes. These putative targets of the florigens became the subject of my project. In particular, I focused my attention on two of them, an F-BOX containing protein and

a Plant Mobile Domain containing protein, characterizing them with the generation of knock-out lines with CRISPR/Cas9 technology.

3. Results and discussion

3.1 Preliminary data

3.1.1 A florigen inducible system can mimic natural inductive conditions

To check the redundancy and differences between the two florigens effect on flowering, and to discern their function from that of the photoperiod as a whole, two inducible lines were created, expressing either *RFT1* or *Hd3a*. The construct was made as seen in Fig. 13A,B and described in Brambilla *et al.*, (2017). The GVG (GAL4, VP16, GR) receptor was put under the control of *pGOS2*, a constitutive promoter, while the florigens under the control of a *4xUAS* promoter; GVG is bound by dexamethasone (DEX), a human hormone, and when this happens, it is released from the membrane, enters the nucleus where it can bind the *UAS* promoter and activate the transcription of the gene downstream of it.

Since the florigens are produced in the leaves, leaves of *GVG:Hd3a* and *GVG:RFT1* plants were sprayed with a solution containing DEX while being kept in LDs, in order to minimize the endogenous production of the florigens. Both leaves and meristems of transgenic lines were sampled after spraying with DEX (2 days after for *GVG:RFT1* and 5 days after for *GVG:Hd3a*): the expression of the exogenous florigens was present in the leaves only (Fig. 13C,D). Also, the expression of known target genes (*OsMADS14, OsMADS15* and *OsMADS34*) was detected only after induction (wild type plants shifted to SDs, or transgenic plants sprayed with DEX), but not in the controls (wild type plants in LDs, or transgenic plants sprayed with a mock solution, Fig. 13F-H).

The flowering time of the transgenic lines was measured too (Fig. 13E). In LDs we see that the inducible lines flower like the wild type when sprayed with a mock solution, while when DEX was applied the artificial *RFT1* could induce flowering at the same time as a wild type shifted to SDs, while the exogenous *Hd3a* could not. Given all these data, the conclusions were that these inducible systems are able to mimic what happens in natural conditions, since the exogenous florigens are only expressed in the leaves but not in the meristems of the transgenics lines. Besides, also the well characterized targets of the florigens can be induced by this system, even if with lower level of expression that the wild type plants. RFT1 was also able to make the plant flower as if it were in SDs, but Hd3a could not, probably because

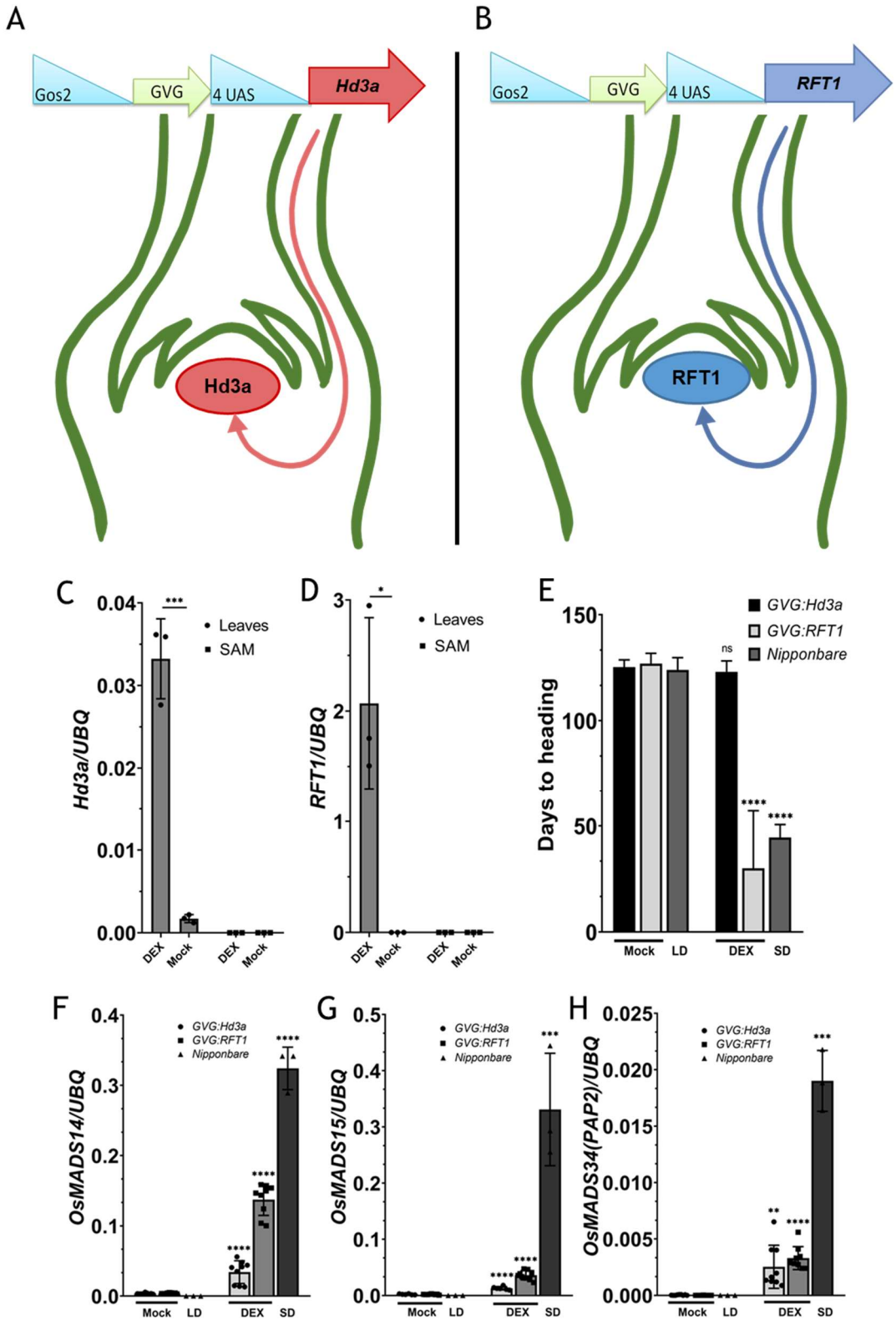

Figure 133. ***Scheme of the DEX-inducible systems and validation of their effectiveness*** *. A,B) Illustration of the vectors harboring the inducible expression cassette for A) Hd3a and B) RFT1; triangles represent promoters, and arrows represent genes. C) Expression of Hd3a in the leaves and meristems of Hd3a-inducible lines, evaluated in DEX- treated and mock-treated plants. D) Expression of RFT1 in the leaves and meristems of Hd3a-inducible lines, evaluated in DEX- treated and mock-treated plants. E) Flowering time of transgenic lines in inductive and non-inductive conditions. F,G,H) Expression of OsMADS15, OsMADS14 and OsMADS34 in the meristems of inducible lines in inductive and non-inductive conditions. DEX: dexamethasone; Mock: mock solution; LD: long day; SD: short-day. * 0.05>p>0.01; ** 0.01>p>0.001; *** 0.001>p>0.0001; **** p<0.0001*

Hd3a alone is not able to sustain the switch to the reproductive phase under LD, or because DEX-induction was sufficient to promote target gene expression but could not reach the threshold necessary to commit the SAM to flowering.

3.1.2 Three independent RNA-seq experiment unraveled ten novel genes controlled by the florigens

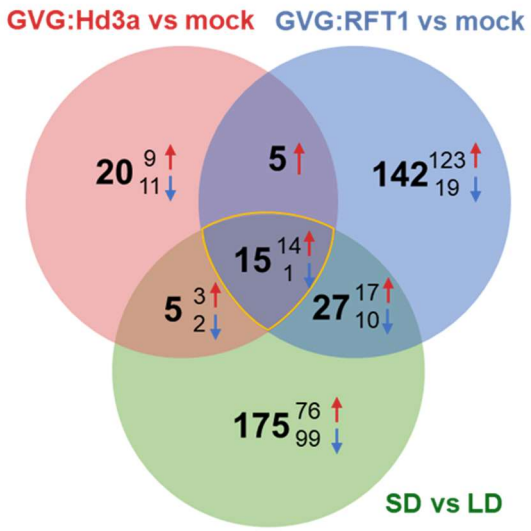

Figure 14. ***Venn diagram representing the differentially expressed genes in the three independent RNA-seq experiments****. Bigger numbers represent the total number of the genes, the smaller numbers by their side the break down in up- (red arrow) and down- (blue arrow) regulated genes*

These same inducible lines were used in two independent RNA-seq experiment. SAMs of transgenic plants grown in LDs and sprayed with DEX, or sprayed with a mock solution, were collected (three biological samples for each condition and for each genotype, for a total of 12 samples, but for the subsequent analysis only two of Hd3a-DEX and Hd3a-mock were used since PCA shown that the third replicate did not cluster with the other two). RNA was extracted and the mRNA sent to sequencing with Illumina HiSeq. The outputs were sets of genes expressed in the two treatments, DEX and mock, which were then compared to identify the differentially expressed genes (DEGs, pvalue < 0.05). A third experiment compared the gene expression of SD induced plants (after 12SDs) with that of plants kept in LDs. The three resulting datasets were then crossed in order to obtain DEGs that were in common to two conditions at a time, or all three (Fig. 14). After setting a stringent condition, being a logFC (Fold Change) > |1.5| we retrieved 15 genes strongly regulated by all the three conditions (Tab. 1). Among them, we found the aforementioned *OsMADS14*, *OsMADS15*, *OsMADS18* and *OsMADS34*, but also *OsFT-L1*, a recently characterized gene necessary to promote panicle determinacy (Giaume *et al.*, 2023). Furthermore, 10 genes were still uncharacterized, and they belonged to very different families, spanning from transposons, an F-BOX containing protein, a B3-AP2 transcription factor, a homologous of *Arabidopsis thaliana* MAIN, some expressed proteins, and IAA2 involved in auxin perception. The finding of the known targets genes inside our datasets gave us a confirmation of the solidity of the

Table 1. Genes differentially expressed in the three conditions, with a logFC > |1,5|. Red boxes mean upregulation, blue boxes downregulation. PINE1 is in the list despite being slightly below the threshold because of its biological relevance.

LOCUS ANNOTATION	GENE NAME	Log2FC Hd3a	Log2FC RFT1	Log2FC SD
LOC_Os07g01820	*OsMADS15*	6,79	8,29	8,87
LOC_Os04g29310	*retrotransposon HELICASE-RELATED/ nucleic acid binding/AT hook motif*	5,59	6,05	4,96
LOC_Os03g54160	*OsMADS14*	5,14	6,39	6,72
LOC_Os01g11940	*OsFT-Like1*	4,41	5,33	6,14
LOC_Os03g54170	*PANICLE PHYTOMERE 2 (PAP2)/OsMADS34*	4,27	5,53	6,49
LOC_Os08g13680	*retrotransposon HELICASE-RELATED*	3,48	4,58	3,52
LOC_Os04g48290	*MATE efflux membrane protein*	3,02	2,30	2,24
LOC_Os12g36680	*expressed protein*	2,46	5,25	3,15
LOC_Os08g37070	*expressed protein*	2,22	3,62	1,64
LOC_Os05g28210	*small hydrophilic plant seed protein/ Late Embryogenesis Abundant (LEA)*	2,21	4,87	3,94
LOC_Os01g09450	*Auxin-responsive Aux/IAA/ARF OsIAA2*	2,09	1,90	1,79
LOC_Os07g41370	*OsMADS18*	1,90	2,19	1,98
LOC_Os07g32406	*Similar to MAIN-LIKE1/plant mobile protein + serine/threonine phosphatase*	1,71	4,64	1,82
LOC_Os04g13150	*BROADER TILLER ANGLE 1 (BRT1) OsFBX125 - F-box domain*	1,51	2,35	3,48
LOC_Os12g42250	*PREMATURE INTERNODE ELONGATION 1 (PINE1)*	-1,36	-1,90	-2,45
LOC_Os01g04750	*AP2-B3 DNA binding domain*	-1,55	-1,62	-3,65

analysis, and we got especially intrigued in those ten uncharacterized genes that are strongly regulated by the photoperiodic induction, but also by the florigens alone.

3.2 Validation of putative targets of the florigens identified by RNA-Seq

We first validated the expression seen in the RNA seq with qRT-PCR. Samples were the meristems of *GVG:Hd3a* and *GVG:RFT1* plants sprayed with either DEX or a mock solution. In the graphs (Fig. 15) we can appreciate the differences in the expression

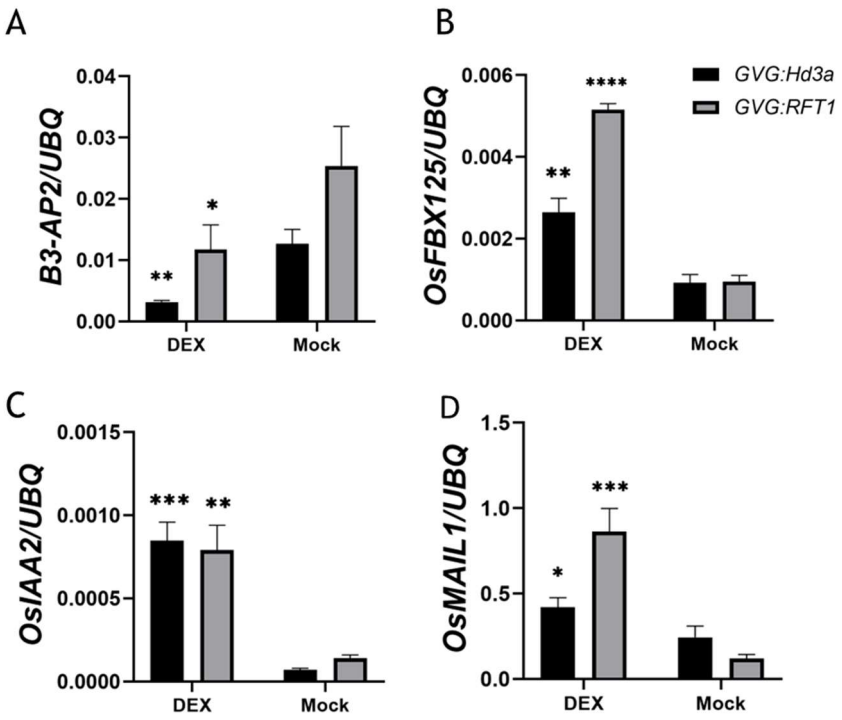

Figure 15. ***Validation of four genes retrieved from the RNA-seq.*** *Expression of B3 (A), OsFBX125 (B), OsIAA2 (C) and OsMAIL1 (D) in meristems of florigen inducible lines, in inductive and non-inductive conditions. Bars represent average values, error bars represent standard deviations. DEX: dexamethasone; Mock: mock solution. Student's t test was performed on DEX vs the respective mock. * 0.05>p>0.01; ** 0.01>p>0.001; *** 0.001>p>0.0001; **** p<0.0001*

levels in the induced (sprayed with DEX) and the non-induced (sprayed with a mock solution, non-DEX) plants. The results show that there is indeed an induction in the expression of 4 novel genes in the induced plants meristems than in the non-induced populations, in accordance with RNA-seq data. B3 (*LOC_Os01g04750*) is the only one in which its expression level is lower in the treated samples than the untreated ones, because it is downregulated during the floral transition as already shown in the table. As for the other three, *OsFBX125*, *OsMAIL1* and *OsIAA2*, the trend of their expression indicates they are upregulated during floral transition as they are much more expressed in treated plants than in the non-treated ones. However, *RFT1* is a stronger activator than Hd3a for at least two of them (*OsFBX125*, *OsMAIL1*) since the expression fold change is much higher for them in the *GVG:RFT1* plants than in the *GVG:Hd3a* plants. With this experiment we confirmed the RNA-seq data and could proceed with the analysis of the novel genes.

3.3 Florigen CRISPR mutants delays flowering in LD and SD

In the laboratory I completed my thesis in there were already stable lines mutated in the florigens, *Hd3a* and *RFT1*, carrying the alleles shown in Tab. 2 (*Hd3a*) and Tab.

Table 2. Hd3a CRISPR alleles

Hd3a CRISPR alleles (5'- 3')		type of mutation
wt	CGTCCGGAGCACCAACC-TCAAGGTCACCTATGGCT	none
hd3a-1	CGTCCGGAGCACCAACC**C**TCAAGGTCACCTATGGCT	1 C insertion
hd3a-2	CGTCCGGAGCACCAAC—TCAAGGTCACCTATGGCT	1 C deletion
hd3a-3	CGTCCGGAGCACCAACC--CAAGGTCACCTATGGCT	1 T deletion
hd3a-4	CGTCCGGAGCACC-----TCAAGGTCACCTATGGCT	4 bp deletion
hd3a-5	CGTCCGGAGCACC**C**AACCTCAAGGTCACCTATGGCT	1 C insertion
hd3a-6	CG----------GGTCACCTATGGCT	19 bp deletion
hd3a-7 IN FRAME	CGTCCGGAGCACCAAC----------GGCT	15 bp deletion

Table 3. RFT1 CRISPR alleles

RFT1 CRISPR alleles (5'- 3')		type of mutation
wt	CCATTCG-TCCGGATCACTAACCTCAGTG	none
rft1-1	CCATTCG**A**TCCGGATCACTAACCTCAGTG	1 A insertion
rft1-2	CCATTCG**T**TCCGGATCACTAACCTCAGTG	1 T insertion
rft1-3 IN FRAME	CCATTCG------TCACTAACCTCAGTG	6 bp deletion

3 (RFT1). The mutants were created using the CRISPR-Cas9 technology following the protocol from Miao et al 2013. The gene scheme of the florigens, the relative position of the gRNA target sequence, and the cutting site, are shown in Fig. 16. Given the high identity percentage between the two genes, only one scheme is presented. We can see that the majority of the mutations cause a frame shift, introducing

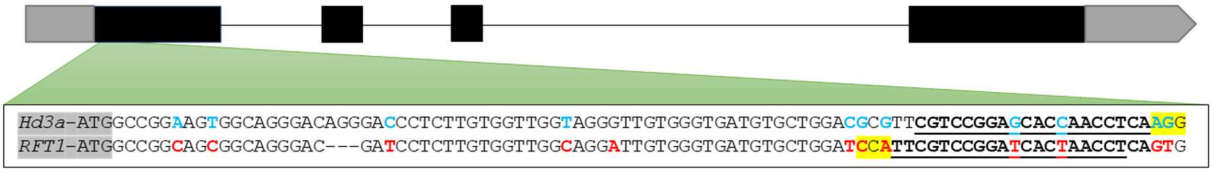

Figure 16. ***Gene structure of Hd3a/RFT1.*** *black boxes represent exons, black lines introns and grey boxes the UTRs (3' UTR is arrow-shaped). Gren shaded area is a closeup on the sequences, written below in the white box. Bolded charatcters are the SNPs between RFT1 (in red) and Hd3a (in blue). The gRNA is underlined, PAM is highlighted in yellow.*

premature stop codons at the 5' end of the gene and, de facto, knocking them out. Only two alleles, one of *Hd3a* and one of *RFT1*, show in-frame mutations (*hd3a-7*, with a 15bp deletion, and *rft1-3*, with a 6bp deletion respectively). *rft1-3* arose during the first round of transformation, while *hd3a-7* was generated in the crossing of *hd3a* and *rft1* parents that still carried the transgene comprising the gRNA and the Cas9. The crossing was made in order to create the double mutant *hd3a rft1*. In an experiment, of which the results are shown in Fig. 17, the *rft1-3* plants were evaluated for their heading time, together with *rft1-1*, *rft1-2*, *hd3a-1*, *hd3a-2*, *hd3a-3*, *hd3a rft1* and the wild type. While the knock-out lines *rft1-1* and *rft1-2* headed significantly later in LDs, *rft1-3* flowered at the same time as the wild type, meaning that the mutation does not impact the florigen function. All three *hd3a* alleles delayed flowering in SDs. The double mutant plants are unable to flower in any

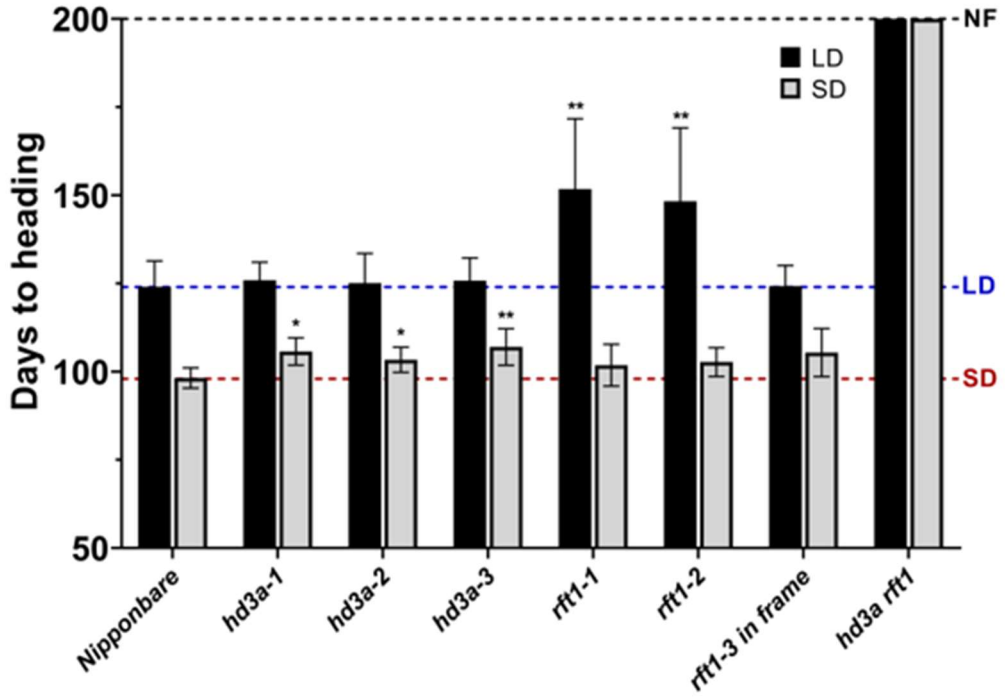

Figure 17. ***Flowering time of florigen CRISPR mutants*** *Bars represent the average value, error bars the standard deviation. LD long days. SD: short days. NF: never flowering. Red dotted line indicated the days to heading of Nipponbare in SDs, blue dotted line indicates days to heading of Nipponbare in LDs. Student's t tests were performed on LD values (black bars) vs the wild type LD value (blue line), and on SD values (grey bars) vs the wild type SD value (red line) * 0.05>p>0.01; ** 0.01>p>0.001*

photoperiodic condition, a further proof that the florigens are essential for flowering (Komiya *et al.*, 2008b), but also that the novel allele *hd3a-7*, despite being in frame, abolish the florigenic function.

3.4 Structural changes in florigen CRISPR mutants

I wanted to understand what causes the opposite behaviors of the protein products of *hd3a-7* and *rft1-3*, and I proceeded to look into their tertiary structure. The protein model for Hd3a was retrieved from PDB (Protein Database, accession: 3axy), and the respective mutant Hd3aΔ5 was modeled on the wild type protein with Swiss Model. RFT1 and the respective mutant RFT1Δ2 were modeled on the Hd3a protein with Swiss Model. The proteins were visualized and rendered with PyMol (ver. 2.5.3). In Fig. 18 we can appreciate the differences between the structures of the wild type protein (on the left) and that of the mutants (on the right), of both Hd3a and RFT1. In Fig. 18A, C the magenta indicates the 5 amino acids (L30V31K32T33Y34) that are missing from the mutant in Fig. 18B, D. We can see that an entire ß-strand is lost in Hd3aΔ5. Fig. 18C-D show the interaction surface between Gf14c (lilac color) and Hd3a (blue), or Hd3aΔ5 (green): the missing ß-sheet falls exactly in the binding interface. These residues have not been indicated as involved in the binding site to Gf14c (Taoka *et al.*, 2011b), but rather residues 32-35 are supposedly part of a loop that, upon binding with bridge proteins, undergoes a conformational change that is transferred to another loop and to the segment B (Nakamura *et al.*, 2019b), an important portion of the PEBP that determines its fate, whether being a florigen or an antflorigen (Ahn *et al.*, 2006b). Although the loop has been found in FT, it is plausible to infer that a similar mechanism works in Hd3a as well, and removing it, or part of it like in this case, heavily hinder the function of the protein. Furthermore, in Fig. 18E, F we can see how the electrostatic potential changes from the wild type to the mutant at the binding site, as a big positively charged region is deleted.

As for RFT1, the tertiary structures of the wild type protein and the mutant are shown in Fig. 18G and 18H respectively. In Fig. 18G, the magenta residues are the ones that have been deleted. The black dotted line indicates the binding region of the Gf14c, and we can see that the two deleted amino acids are far from it, and can thus conclude that, regarding the formation of the FAC, they are not essential and RFT1Δ2 can still work properly.

wt
mutant
Hd3a, ribbon view
Hd3aΔ5, ribbon view
A
B
Hd3a and Gf14c interaction
Hd3a Δ5 and Gf14c interaction
C
D
Hd3a and Gf14c interaction (electroastatic potential)
Hd3a Δ5 and Gf14c interaction (electroastatic potential)
E
F
RFT1 ribbon view
RFT1 Δ2 ribbon view
G
H

Figure 18. (on previous page) ***3D structures of the in-frame mutants of the florigens.*** *A) Hd3a wild type, in magenta the residues which are lost in the Hd3aΔ5 mutant (B). Binding interface of Hd3a (blue, C) and Hd3aΔ5 (green, D) with Gf14c (lilac). Binding interface of Hd3a (E) and Hd3aΔ5 (F) with Gf14c (lilac), with a surface potential representation. G) RFT1 wild type, in magenta the residues which are lost in the RFT1Δ2 mutant (H). Black dotted curves represent the binding site with Gf14c.*

3.5 Spatio-temporal expression of the uncharacterized genes from the dataset

To start the analysis of the ten uncharacterized genes that we retrieved as differentially expressed in the three conditions of the RNA-seq experiments, I used a repository at The Bio-Analytic Resource for Plant Biology (BAR, bar.utoronto.ca). It collects data from microarrays on different tissues, at different developmental stages and in various growth conditions for a number of plants. The aims were to check whether the Microarray data were matching the RNA-seq data, and also obtain informations about the tissues and the life phase in which each gene is expressed. I downloaded the raw data of the ten genes for the desired timepoints and tissues, and plotted the graphs shown in Fig. 19.

LOC_Os04g29310

LOC_Os04g29310 is expressed in almost all the tissues and stages, except for the ovary and the young roots, where it is negligible. It increases during seed development.

LOC_Os08g13680

LOC_Os08g13680, again is expressed in every tissue under exam: the expression increases during seed development and is particularly present in the roots.

MATE

The mate efflux protein has generally a low expression, except for the young leaves, the first and last stages of seed development, and the shoot.

LOC_Os12g36680

LOC_Os12g36680 has generally a high expression in all the samples, but the young roots, the SAM and the endosperm.

LOC_Os08g37070

LOC_Os08g37070 has a more or less constant expression throughout the life of the plant, but peaks in the late stages of seed development and in the shoot, and is not expressed in the endosperm.

LOC_Os05g28210

LOC_Os05g28210 follows a similar pattern as the previous one.

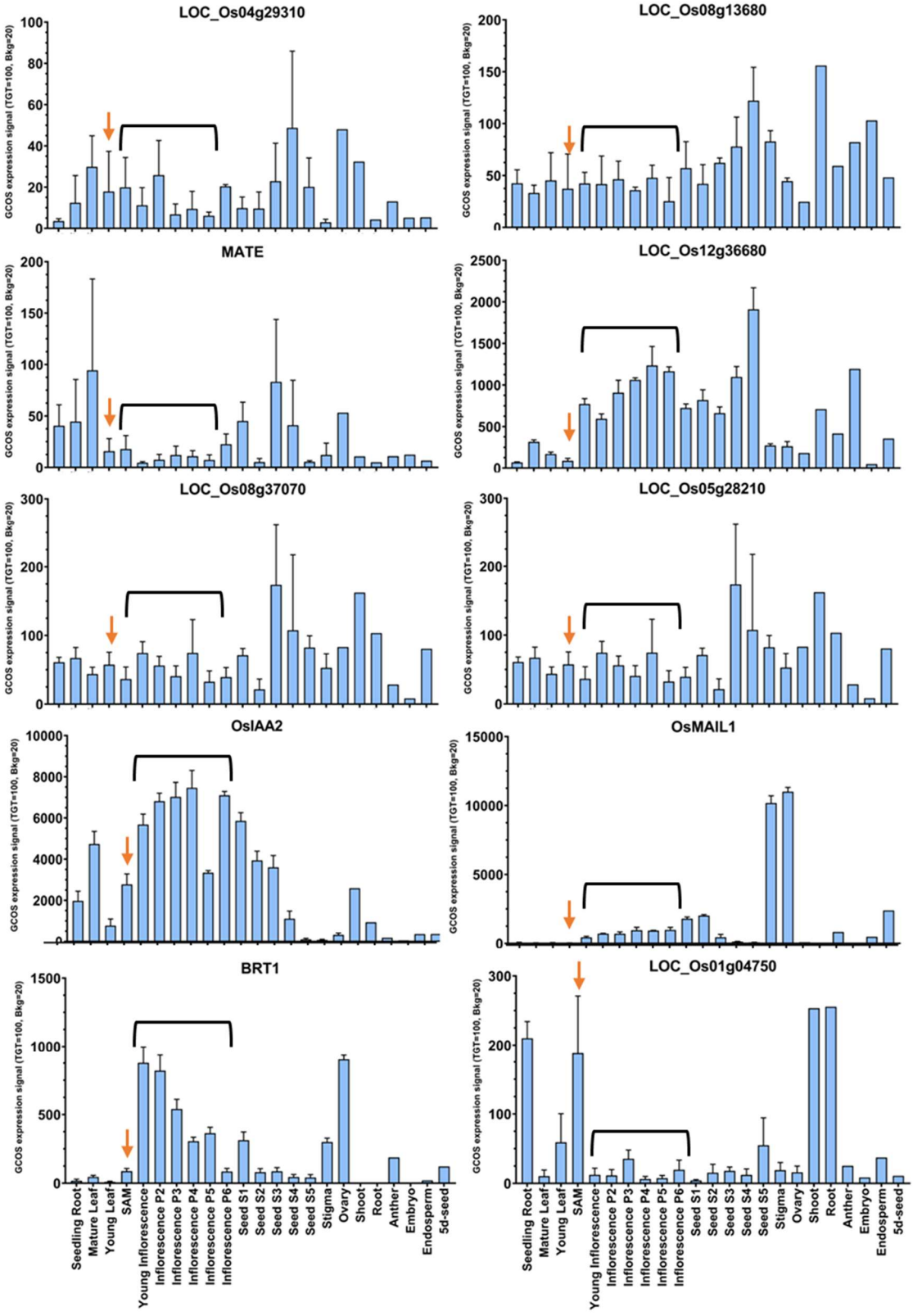

Figure 19. ***Spatio-temporal expression of putative targets of the florigens.*** *Orange arrow indicates the SAM expression level, the black brackets indicates the developing inflorescence*

OsIAA2

OsIAA2 expression increases in the switch from vegetative to reproductive stage, and decreases during seed development. It is not present in the female and male organs.

OsMAIL1

The expression of *OsMAIL1* is more localized in the stigma and ovary. It also increases during the floral transition, and it is not present in the SAM at all.

BRT1

BRT1 as well has an interesting expression pattern: it is poorly expressed in the SAM, and dramatically increases in the first stages of inflorescence development, only to decrease again in the later stages. It is also highly expressed in the ovary.

LOC_Os01g04750

LOC_Os01g04750 is generally lowly expressed: it peaks in the SAM and young roots, but also in mature shoot and root.

For half of the genes, the expression follows the same trend as seen in the RNA-seq experiment. *LOC_Os12g36680, IAA2, OsMAIL1* and *BRT1* transcript levels are low in the SAM (orange arrow in Fig. 19) but increases in the subsequent stages of inflorescence development (black bracket in Fig. 19); *LOC_Os01g04750* is highly expressed in the SAM, but then immediately decrease to become barely detectable in the inflorescence. I cannot explain the behavior of the other genes in apparent contrast to the RNA-seq data, I can only speculate that it could be due to the different growing conditions (the BAR data come from field-grown plants), or to the different sampling.

3.6 Promoter analysis

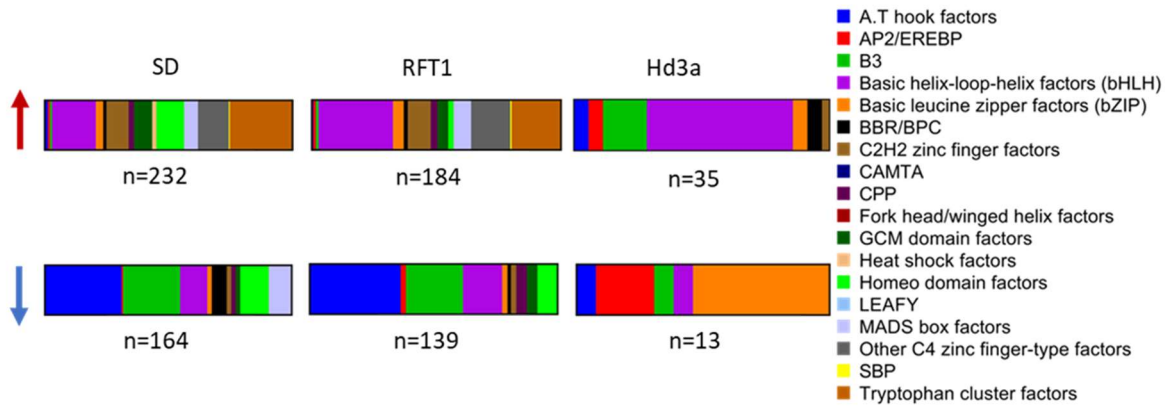

Figure 20. ***TF families whose binding sites are present in the promoter regions of the putative targets of the florigens****. Red arrow means up regulated (upper row of graphs), and blue arrow means downregulated genes (bottom row of graphs)*

We wanted to see if the putative promoter regions of all the DEGs retrieved from the RNA-seq experiments were enriched in binding sites of specific transcription factor families and if there were differences or similarities in the subsets in which the motifs were divided. We arbitrarily took 900bp upstream the ATG of each gene (from -100 to -1000), since rice transcription start sites (TSS) are not well annotated, and it was not possible to predict them. The putative promoters were divided in six groups, SD-, *Hd3a*- and *RFT1*-induced, and up and downregulated in said conditions, and then we searched if there were known TF motifs in their sequence. The matrices of the motifs were retrieved from JASPAR, and both cereals and Arabidopsis motifs were used, since rice motifs seemed to be a restrictive choice. What was found is seen in Fig. 20: in the SD-induced plants the most represented motif is the one bound by the tryptophan cluster factor, followed by the bHLH family. Other highly represented families are homeo domain factors, C4 zinc fingers and C2H2 zinc fingers. Regarding the promoters of the downregulated genes in SD-condition, we found different motifs: they are bound mostly by AT hook factors and B3-containing transcription factors, but also bHLH, homeo-domain and MADS boxes. As for RFT1-induced genes that are upregulated, their promoter is mainly bound by bHLH and tryptophan cluster factors, but also C_2H_2 and C4 zinc finger-type factors. The RFT1-induced genes that are downregulated, on the other hand, possess promoters with AT hook factor and B3 transcription factors, followed by the bHLH. The profiles of SD and *RFT1* induced gene's promoters are very similar, with the most represented TF families being bHLH and Tryptophan cluster factors (represented in lilac and okra

in Fig. 20) for the upregulated genes, and AT hook factors and B3 transcription factors for the downregulated genes. The *Hd3a*-regulated genes promoters, on the other hand, have a very different pattern, with bHLH transcription factors greatly overrepresented in the upregulated batch, and the bZIP transcription factors, the family to which *OsFD1*, essential part of the FAC, belongs, in the downregulated one. That said, it may be worth noticing that the total number of matrices is way smaller in the *Hd3a* datasets than in the other two, reflecting the low number DEG in the datasets from which this analysis is derived. Furthermore, the high similarity between SD and RFT1 profiles can simply be explained by the fact that the genes from which the promoters have been analyzed are almost the same. Looking at the differences, like the fact that in *RFT1* downregulated the homeo domain completely disappear, could be a starting point to elucidate the different families of transcription factors that are independently acting regard to the florigens.

3.7 Florigens are necessary to activate the putative targets

The RNA-seq experiments, together with the subsequent validation with qRT-PCR, identified ten uncharacterized genes that are regulated by the florigens (*Hd3a* and *RFT1*) and the photoperiodic induction. These findings told us that the florigens are sufficient to activate, or suppress in the case of *LOC_Os01g04750*, their transcription. The question that immediately arose was: are *Hd3a* and *RFT1* also necessary to regulate the expression of the aforementioned genes? To address this question, we checked the expression of the ten genes in three backgrounds: *hd3a* and *rft1* single mutant lines (Fig. 21A-J), and in the *hd3a rft1* double mutant line (Fig. 21K-R), the one unable to commit to flowering. The RNA was extracted from the scalpel-dissected meristems of plants grown in LDs (and thus still in vegetative phase), and after 7 SDs and 12 SDs for the single mutants, and after 8 SDs and 15 SDs for the double mutant. The expression has been normalized on ubiquitin.

LOC_Os04g29310

In Fig. 21A,K is reported the time course of the expression of *LOC_Os04g29310* in the single mutants and the double mutants respectively. The black line is the *Nipponbare* wild type control, and we can see that it is upregulated during the first phases of the floral transition with a ten-fold increase. In Fig. 21A, we appreciated a significant

decrease in the level of the expression in both the single mutant lines (red line for *hd3a* and blue line for *rft1*), that is around one-third of the wild type at 12SDs, while in Fig. 21K the expression at 15SDs is almost non-existent. The expression is lower in *rft1* than in *hd3a*.

LOC_Os08g13680

In Fig. 21B,L is reported the time course of the expression of *LOC_Os08g13680* in the single mutants and the double mutants respectively. In the *Nipponbare* wild type

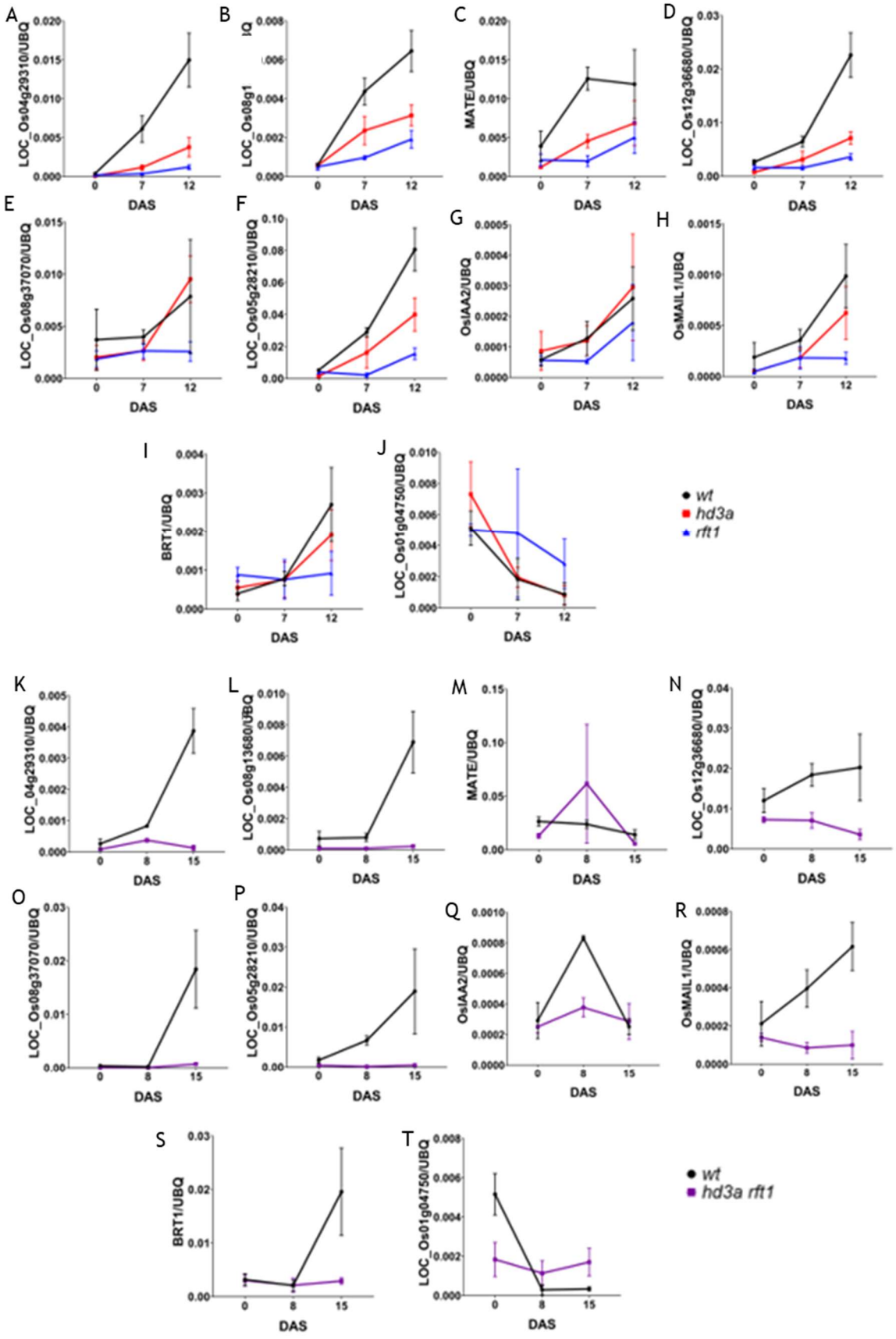

Figure 21. ***Time course of the expression of putative targets of the florigens in florigen mutant lines.*** *Dots represent the average values, bars the standard deviations. DAS: Days after shift (to short days)*

control we can see that it is upregulated during the first phases of the floral transition with a ten-fold increase. In Fig. 21B, we appreciated a significant decrease in the level of the expression in both the single mutant lines, which halves, while in Fig. 21L the expression at 15SDs is close to zero. The expression is still lower in *rft1* than in *hd3a*.

LOC_Os04g48290 MATE

In Fig. 21C,M is reported the time course of the expression of MATE in the single mutants and the double mutants respectively. In the *Nipponbare* wild type control we can see that it is upregulated during the first phases of the floral transition, but after 7SDs it is stable (Fig. 21C). In Fig. 21C, we appreciated a significant decrease in the level of the expression in both the single mutant lines, which halves. Unexpectedly, the control in Fig. 21M has a different behavior, as the expression stays constant during the floral transition. The expression in the double mutants is also not reduced compared to controls. We currently can't explain this pattern.

LOC_Os12g36680

In Fig. 21D,N is reported the time course of the expression of *LOC_Os12g36680* in the single mutants and the double mutants respectively. In the *Nipponbare* wild type control we can see that it is upregulated during the first phases of the floral transition with an eight-fold increase. In Fig. 21D, we appreciated a significant decrease in the level of the expression in both the single mutant lines, while in Fig. 21N the expression at 15SDs is very low, almost one-tenth of the wild type control. Again, the expression is lower in *rft1* than in *hd3a*.

LOC_Os08g37070

In Fig. 21E,O is reported the time course of the expression of LOC_Os08g37070 in the single mutants and the double mutants respectively. In the *Nipponbare* wild type control we can see that it is upregulated during the first phases of the floral transition. In Fig. 21E, we appreciated a decrease in the level of the expression in *rft1*, which halves, but not in *hd3a*, in which the expression is comparable with the control. In Fig. 9O the expression at 15SDs is almost non-existent.

LOC_Os05g28210 LEA

In Fig. 21F,P is reported the time course of the expression of LOC_Os05g28210 in the

single mutants and the double mutants respectively. In the *Nipponbare* wild type control we can see that it is upregulated during the first phases of the floral transition with more than ten-fold increase. In Fig. 21F, we appreciated a significant decrease in the level of the expression in both the single mutant lines, while in Fig. 21P the expression at 15SDs is close to zero. The expression is once again lower in *rft1* than in *hd3a*.

LOC_Os01g09450 OsIAA2

In Fig. 21G,Q is reported the time course of the expression of *OsIAA2* in the single mutants and the double mutants respectively. In the *Nipponbare* wild type control we can see that it is upregulated during the first phases of the floral transition (Fig. 21G). We can also see a slight decrease in the level of the expression in *rft1*, but not in *hd3a*. Fig. 21Q shows a very different trend for the wild type, since it is highly expressed after 8SDs but then drops at 15SDs. The speculation is that the three days delay with the wild type in Fig. 21G could be enough to see the expression decrease in such way, also considering that not every meristem is in the same exact stage at the sampling date. The pattern in the double mutant is similar to that of the wild type, although mitigated.

LOC_Os07g32406 OsMAIL1

In Fig. 21H,R is reported the time course of the expression of OsMAIL1 in the single mutants and the double mutants respectively. In the *Nipponbare* wild type control we can see that it is upregulated during the first phases of the floral transition with a regular trend. In Fig. 21H, we can see a decrease in the level of the expression in both the single mutant lines, while in Fig. 21R the expression at 15SDs is close to zero. The expression is much lower in *rft1* than in *hd3a*.

LOC_Os04g13150 BRT1

In Fig. 21I,S is reported the time course of the expression of *BRT1* in the single mutants and the double mutants respectively. In the *Nipponbare* wild type control we can see that it is upregulated during the first phases of the floral transition. In Fig. 21I, we can see a decrease in the level of the expression in both the single mutant lines, although is stronger in *rft1*, while in Fig. 21S the expression at 15SDs is close to zero.

LOC_Os01g04750 B3

In Fig. 21J,T is reported the time course of the expression of *LOC_Os01g04750* in the single mutants and the double mutants respectively. In the *Nipponbare* wild type control we can see that it is downregulated during the first phases of the floral transition, to reach a null expression level after 12/15 SDs. In Fig. 21J, we can see that the level of the expression in *rft1* lines stays higher, while the expression in *hd3a* is compatible with the wild type. In Fig. 21T the expression in the double mutant is constant and does not decrease, but it is noteworthy that it was already lower than the wild type at the beginning.

In Fig. 22, the data of Fig. 21 have been summarized. Only the values of the last time point are shown (12SDs for single mutants and 15SDs for double mutants), and are expressed as the ratio between the value of the mutant and the value of the respective wild type.

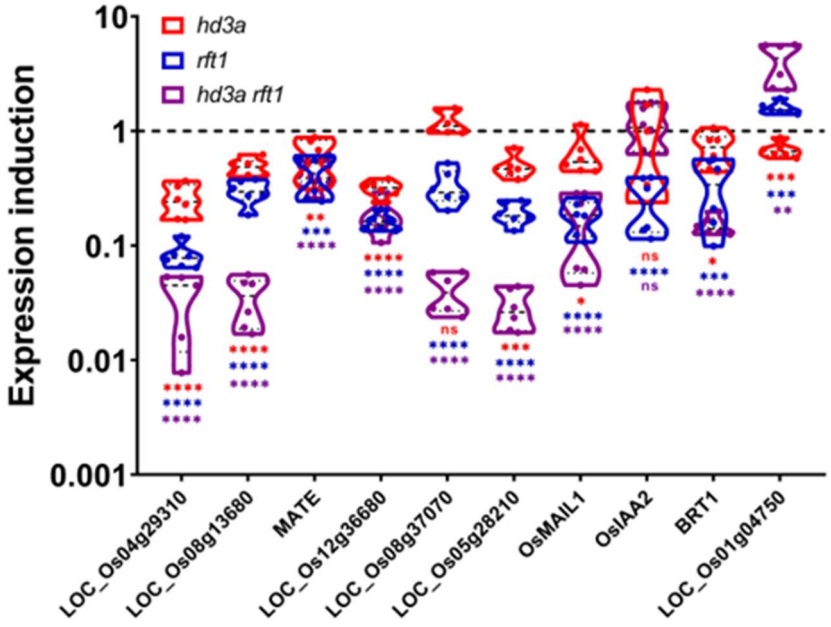

Figure 22. ***Violin plots of the expression of the 10 genes at the commitment to flower****. Graphs represent the ratio of the expression of the ten genes under analysis in florigen CRISPR mutants (single and double) respect to the expression in the wild type, represented by the dotted black line. Dotted line inside the violins represent the average. Student's t test was conducted on mutant vs the respective wild type. * 0.05>p>0.01; ** 0.01>p>0.001; *** 0.001>p>0.0001; **** p<0.0001*

What we can deduct from this experiment is that the florigens are not only sufficient to induce the expression of ten novel genes, but are also necessary for *LOC_Os04g29310*, *LOC_Os08g13680*, *LOC_Os12g36680*, *LOC_Os08g37070*, *LOC_Os05g28210*, *OsMAIL1*, *BRT1* and *LOC_Os01g04750*. More in detail, it is evident

that *RFT1* plays a major role in the regulation, as in the *rft1* lines the impact on the expression level of the targets is stronger than in *hd3a* lines.

Furthermore, the fact that in the double mutants the expression is brought down to zero (or, for *LOC_Os01g04750,* stays constitutively higher) is a further proof of the fact that the florigens have an additive effect in activating the downstream targets.

3.8 Tissue localization of three florigen targets

Continuing with the study of the downstream target of the florigens, I checked the spatial expression of three selected genes with *in-situ* hybridization, in meristematic tissues induced to flower after exposure to SDs. Samples were taken at 0SDs, in the vegetative phase, and at 14SDs, at the secondary branches stage, and collected in FAA solution. The tissues were then dehydrated and cut into 7µm thick slices. Digoxygenin-labelled probes were designed to target *OsIAA2*, *OsMAIL1* and *MATE*. The results of the hybridization at 60°C and subsequent detection with anti-digoxygenin are shown in Fig. 23.

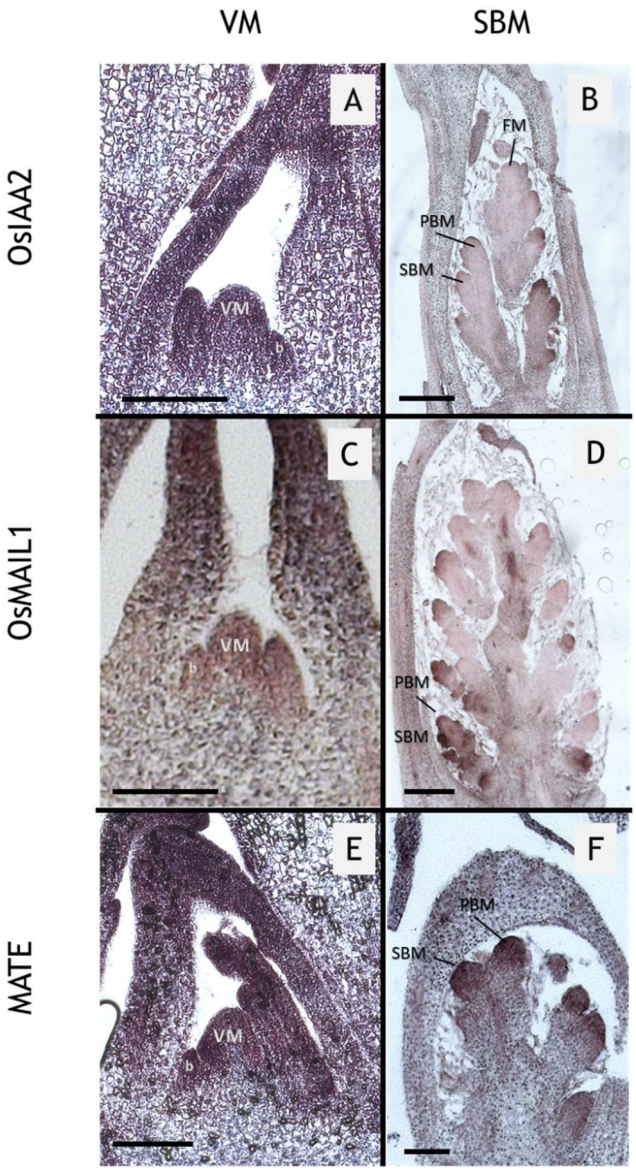

Figure 23. ***Tissue localization of three putative target genes of the florigens.*** *VM: vegetative meristem. PBM: primary branch meristem. SBM: secondary branches meristem. FM: floret meristem. Scale bar = 100µm*

OsIAA2

OsIAA2 is slightly expressed in the vegetative meristem and meristematic leaves (Fig. 23A), consistently with the qRT-PCR results. At the SB stage (Fig. 23B) the signal is localized at the tips of the primary and secondary branches primordia.

OsMAIL1

OsMAIL1-probe signal at the VM stage is almost negligible (Fig. 23C), while at the second developmental stage analyzed it becomes focused in the tips of the primordia of the primary and secondary branches, but also in the spikelet meristems SM (Fig. 23D). It is also interesting to notice that there is a gradient in the signal, because it is more intense at the bottom of the inflorescence on the first formed branches than in the upper, and newly formed, branches.

MATE

MATE is slightly expressed in the vegetative meristem and meristematic leaves (Fig. 23E), consistently with the qRT-PCR results. At the SB stage (Fig. 23F) the signal is localized in the primary and secondary branches primordia, although not in a specific district as it is for *OsIAA2*.

3.9 Characterization of *BRT1* and *OsMAIL1*

The last step in the analysis of the genes was a functional characterization. I chose two from the datasets to begin with, being *BRT1* and *OsMAIL1*. The reasons behind the choice are that i) they both belong to a known family, so there were already data available in scientific literature for both F-BOXs and the Plant Mobile Domain containing protein (to which *OsMAIL1* and its Arabidopsis homologues *MAIN*, *MAIL1*, *MAIL2* and *MAIL3* belong), and ii) the data from BAR, expression analysis and *in-situ* hybridization were encouraging. The functional characterization was carried out thanks to the CRISPR-Cas9 technology.

3.10 Editing of BRT1 – ΔC lines

The transformation vector, harboring the Cas9-encoding gene, and the gRNA targeting BRT1 was assembled according to (Miao *et al.*, 2013). A closeup of the genic region targeted by the Cas9-gRNA construct is shown in Fig. 24A. Technical restraints forced us to target a region far from the beginning of the coding sequence. The PAM recognized by this Cas9 (NGG) allowed the design of few efficient gRNAs, and none of those was in the first half of the gene. Thus, I decided to target a region close to the FBA in order to disrupt its protein-protein interaction domain, and *BRT1* function with it. After co-cultivating embryogenic rice calli together with *R. rhizobium*

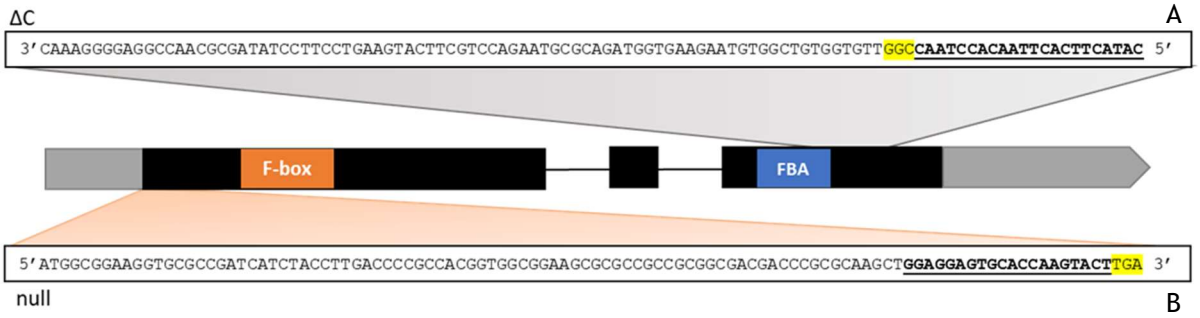

Figure 24. ***Gene structure of BRT1****. Black boxes represents exons, black lines introns and grey boxe the UTRs (3' UTR is arrow-shaped). The F-box domain is represented in orange, the FBA in blue. Gray and orange shaded area are closeups on the gene sequences, written above (A) for the ΔC lines, and below (B) for the null lines in the white box. The gRNAs of both editing events are underlined, PAM is highlighted in yellow.*

carrying the final vector, the calli were selected with two rounds of plating with increasing concentration of hygromycin, and the regenerated plants put into soil. DNA was extracted from the leaves of these T_0 plants, and the presence of the transgene was assessed. Among those which were positive, 13 were sequenced in *BRT1* to check the potential editing events. The alleles that were generated are recapitulated in Tab. 4. As expected, most of the mutations are indels (insertion/deletion) of 1bp, but I found also bigger deletions and a combined

Table 4. Alleles of brt1-ΔC plants

BRT1 ΔC alleles		Type of mutation
wt	TTGGCCAATC-CACAATTCACTTCATACTCCATTGA	
brt1-1	TTGGCCAATC**G**CACAATTCACTTCATACTCCATTGA	1 G insertion
brt1-2	TTGGCCAATC**T**CACAATTCACTTCATACTCCATTGA	1 T insertion
brt1-3	TTGGCCAATC**A**CACAATTCACTTCATACTCCATTGA	1 A insertion
brt1-4	TTGGCCAATC**C**CACAATTCACTTCATACTCCATTGA	1 C insertion
brt1-5	TTGGCCAATC--ACAATTCACTTCATACTCCATTGA	1 C deletion
brt1-6	TTGGCCAATC------TTCACTTCATACTCCATTGA	5 bp deletion
brt1-7	TTGGCCAATC--------CACTTCATACTCCATTGA	7 bp deletion
brt1-8	TTGGCC----------CACTTCATACTCCATTGA	11 bp deletion
brt1-9	TTGGCCAATC**G**-----TTCACTTCATACTCCATTGA	1 G insertion – 5 bp deletion

Table 5. Allelic status of T0 brt1-ΔC plants

Wild type	0
Biallelic	10
Homozygous	3
Heterozygous	0
Total plants	13
efficiency	100%

mutation (*brt1-9*). The allelic states of the plants are shown in Tab. 5. No wild type plants, nor heterozygous, were found, meaning that the editing was very efficient reaching the 100%. 10 plants were biallelic, and 3 homozygous already in the transformed generation. Plants were grown to the T_2, and the transgene segregated to avoid continued expression of Cas9 in the background.

3.11 *BRT1* is still expressed in *brt1*-ΔC lines

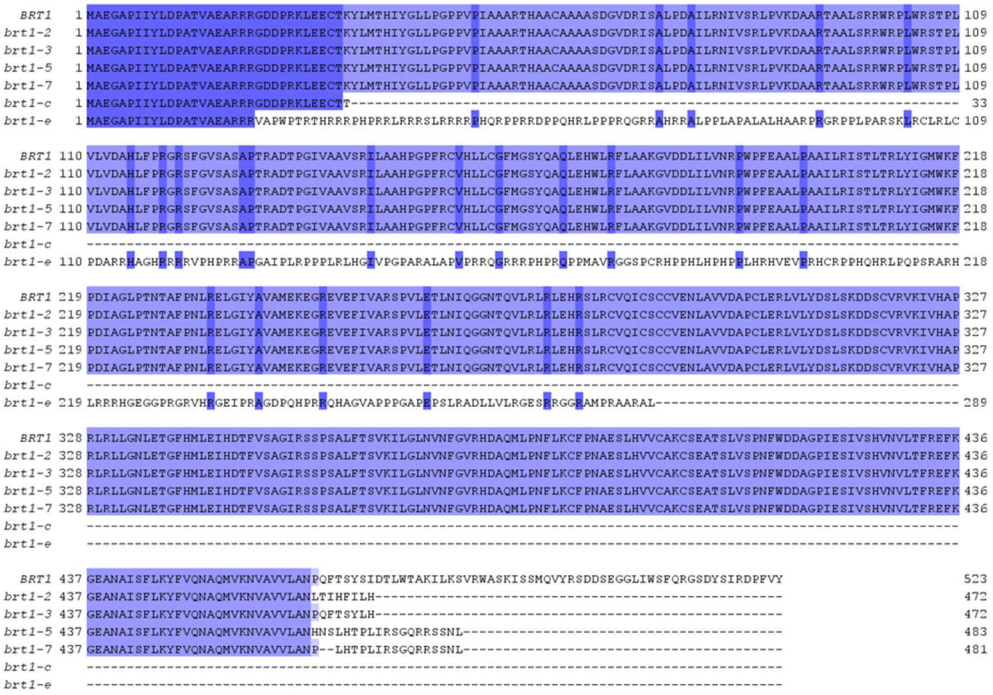

*Figure 25. **Aminoacidic sequences alignment of predicted protein products of BRT1-ΔC alleles**. Purple-highlighted residues are the conserved ones.*

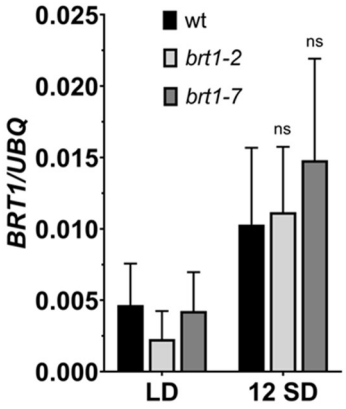

*Figure 26. **Expression of BRT1 in BRT1-ΔC lines**. Bars represent average values, error bars represent standard deviations. LD: long day. SD: short day. UBQ: ubiquitin*

To understand whether I created a knockout mutant or not, I checked the expression of *BRT1* in homozygous, Cas9-free plants, carrying the alleles *brt1-2* and *brt1-7*. Those were chosen since they encode for versions of BRT1 with different C-termini, also different from the wild type protein (Fig. 25). The time points chosen were at 0SDs (LD), and at 12SDs (Fig. 26). We can see in the graph that the transcript is still present in both mutant lines in an amount that is comparable to the wild type, hence we concluded that also the relative protein product

might be expressed. These products, though, lack the C-terminus that is substituted by few amino acids. The predicted aminoacidic sequences are shown in Fig. 25. For this reason, we called this set of mutants *brt1*-ΔC.

3.12 Phenotyping of *brt1*-ΔC

T_2 homozygous plants carrying different alleles were sown and grown to look for potential phenotypes, which were expected after the flowering induction given the way *BRT1* was discovered. Surprisingly, after one month of vegetative growth, the plants appeared as shown in Fig. 27. When the tillering phase started, the tillers of *brt1-5* and *brt1-7* opened more than the wild type, while the tillers of *brt1-2* had an angle similar to the *Nipponbare* control. The angle stayed constitutively wider for the entire life cycle of the plants. We decide to call this F-BOX-protein-encoding gene *Broad Tillering1* (*BRT1*).

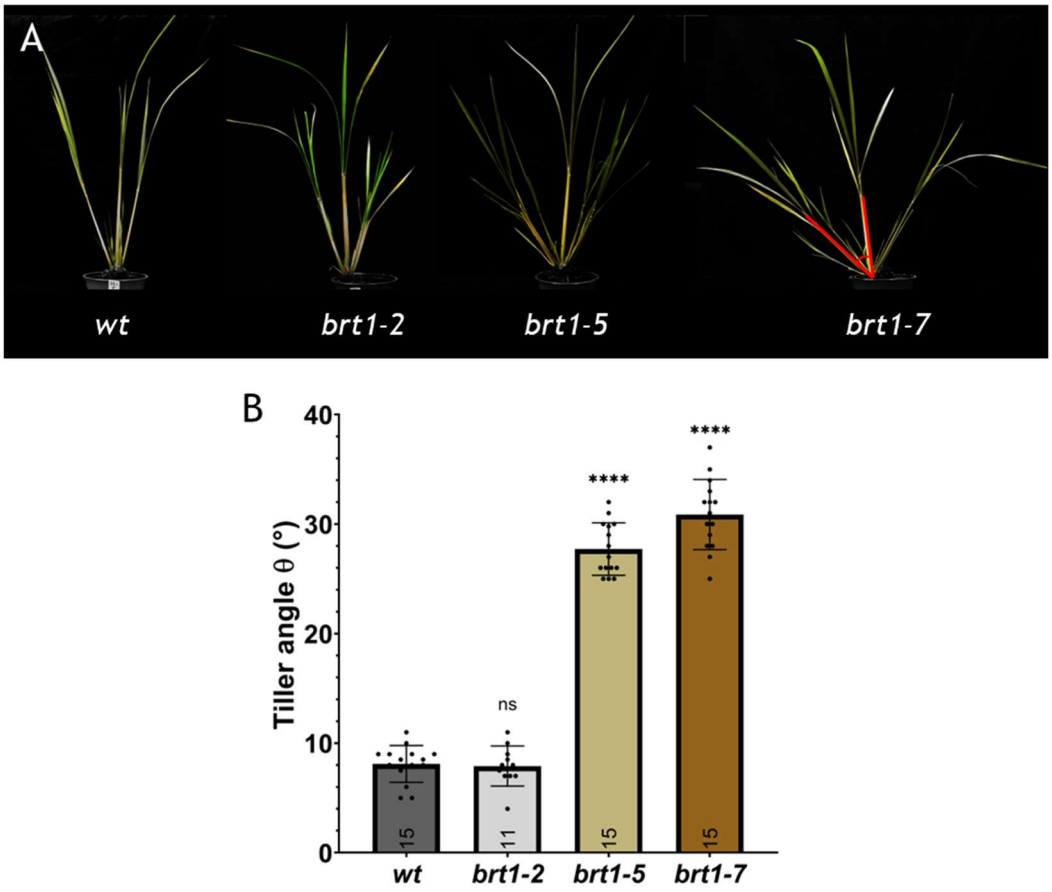

Figure 27. ***Phenotype of different BRT1-ΔC alleles****. A) Plants were 4 weeks old. The red angle on brt1-7 plant represents the way the angle was measured. B) measure of the angle of the same 4 weeks old plants. Bars represent average values, error bars represent standard deviations. Student's t test was performed on the values of the angles of the mutant alleles of BRT1 vs the angles of the wild type * 0.05>p>0.01; ** 0.01>p>0.001; *** 0.001>p>0.0001; **** p<0.0001*

3.13 Protein structure prediction with Alphafold

Being a novel gene, with no literature comprising it up to now, no crystallographic structure has been made available. Thanks to a new online tool, Alphafold (Jumper *et al.*, 2021), it was possible to predict the 3D structure of the wild type BRT1. The

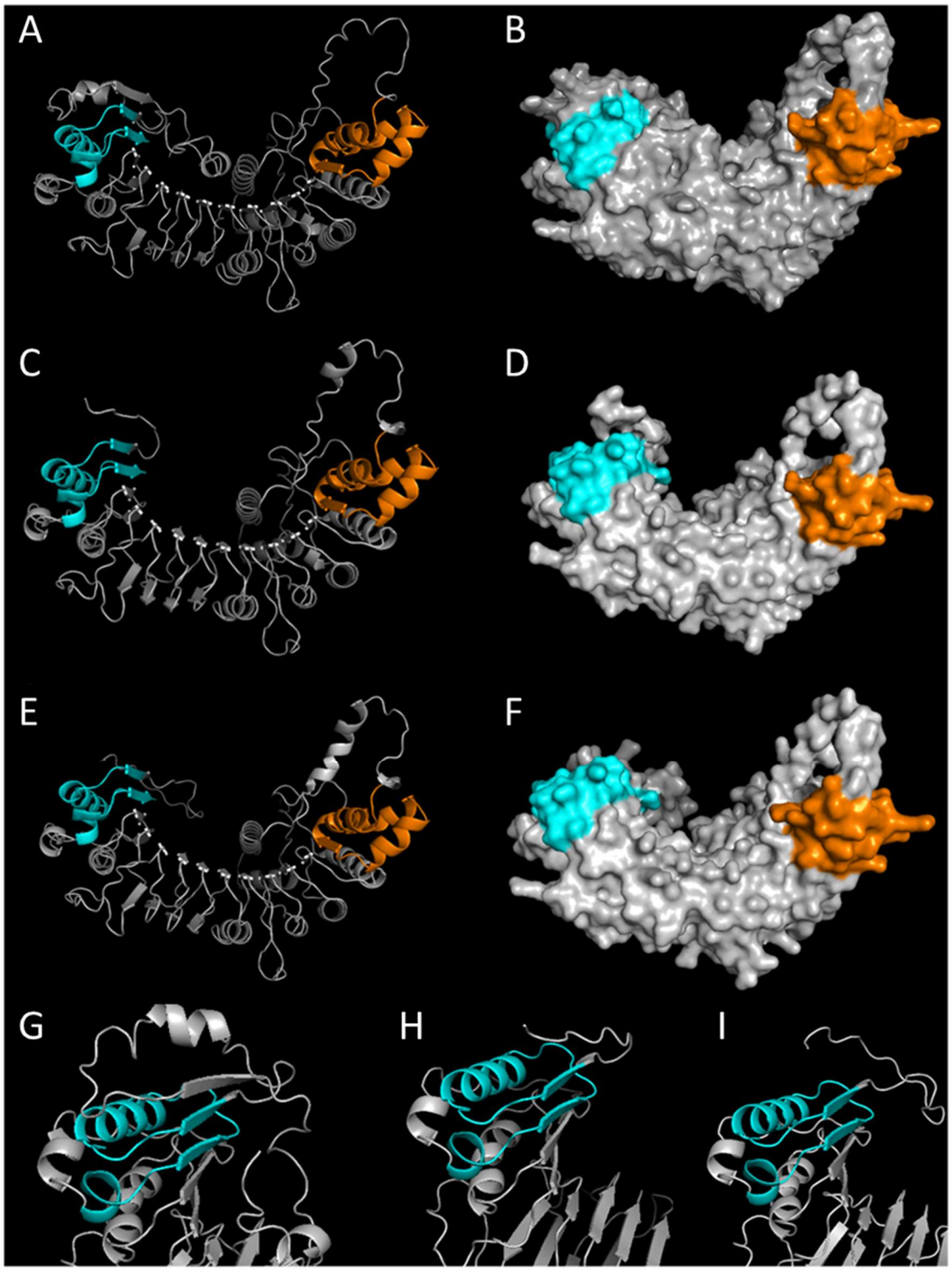

Figure 28. ***Prediction of brt1-ΔC protein products with Alphafold2.*** *On the left (A, C, E) ribbon view, on the right surface view (B, D, F). A, B, G) wild type BRT1, C, D, H) brt1-2, E, F, I) brt1-7. orange reprents the F-BOX domain, blue the FBA domain*

file was then visualized and rendered with PyMol Fig. 28A,B,G. The protein indeed resembles an F-BOX, with the characteristic "U" shape made of ß-strands and α-helices. I colored orange the F-BOX domain properly named, and in blue the FBA domain. I also folded and rendered the two mutants with a different behavior, brt1-2 (Fig. 28C, D, H) and brt-7 (Fig. 28E, F, I). We can see that an important portion of the C-terminus is missing from brt1-2, while in brt1-7, completely different residues form the C-terminus which is also smaller than the wild type. For example, there is a proline forcing the backbone to abruptly turn, and also two consecutives arginine and two serine residues, that could have become phosphorylation targets. We cannot draw any definitive conclusions with these data about the phenotype we observe, but it is evident that it must have to do with how the new protein product created by the CRISPR editing is composed and folded.

3.14 BRT1 has no effect on the plastochron

Given the unexpected phenotype, and its action on the vegetative growth of the plant, and its architecture, we wondered whether BRT1 could have an effect on the way, and the timing, leaves and tiller emerge. 24 plants homozygous for *brt1-7* were sown and grown in LDs for two months, and the number of leaves and tillers was counted every three days. Both the leaves and the tillers of the mutant line emerged at the same rate as the wild type (Fig. 29). We concluded that, despite being involved in the regulation of the tillering angle, *BRT1* does not modify the plastochron, nor in the phyllotaxis of the rice plants, since also the pattern of emergence is not impacted.

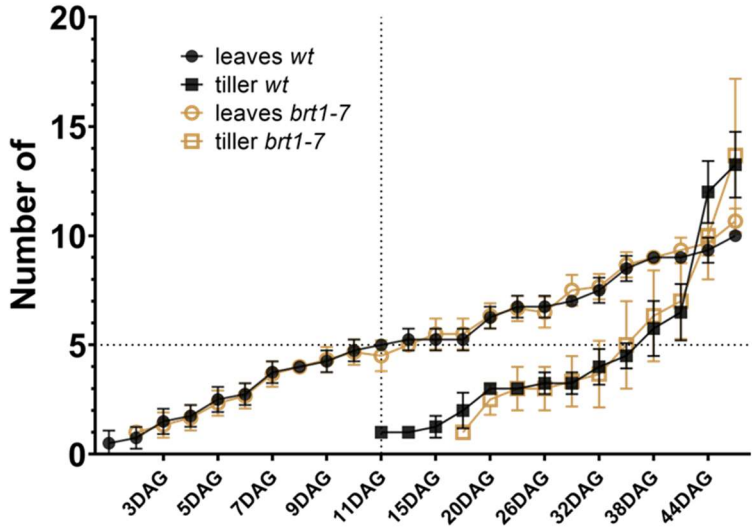

Figure 29. ***Plastochron of brt1-7 plants.*** *Dots represent average values, error bars standard deviations. Dotted line marks the fifth leaf at which tillers start to emerge. DAG: days after germination.*

3.15 Editing of *brt1*-null mutants

We followed a new strategy to confirm or confute the *brt1*-ΔC phenotype. To this end, we used a new Cas9 (Cas9-VQR) that became available for plants, following its development in the human field (Hu *et al.*, 2018). This new endonuclease recognizes a different PAM, NGA, and this allowed me to design another gRNA as seen in Fig. 24B, this time close to the start codon and with the potential to knock the *BRT1* out. The transformation was carried out as previously described, and after genotyping the plants, the alleles shown in Tab. 6 were obtained. These lines were called *brt1-null* since the Cas9 cuts towards the 5' end abolishing the transcript presence.

Table 6. BRT1 CRISPR alleles – null lines

BRT1 null alleles		
wt	CGCAAGCTGGAGGAGTGCACCAAGTACTTGATGAC	
brt1-a	CGCAAGCTGGAGGAGTGCACCAAG-ACTTGATGAC	1 bp deletion
brt1-b IN FRAME	CGCAAGCTGGAGGAGTGCACCA---ACTTGATGAC	3 bp deletion
brt1-c	CGCAAGCTGGAGGAGTGCACCA----CTTGATGAC	4 bp deletion
brt1-d	CGCAAGCTGGAGGAGTGCAC----TACTTGATGAC	4 bp deletion
brt1-e	CGCCGC**(-60)A**GGGTTGCTCCCTGG	1 A insertion – 60 bp deletion

3.16 BRT1 links the photoperiod and the tiller angle control in SD

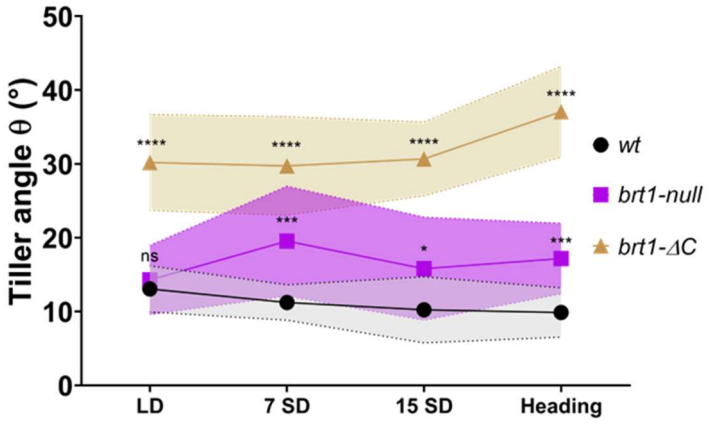

Figure 30. ***Tiller angle along the flowering transition of brt1-ΔC and brt1-null plants.*** *Tiller angle was measured as the angle between the main culm and the most spread of its tillers. Dots represent average values, shaded area the standard deviation. LD: long day; SD: short days. Student's t test was conduced for the value of the mutant vs the value at the same time point of the wild type. * 0.05>p>0.01; ** 0.01>p>0.001; *** 0.001>p>0.0001; **** p<0.0001*

Homozygous plants for two independent alleles, *brt1-c* and *brt1-e*, were grown in LDs for 8 weeks and then shifted to SDs to induce flowering. At first, no obvious phenotype was detectable in the vegetative growth. As said in the introduction, plants tend to straighten up during flowering, and the tiller angle becomes narrower (Yu *et al.*, 2007b). *brt1-null* plants, though, maintained a wider tiller angle during all stages of reproductive growth (Fig. 30). The time points at which the tiller angle was measured were at 0 SDs (LD), at 7 and

15SDs and at the heading date, which occurred at 30SDs on average for both the mutants and the control; the angle was measured using ImageJ.

3.17 *brt1-null* also alters panicle development

To predict possible phenotypes in *brt1* plants I used another online repository, RiceXPro (https://ricexpro.dna.affrc.go.jp/), a collection of gene expression profiles obtained from microarray analysis of tissues and organs covering the entire growth of the rice plant in natural field conditions. Differently from BAR, it is more detailed in the analyzed tissues (Suppl. Fig. 1). We can see that, besides the inflorescence and ovary, *BRT1* is also expressed in the palea and lemma. I proceeded to look at all these organs in the *brt1-null* plants to check for potential aberrations.

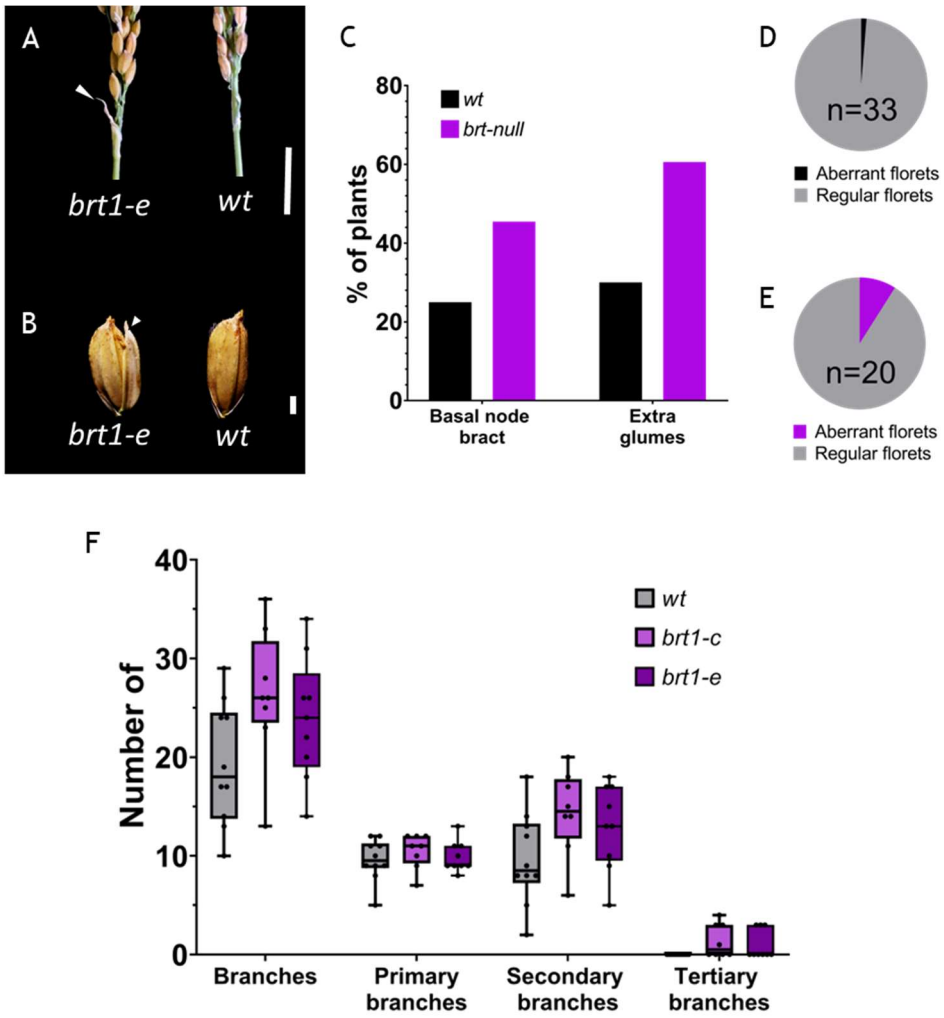

Figure 31. ***Additional phenotypes of brt1-null mutants.*** *A) Arrow indicates the basal node bract that is present in a higher percentage in the mutant population. Scale bar: 1cm. B) Arrow indicates the extra glumes on mutant spikelets. Scale bar: 1mm. C) Grpah reporting the rate of occurrence of the basal node bracts and the extra glumes. Pie charts of the percentage of aberrant florets in wild type plants (D) and brt1-null mutants (E). F) Box plot of the number of total, primary, secondary and tertiary branches.*

The findings are summed up in Fig. 31. The mutant panicles had a bract at their basal node (Fig. 31A) much more frequently than the wild type (45% vs 25%, Fig. 31C). Besides, florets from the *brt1-null* plants presented the development of a rudimentary glume into a full one (Fig. 31B); this time, the aberration occurred twice as much in the mutants than in the wild type (60% vs 30% Fig. 31C). More in detail, I counted how many florets had this extra glume only on the panicles that had at least one and discovered that only 1% of the wild type florets per panicle had an extra glume (Fig. 31D), while 9% of the mutant florets had it (Fig. 31E). Lastly, I counted the number of branches divided by type (Fig. 31F), and also the number of spikelets per panicle and the percentage of sterility (data not shown), but none of these traits was affected. This finding, together with the phenotype in the tiller angle, suggest that *BRT1* is active in suppressing traits that are typical of the vegetative phase, such as a wide tiller angle, and the development of leaf-like organs, such as bracts and glumes. Also, this might explain its upregulation when for the plant it is time to flower.

3.18 Editing of *OsMAIL1*

OsMAIL1 was edited following the protocol of Miao et al., 2013. As shown in the gene structure (Fig. 32) it was possible to design a gRNA targeting the start of the second exon granting, in case of successful editing, a knockout mutant. Transformation and selection were performed as described for *BRT1*. 176 T_0 plants were regenerated, and 137 tested for the presence of the transgene. All of them tested positive, for a transformation efficiency reaching 100%. 75 plants were then genotyped in *OsMAIL1* for editing events. The alleles shown in Table 7 were obtained. Again, most of the events were small indels. 33 plants were biallelic, 37 homozygous, 5 heterozygous and 0 wild type, for a total of only 5 copies of *OsMAIL1* that were not edited (Table 8). Sadly *osmail1-6* was lost in the following generations due to the death of the plant, so no in-frame alleles remained.

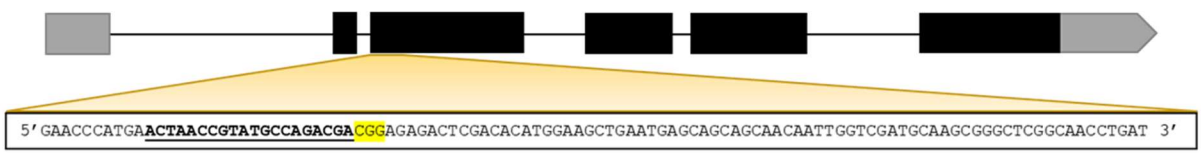

Figure 32. ***Gene structure of OsMAIL1.*** *Black boxes represents exons, black lines introns and grey boxe the UTRs (3' UTR is arrow-shaped). Yellow shaded area is a closeups on the gene sequences, written in the white box. The gRNA is underlined, PAM is highlighted in yellow.*

Table 7. OsMAIL1 CRISPR alleles

OsMAIL1 alleles		
wt	GAACCCATGAACTAACCGTATGCCAGA--CGACGGAG	
Osmail1-1	GAACCCATGAACTAACCGTATGCCAGA-**A**CGACGGAG	1 A insertion
Osmail1-2	GAACCCATGAACTAACCGTATGCCAGA-**T**CGACGGAG	1 T insertion
Osmail1-3	GAACCCATGAACTAACCGTATGCCAGA-**C**CGACGGAG	1 C insertion
Osmail1-4	GAACCCATGAACTAACCGTATGCCAGA-**G**CGACGGAG	1 G insertion
Osmail1-5	GAACCCATGAACTAACCGTATGCCAGA---GACGGAG	1 C deletion
Osmail1-6 IN FRAME	GAACCCATGAACTAACCGTATGCCAGA-----CGGAG	3 bp deletion
Osmail1-7	GAACCCATGAACTAACCGTATGCCAG**-GT**CGACGGAG	1 A deletion – 2 bp insertion

Table 8. Allelic status of mail1 T0 plants

Wild type	0
Biallelic	33
Homozygous	37
Heterozygous	5
Total plants	75
efficiency	[(75*2)-5]/(75*2) = **96.7%**

3.19 *OsMAIL1* is involved in shaping the female organs morphology

The phenotype was evaluated for T_1 plants that had segregated the transgene away and carrying homozygous *mail1-3*. Following the clear indication given by the expression pattern of *OsMAIL1* retrieved by BAR (Fig. 19), I looked into the florets for potential developmental problems. What I found were ovaries with three stigmas instead of the canonical two (Fig. 33A). This defect was not always present but affected, on average, 40% of the pistils of the five panicles I observed (Fig. 33B). The wild type, on the other hand, had pistils with two stigmas in the 100% of the florets. I concluded that *OsMAIL1* plays an important role in the development of the pistil, although its penetrance is not full, since 60% of the florets developed normally. Its DNA-protecting role may not be fulfilled properly in this tissue, leading to the development of an organ that would be otherwise suppressed.

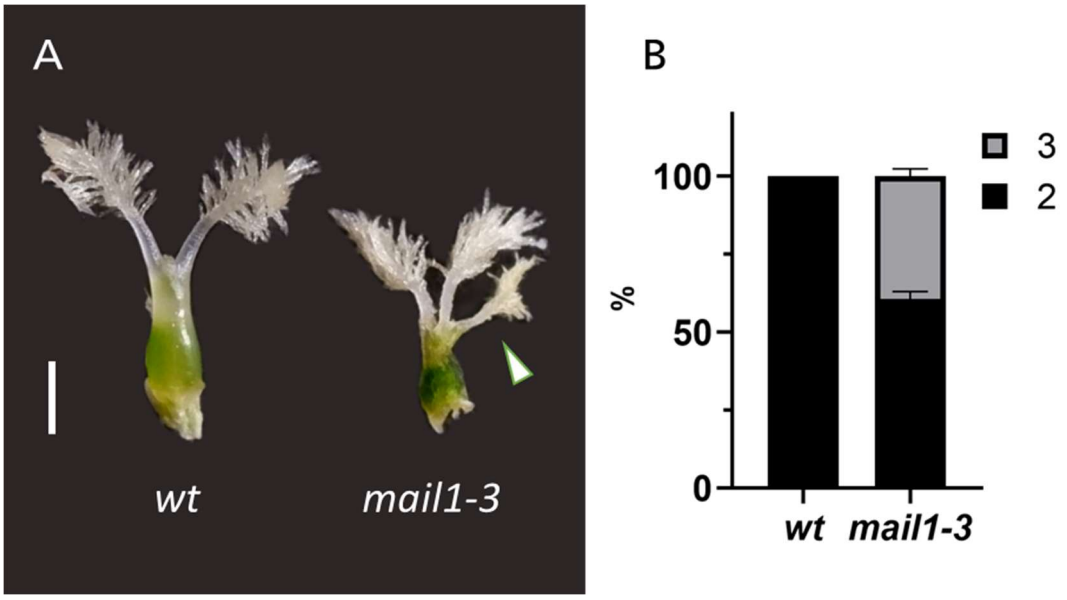

Figure 33. ***Phenotype of mail1.*** *A) The arrow points at the extranumerary stigma in the mail1 mutant. B) bar chart reporting the occurrence of three-stigma pistils in mail1 mutants*

3.20 *mail1-1* transcriptome analysis reveals that OsMAIL1 is upstream of carpel identity genes

We performed an RNA-seq experiment to check the change in transcriptome profiles in *mail1-1* mutants in key developmental stages of flowering, in order to isolate the gene(s) responsible for the phenotype I observed in the mutants. *mail1-1* and *wild type* inflorescences were collected from SD induced plants at 15SDs, a timepoint chosen because of the expression data from section 3.7, and 21SDs, a time point chosen based on phenotypic data to catch the moment in which the female organs are beginning to form. Three biological replicates per sample were used, although for the analysis one wild type 15SDs and one *mail1-1* 15SDs samples were discarded since they did not cluster together with the other two. Total RNA was extracted and sent to the sequencing facility: a non-stranded cDNA library was prepared and sequenced with NGS. The obtained reads were mapped on rice reference genome, and the transcriptomes of *mail1-1* mutants in the two time points were compared to those of the wild type to obtain the differentially expressed genes (DEGs, Fig. 35), that were divided in up- and down-regulated. What we observed is that there are many more DEGs in the 15SDs condition than in 21SDs, 1526 up and 834 down versus 189 up and 161 down respectively. Then, we looked for enrichment in Gene Ontology biological processes terms, and the results are shown in Fig. 36.

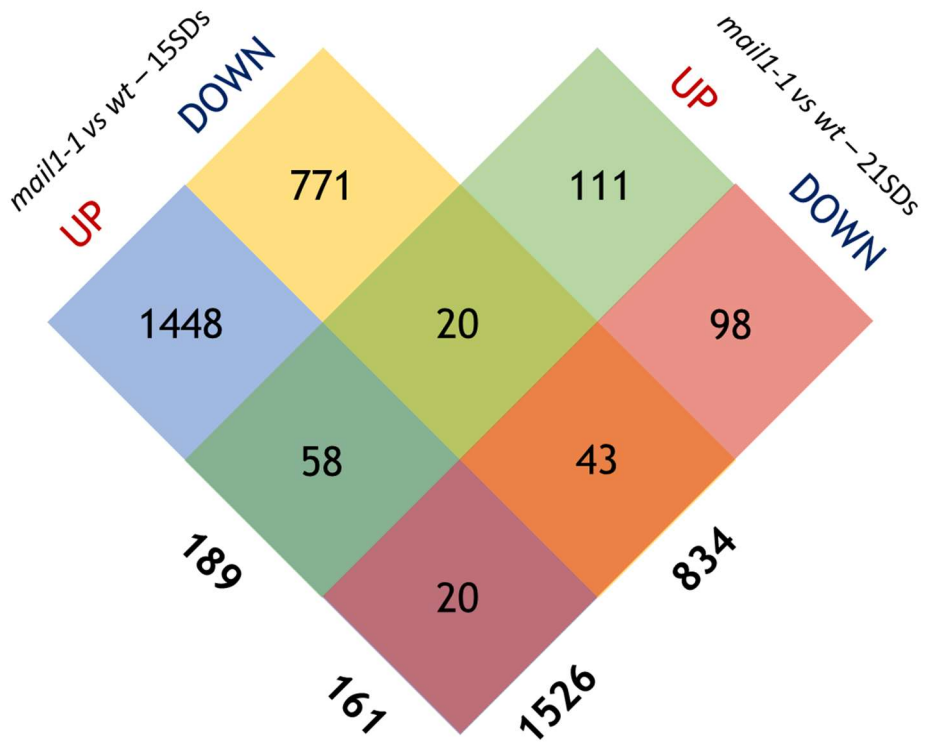

Figure 34. ***DEGs between mail1 and wild type****. Bolded numbers outside of the Venn diagram are the total DEGs*

In the GO-terms associated to the DEGs that are upregulated in the *mail1-1* mutants respect to the wild type (Fig. 36A) we see an enrichment in terms associated with stress response, such as drought and temperature, together with RNA metabolism terms. In the GO-terms associated to the DEGs that are downregulated in the *mail1-1* mutants respect to the wild type we see an enrichment in terms associated with floral development (Fig. 36B), but also pistil development and morphogenesis, and regulation of transcription. Lastly, it was not possible to look for GO-terms enrichment in the datasets of *mail1-1* vs *wild type* at 21SDs separately because the number of DEGs was too low, and we had to put together up- and down-regulated genes; the enriched terms are related to protein folding (Fig. 36C).

Taken together, the number of DEGs and GO-term enrichment suggest that the biggest transcriptional change, when *OsMAIL1* is knocked out, happens at 15 SDs, morphologically corresponding to the SBM developmental stage. This is in accordance with both the DEX RNA-seq data and the expression analysis with qRT-PCR, that saw an upregulation of *OsMAIL1* at this precise phase. Furthermore, the fact that the genes that are downregulated in *mail1-1* mutants at 15SDs are involved in carpel development fits with phenotypic data.

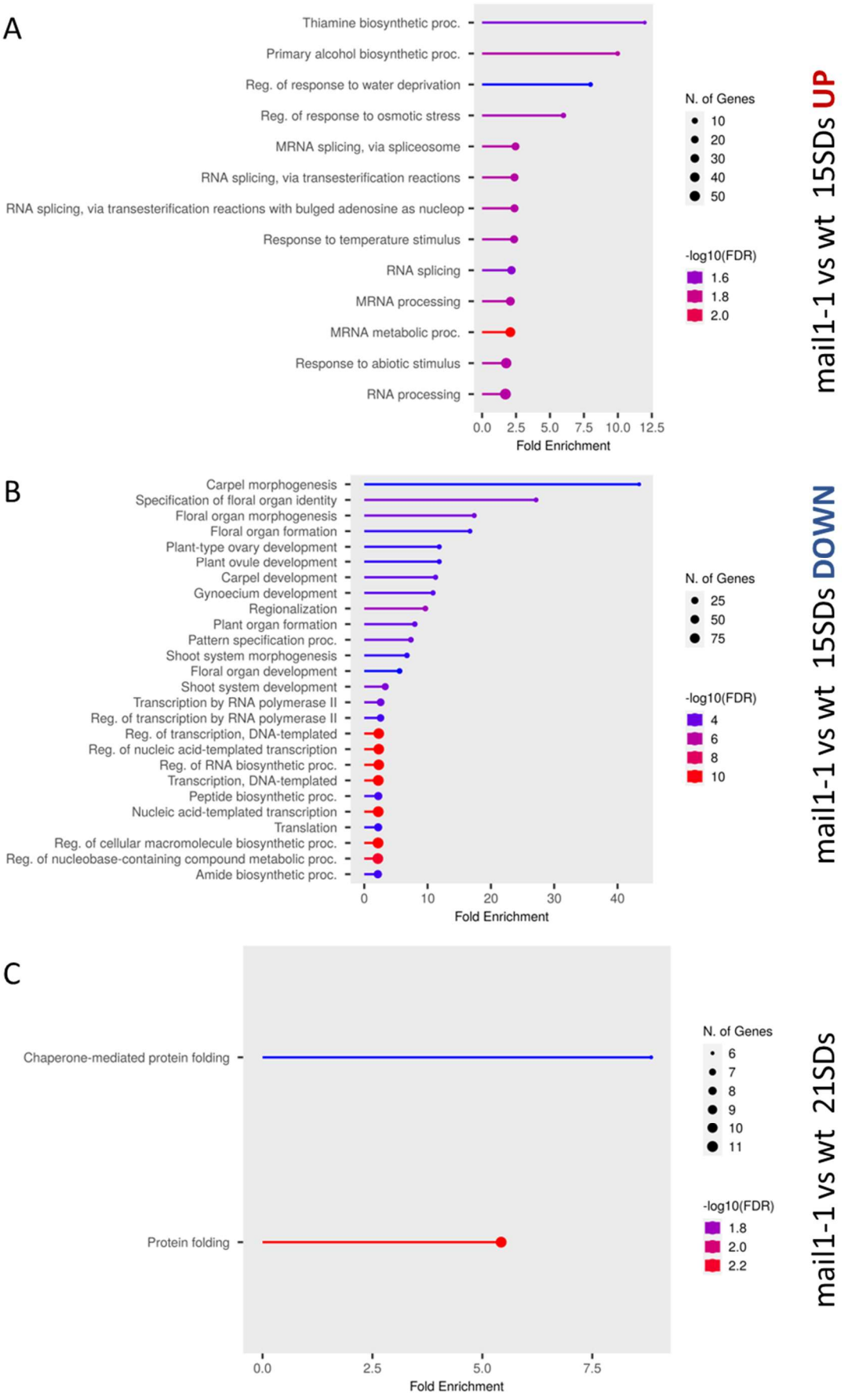

Figure 35. ***GO terms enrichment analysis on mail1 DEGs***

3.21 *BRT1* and *OsMAIL1* have no role in flowering time

Lastly, I checked if *BRT1* and *OsMAIL1* played a role in regulating flowering time, since they are targets of the florigens. Mutant plants were grown in LDs for 8 weeks, shifted to SDs and the heading date was recorded. From Fig. 36 we can deduce that these two genes do not influence flowering time, since mutants took the same time as the wild type to flower.

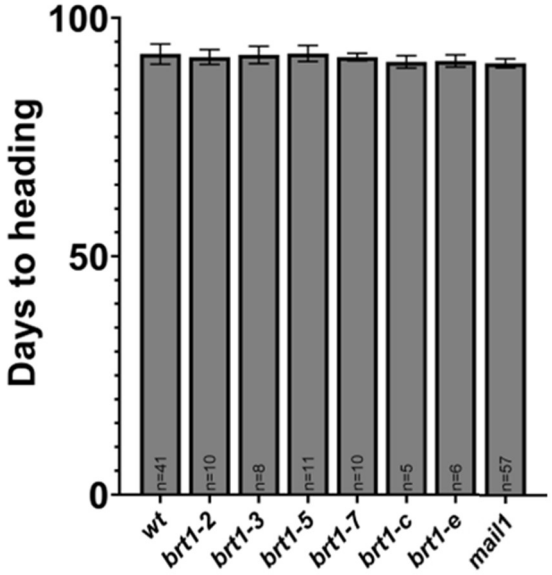

Figure 36. ***Flowering time of mutants in the putative florigen targets***

4. Conclusions and future perspectives

Rice plants rely on its florigens *Hd3a* and *RFT1* to flower at the right time of the year. They act as the final recipient of the photoperiodic signal in the leaves, and then carry that signal to the SAM in order to catalyse the switch to the reproductive phase. While their transcriptional regulation is well understood, and helps explaining the partial redundancy of their function, little is known about their activities once they enter the meristem. In this work, the major aim was to delve deeper into what happens downstream of the florigens when the flowering process begins, and also look more in detail at the contribution of each florigen to it. From three RNA-seq experiments on transgenic plants sprayed with DEX and selectively expressing Hd3a or RFT1, as well as wild type plants shifted to short days, it became clear that florigenic and photoperiodic inductions are not completely interchangeable in activating later developmental steps. The *Hd3a*-related pool seems to be way more restricted in terms of number of genes, but also the families to which the genes belong to are very different than in the other two conditions, while the *RFT1*-regulated genes are many more, and even more so the photoperiod-dependent genes. This is also suggested by the promoter analysis where the *Hd3a*-regulated genes have a very different profile of putative transcription factors that bind their promoter, compared to that of *RFT1* or SDs, which in turn are much more similar to one another. The florigens may be essential for flowering (Komiya *et al.*, 2008a), but the overall effect of the photoperiod is much more extensive.

An interesting aspect was that, besides the expected floral identity genes *OsMADS14*, *OsMADS15*, *OsMADS18* and *OsMADS34*, ten uncharacterized genes belonging to very different families were retrieved by the crossing of the DEGs in the three conditions. We found an F-BOX-containing protein, a B3/AP2 transcription factor, an auxin-responsive gene *OsIAA2*, a MATE gene involved in detoxification, a helicase-related gene, a LEA (Late embryogenesis abundant) gene, and MAIN-isoform like gene, and two other non-annotated genes. This indicates that the flowering effect of the florigens is only one facet of the global role they take on in the plant, as already demonstrated in the work of Tsuji *et al.* (2015) where Hd3a was found capable of assembling an alternative complex at the level of the axillary buds that promotes branching.

The subsequent analysis carried out in CRISPR mutant lines of the florigens, harbouring non-functional alleles of *Hd3a* and *RFT1* by qRT-PCR confirmed the observation on the ten novel genes made on the RNA-seq. The florigens are not only sufficient, but are also necessary to activate the transcription for the majority of them. Furthermore, this expression analysis has also shown that in *rft1* plants the impact on their expression is greater than in *hd3a* plants. Our observations indicates that *RFT1* is better at compensating for when *Hd3a* is missing than the other way around (an observation also made by (Komiya *et al.*, 2009). The differences between the florigens are deeper than expected in terms of types of target activation, but also in the strength of activation. Besides, the fact that in the double mutants *hd3a rft1* there is almost no change in the expression levels of the genes along the floral transition where it is supposed to increase (or decrease in the case of *LOC_Os01g04750*) is an indication that the florigens cooperate to reach an appropriate amount of transcript of their targets. Among these, the attention was focused, to start with, on two of them.

The first one is *OsFBX125,* an F-BOX containing protein that has been then renamed *Broader Tillering1* (*BRT1*). The *brt1-null* mutants, in which the coded protein is completely absent, are showing the persistence of vegetative traits in an advanced stage of reproductive development. We found a bract at the neck of the panicle, that usually gets suppressed early in development of the inflorescence (when the primary branches begin to form at the tip of the meristem, Wang *et al.*, 2021). We also observed the abnormal development of the sterile glumes, that are leaf structures like the panicle bract. The most prominent effect, though, was on the tillering angle. In wild type plants it reaches its widest point in the tillering phase, that occurs during the vegetative growth, for then slightly decreasing in the reproductive phase, while the panicle is growing in the culm (Wang *et al.*, 2022). In the mutant this did not happen, and the angle stayed wider till the panicle emerged from the boot, as if the signal to straighten up was not delivered or perceived. This could become the object of future studies to assess the origin of this behaviour, taking into account also the family to which the protein belongs to, the F-BOX family. F-BOX proteins are usually part of the SCF complex, a type of E3 ligase that ubiquitinates proteins that need to be degraded. The target of *BRT1* might be needed for the plant to mediate between the perception of the florigenic signal (and thus

the beginning of the flowering process), and tillering (when tillers need to become more erect). Alternatively, it could be a response factor that effectively reduces the tiller angle, for example by degrading an effector that, until then, was in charge of widening such angle. We can speculate that this happens through the auxin pathway, as auxin is the hormone responsible for the curvature of the shoots. Its asymmetrical distribution determines the direction of growth of tillers, but also leaves and roots. This could also explain the aberrant phenotypes we see in the panicle, because auxins are also related to growth of this types of tissues(Zhu *et al.*, 2022a). Bract and glumes are leaf-like organs, and it has been demonstrated that in grasses auxin transporters of the *PINOID* (*PIN*) family, are highly expressed in floral organ primordia, including lemmas (O'Connor *et al.*, 2014). Here, they regulate auxins influx and efflux in order to create a spatio-temporal gradient that directs organ development.

A recent work on *Unusual floral organ* (*UFO*, Rieu *et al.*, 2023), although, could suggest a different idea on how *BRT1* works. As an F-BOX protein, UFO was expected to act in an SCF complex with the task of degrading a target. Instead, it has been demonstrated to form a transcriptional complex together with LEAFY and an Skp-like protein: this complex activates B genes like *APETALA3*. This findings are also supported by an older paper (Chae *et al.*, 2008) that demonstrated that UFO is recruited at the *AP3* promoter in a LFY-dependent manner, although it was suspected to be part of the proteasome-mediated degradation of LFY itself, or some other transcriptional co-facotor. Instead, Rieu et al. shown that the F-BOX domain is superfluous in the context of DNA binding and *AP3* activation, as depleting it does not impact its LFY-binding capabilities. The depletion, though, still partially modify *UFO* activity, because minor defects in the flower of *35s::UFOΔFBOX* plants were detected, similar to those of *ufo* mutants, even though the penetrance was not as full. This suggests a dual role for *UFO*, a major one as a transcriptional co-regulator and a minor one as part of an SCF^{UFO} complex.

This dualism could also help explaining the *brt1-ΔC* mutant phenotypes, since from a truncated version of the protein we did not expect the phenotype to be this much stronger than in the knock-out mutants. An explanation in this sense could be that the truncation only impact one of the two functions of *BRT1* (the one involved in tillering angle control), while the other one would still be functional (the one

controlling bracts and glumes development). Another speculation regarding the behaviour of these mutants has to do with the nature itself of the F-Box protein. It possesses a protein-protein interaction motif, and the premature stop codon giving rise to the alternative C-terminus in *brt1-ΔC* could have led to a mistargeting or a sequestering, rather than a degradation, of the target, or also the formation of *BRT1* aggregates that could not carry on their function although being expressed.

Another characterized F-BOX in rice is *DWARF3* (*D3,* Ishikawa *et al.*, 2005). Interestingly, it has been shown to suppress tiller buds outgrowth, since *d3* plants produce more tillers than the wild types. It has been proposed to act as part of a strigolactones(SL)-dependent SCF complex that degrades a repressor of SL responsive genes, *D53*, allowing for the proper plant architecture to be achieved (Zhou *et al.*, 2013). We can hypothesize that a similar mechanism involves *BRT1,* but instead of being SL-dependent it could be auxin-dependent, since gravity perception and shoot curvature are related to auxins.

The other gene under examination was *OsMAIL1* (Oryza sativa MAIN-like 1), which has four homologues in *Arabidopsis thaliana: MAIN*, *MAIN-like1* (*MAIL1*), *MAIL2* and *MAIL3*. *MAIN*, *MAIL1* and *MAIL2* share a very similar structure with a Plant Mobile Domain (PMD), while *MAIL3* also possess a serine/threonine-specific protein phosphatase domain. AtMAIN is supposedly involved in meristem maintenance (hence the name) and genome stability : it acts by silencing potentially deleterious transposable elements. The meristems, both the shoot one and root one, of *main* mutant plants are disorganized; besides the stem of the plants is fasciated and the flowers as well (Wenig *et al.*, 2013). *mail1* mutants have an even severer phenotype, with shorter, non-gravity-responsive roots, smaller leaves with an impaired photosynthetic activity (Ühlken *et al.*, 2014). The effect was also epistatic with *main*. In rice plants mutated in *OsMAIL1,* we discovered that the pistil was altered in the number of stigmas, that are usually two but were three in these mutants. That meant that, directly or indirectly, the florigens control the female organ development as well. There must be other factors involved, since not all the flowers are aberrant, such as other PMD-containing proteins (a scan on UniProt gave 539 putative PMD proteins in rice). A thorough phenotyping must be performed in the

future also in organs different from the SAM and the panicle. Although the roots in *Os-mail1* plants looked similar to the wild type roots, there could be a disorganization at a cellular level. Also, the DNA damage in meristematic cells needs to be assessed, as it was done in *main* and *mail1 A. thaliana* plants. Wenig et al. observed that there was an accumulation of dead cells in the root apices of *main* plants, who were also more susceptible to DNA-damaging agents such as zeomycin respect to the control. To conclude on *OsMAIL1*, the RNA-seq we performed on knockout mutants confirmed that 15SDs, that is secondary branches meristem (SBM) stage, is a crucial time point for it to act on inflorescence development. This is supported by the high number of genes that are differentially expressed in this timepoint, 2360, versus the 350 DEGs at 21SDs. Not only that, but the Gene Ontology terms analysis has shown that there is an enrichment in terms related to carpel morphogenesis in the downregulated DEGs, in a perfect accordance with phenotypic data. We can postulate that *OsMAIL1* is an activator of carpel identity genes but is not directly involved in its development, because this process happens days after the peak in *OsMAIL1* expression.

From the study of *BRT1* and *OsMAIL1,* what appears evident is that the florigens in rice, as already seen previously and also in other crops such as tomato and poplar, have a role beyond flowering, being also responsible for shaping plant architecture, directing floral organ development.

5. Materials and methods

5.1 Plant growth conditions and DEX treatments

The cultivar used for all the experiments is Nipponbare. Plants were grown in a greenhouse with 16 hours light/8 hours dark, 28°C during the day and 24°C during the night, for 8 weeks (LD). Short day induction was obtained shifting the plants to 10 hours light/14 hours dark, 28°C during the day and 24°C during the night. Transgenic plants were sprayed on the leaves with a 10mM dexamethasone solution (+ 0.2% Tween) or mock treated. Construction and validation of *GVG:Hd3a* and *GVG:RFT1* transgenic plants is described in Brambilla et al., 2017. the variability of transgene induction in leaves in the selected *GVG:Hd3a* and *GVG:RFT1* lines required pretesting to assess the optimal spraying length: a comparable induction of Hd3a and RFT1 was achieved by spraying *GVG:Hd3a* leaves for 5 consecutive days and *GVG:RFT1* leaves for 2 consecutive days; DEX was applied at ZT10, and the sampling was made at ZT0 of the subsequent day.

5.2 RNA extraction and RNA-seq (DEX)

The RNA-seq analyses were performed with biological triplicates, with the exception of Hd3a DEX/mock: one DEX sample and one mock sample were discarded because PCA indicated that they did not cluster together with the respective replicates. Three pools of 4-5 SAM manually dissected with a scalpel under a stereomicroscope were sampled. RNA was extracted using NucleoZOL (Macherey-Nagel) and genomic DNA eliminated using DNase I (Turbo™ DNAse, Invitrogen). A stranded cDNA library was prepared and sequenced with 150 bp paired-end reads (about 35M pairs of reads per sample were obtained) with Illumina HiSeq2500 at IGA, Udine, Italy. Exploratory analyses based on dimensionality reduction of gene expression profiles (MDS-plot) were performed to assess the overall consistency of biological replicates. Reads were aligned to the MSU reference of the Os-Nipponbare-Reference-IRGSP-1.0 genome as available from http://rice.uga.edu/, by means of the bowtie2 software; gene expression levels were estimated by RSEM. Differential analyses of gene expression were executed by means of the edge R; the Genewise Negative Binomial Generalized (glmQLFTest) was applied to test for statistically significant differences. P-values were corrected using the Benjamini Hochberg procedure for the control of the False Discovery Rate. Only genes showing a p-value <= 0.05 following the FDR adjustment

were considered to be differentially expressed (DEGs). Venn Diagrams were made with the online tool of the Bioinformatics and Evolutionary Genomics platform. All genes except three (LOC_Os01g59410, LOC_Os07g41410 and LOC_Os09g09040) and two (LOC_Os05g09500, LOC_Os06g36560) in the intersection between and *GVG:RFT1* or *GVG:Hd3a* respectively and SD in Fig. 14 were differentially expressed in the same direction; these five genes were assigned in the Venn diagram to the change in direction observed under SD.

5.3 qRT-PCR

RNA extracted for qRT-PCR analyses was retrotranscribed with ImProm-II™ Reverse Transcriptase (Promega). 1 µg of total RNA was used as a template. Ubiquitin expression levels were used for normalization. For each sample, three biological replicates were used. We used Maxima SYBR Green qPCR Master Mix (Thermofisher) in a RealPlex2 thermocycler (Eppendorf). All primers are listed in Suppl. Table 1.

5.4 Florigen structures

Hd3a 3D structure was retrieved on PDB (accession 3AXY), while RFT1 was modeled on Hd3a structure using Swiss model by Expasy (SWISS-MODEL (expasy.org)). Models were visualized and rendered with PyMOL.

5.5 Spatio-temporal expression data and Promoter analysis

Affymetrix microarray expression profiles were retrieved from BAR (http://bar.utoronto.ca/). Promoters were defined as regions spanning 1100 bp (from –1000 upstream to +100 bp downstream) from the transcription start site (TSS) of the MSU rice gene models; those of DEGs were analyzed by Pscan to identify over-represented position frequency matrices (PFMs), that summarize occurrences of each nucleotide at each position in a set of observed transcription factor-DNA interactions. PFMs were obtained from the non-redundant core collection of plants PFMs as available from the 2020 release of the Jaspar database (https://jaspar.genereg.net/). Only PFMs pscan pValue <0.01 were considered significantly enriched.

5.6 In situ hybridizations

Wild type *Nipponbare* meristems were collected in FAA solution (5:5:50:40 formaldehyde, glacial acetic acid, 96% ethanol, water) choosing based on the morphology in order to obtain the desired developmental stages (vegetative meristem, VM and secondary branches meristem SBM); samples were then dehydrated with increasing concentrations of t-butyl-alcohol, and lastly embedded in Paraplast. Paraffinx blocks containing the meristems were cut in longitudinal sections with a thickness of 7µm and put on slides. Non-hydrolyzed probes (between 150 and 200 bp) were synthesized from PCR products (see primers in Suppl. Tab. S1) using DIG-RNA labelling kit (Roche). Samples were freed from paraffin with Hystolemon and rehydrated with alcohol/water solutions with decreasing alcohol concentrations. Hybridization was performed at 60°C overnight. Excess probe was washed away with 4x and 0.5x SSC solutions. Detection was performed with Roche's BCIP and NBT solutions at 30°C for 2 hours, and then washed away. The protocol is described in Toriba et al. (2019).

5.7 Rice transformation and CRISPR mutant generation

Constructs used for CRISPR were described in Miao et al., 2013 (Hd3a, RFT1, BRT1-ΔC and OsMAIL1) and Hu et al., 2016 (BRT1-null). Guide RNAs (Suppl. Tab. S1) were designed using CRISPR-P v2.0, (hzau.edu.cn) in the genes positions as described in Figs. . BRT1-ΔC and OsMAIL1 specific were cloned in pOs-sgRNA and then in pH-Ubi-cas9-7 using LR recombinase (Invitrogen). BRT1-null gRNA was cloned in SKm-gRNA and then in pC1300-UBI:VQR. *R. radiobacter* containing the final constructs was grown to OD=0.5 and co-cultivated with embryogenic calli for 4 days. Excess R. radiobacter was removed with a solution of 250mg/L cefotaxime, and calli were put on two rounds of selective medium, containing 50mg/L and 100mg/L hygromycin respectively. Surviving calli were put on regeneration media and, once shoot and root developed, on rooting medium. After two weeks, plantlets were put into soil in growth chambers. Phenotypic analyses were performed on homozygous, transgene-free T2 plants.

5.8 Protein products prediction

Putative 3D protein products of CRISPR alleles of *brt1*-ΔC were predicted with an opensource version of Alphafold, available on the Python environment Google Colab

(colab.research.google.com/github/deepmind/alphafold/blob/main/notebooks/AlphaFold.ipynb?pli=1).

5.9 Tiller angle measurements

Plants were grown for eight weeks under LD and then shifted to SD. Tiller angles were measured on pictures taken so that the main culm and the widest tiller lie on a plane parallel to the camera, in order to avoid parallax error in the angle measurement. Images were analyzed with ImageJ as described by the angle between the main culm and the widest culm deriving from its axillary meristems.

5.10 Flowering time

Flowering time was recorded as the day at which the first panicle spikelet emerges from the boot.

5.11 RNA-seq *mail1*

Plants were grown in a greenhouse with 16 hours light/8 hours dark, 28°C during the day and 24°C during the night, for 8 weeks (LD). Short day induction was obtained shifting the plants to 10 hours light/14 hours dark, 28°C during the day and 24°C during the night. Shoot apices were manually sampled at 15SDs and 21SDs with a scalpel. Three biological replicates for each genotype and time points were collected (5 meristems for 15SDs and 3 young inflorescences for 21SDs). RNA was extracted with RNeasy© Plant Mini kit (QIAGEN). Genomic DNA was removed using DNase I (Turbo™ DNAse, Invitrogen). Non-stranded cDNA library was prepared and sequenced with Illumina NovaSeq 6000. Reads were paired-end, 150bp long. Reads were trimmed with Fastq mcf, mapped with STAR (Dobin *et al.*, 2013) on MSU reference of the Os-Nipponbare-Reference-IRGSP-1.0 genome (as available from http://rice.uga.edu) and counted with htseq (Putri *et al.*, 2022). Differential expression analysis was done with DESeq2 on R (Love *et al.*, 2014): only genes with $p < 0.05$ were considered as statistically different.

Figures sources

Figure 1. A) Open source. B,C)(Yoshida & Nagato, 2011)

Figure 2. Part of the image collection of the International Rice Research Institute (IRRI).

Figure 3. (Hoshikawa, 1989)

Figure 4. (Karlgren *et al.*, 2011)

Figure 5. A;B) (Tamaki *et al.*, 2007b; Komiya *et al.*, 2008a)

Figure 6. A-G) Adapted from **(**Tamaki *et al.* 2015)**.** H,I) Adapted from (Komiya *et al.*, 2009)

Figure 7. A,B) (Komiya *et al.*, 2009). C) (Komiya *et al.*, 2008a)

Figure 8. Adapted from (Nakamura *et al.*, 2019a)

Figure 9. Adapted from (Nuñez & Yamada, 2017)

Figure 10. A; B) (Yu *et al.*, 2007b; Wang *et al.*, 2022)

Figure 11. (Price & Abu Kwaik, 2010)

Figure 12. (Xu *et al.*, 2009)

Supplementary informations

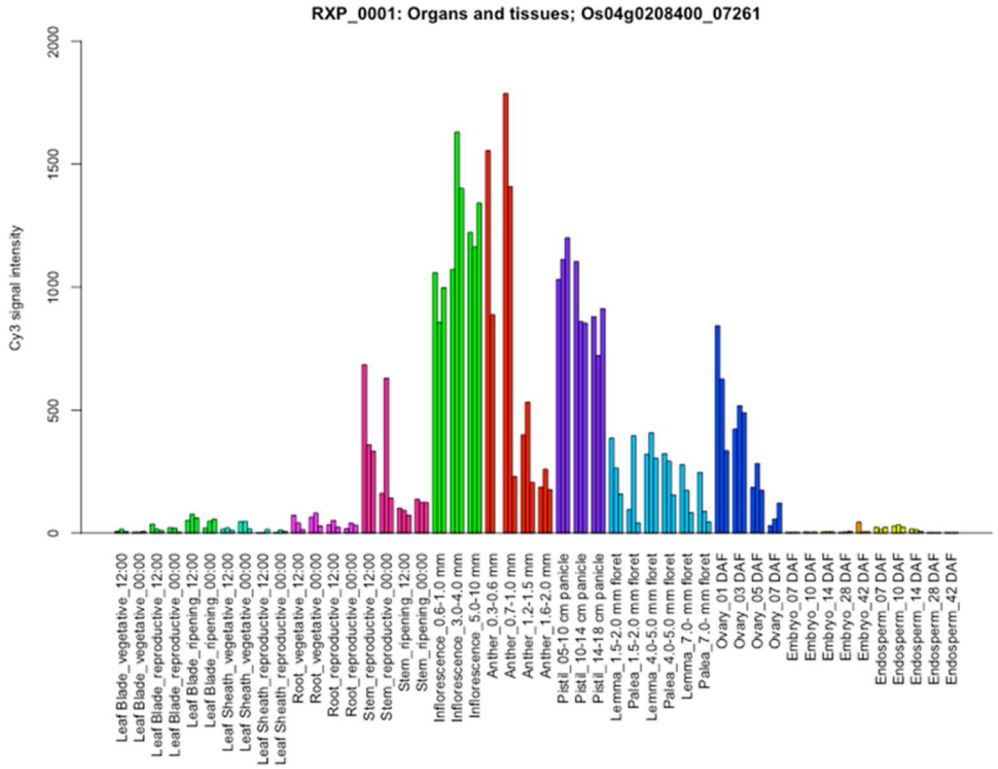

Figure S1. Spatio temporal expression of BRT1 during growth in the field. RiceXPro

Table S1. Primer list. FW: forward. RV: reverse. ISH: in situ hybridization

Gene	5'-3' sequence	primer name
BRT1	GCATTGTTCACGAGCGTCAA	qRT-PCR primer FW BRT1 (OsFBX125) LOC_Os04g13150
BRT1	GAGGAAGTTGGGCAGCATCT	qRT-PCR primer RV BRT1 (OsFBX125) LOC_Os04g13150
LOC_Os01g04750	GAACAGCTTGACGACGACAC	qRT-PCR primer FW LOC_Os01g04750
LOC_Os01g04750	AAGCACCTCCTCATCGACTG	qRT-PCR primer FW LOC_Os01g04750
OsIAA	CCTCCTAGCCGCTCAGAG	qRT-PCR primer FW OsIAA2 LOC_Os01g09450
OsIAA2	ATGAACATCTGCCAGGGAAC	qRT-PCR primer RV OsIAA2 LOC_Os01g09450
LOC_Os04g29310	AGATGGGTCTTGGTGGTACG	qRT-PCR primer FW retrotraspo LOC_Os04g29310
LOC_Os04g29310	CTCCACCTCCACAGCGATAT	qRT-PCR primer RV LOC_Os04g29310
LOC_Os08g13680	GGTGTCGCTTCTTTTGGTGT	qRT-PCR primer FW LOC_Os08g13680
LOC_Os08g13680	GAACCTGACAGCCTCCCTAG	qRT-PCR primer RV LOC_Os08g13680
MATE	TCAACCTCCGCTCCTTCTAC	qRT-PCR primer FW mate efflux LOC_Os04g48290
MATE	GAGGCCCCTGAAGTCCAAG	qRT-PCR primer RV LOC_Os04g48290
LOC_Os12g36680	GAACGGTGAAGAAAGGGCAG	qRT-PCR primer FW LOC_Os12g36680
LOC_Os12g36680	CTCATTCAGCTCACCGTTGG	qRT-PCR primer RV LOC_Os12g36680
LOC_Os05g28210	CTCGAGGCCCAGGAGAAC	qRT-PCR primer FW small seed protein LOC_Os05g28210
LOC_Os05g28210	CATCTCGCGGTACCCTTCC	qRT-PCR primer RV LOC_Os05g28210
OsMAIL1	CAGTTTGGGCAAGAACAGCA	qRT-PCR primer FW main-like LOC_Os07g32406
OsMAIL1	TACATCAGGCTCCAGTCCAC	qRT-PCR primer RV
LOC_Os08g37070	TCTTCTGCGTCGACTGATCA	qRT-PCR primer FW LOC_Os08g37070
LOC_Os08g37070	TGATCTTCCCCTTGTTGCCT	qRT-PCR primer RV LOC_Os08g37070
UBQ	GACAACGTGAAGGCGAAGA	qRT-PCR primer FW LOC_Os06g46770 UBQ
UBQ	CACCAGGTGGAGTGTGGAC	qRT-PCR primer RV Os06g46770 UBQ
Hd3a	CGATCTGCTGCATGCTCAC	qRT-PCR primer FW Hd3a
Hd3a	CCTTAGCCTTGCTCAGCTATTT	qRT-PCR primer RV Hd3a
RFT1	TGGGTTAGCTGACCTAGATTCAA	qRT-PCR primer FW RFT1
RFT1	GCCGGCCATGTCAAATTA	qRT-PCR primer RV RFT1
OsMADS15	CACGAGATCTCCGTCCTCTG	qRT-PCR primer FW OsMADS15
RFT1	**GGCA**AAGGTTAGTGATCCGGACGA	gRNA RFT1 forward + **restriction site**
RFT1	**AAAC**TCGTCCGGATCACTAACCTT	gRNA RFT1 reverse + **restriction site**
Hd3a	**GGCA**CGTCCGGAGCACCAACCTCA	gRNA Hd3a forward + **restriction site**
Hd3a	**AAAC**TGAGGTTGGTGCTCCGGACG	gRNA Hd3a reverse + **restriction site**
BRT1-dC	**GGCA**GTATGAAGTGAATTGTGGAT	gRNA BRT1 (FBX125) forward + **restriction site** (dC mutants)
BRT1-dC	**AAAC**ATCCACAATTCACTTCATAC	gRNA BRT1 (FBX125) reverse + **restriction site** (dC mutants)
BRT1-null	**GGCA**GGAGGAGTGCACCAAGTACT	gRNA BRT1 (FBX125) reverse + **restriction site** (null mutants)
BRT1-null	**AAAC**AGTACTTGGTGCACTCCTCC	gRNA BRT1 (FBX125) reverse + **restriction site** (null mutants)
OsMAIL1	**GGCA**ACTAACCGTATGCCAGACGA	gRNA OsMAIL1 forward + **restriction site**
OsMAIL1	**AAAC**TCGTCTGGCATACGGTTAGT	gRNA OsMAIL1 reverse + **restriction site**
OsMAIL1	TTGCTGAACCTTCCTTTGGC	OsMAIL1 primer FW for sequencing
OsMAIL1	TATGCCCTGGTGCCATACAT	OsMAIL1 primer RV for sequencing
BRT1-dC	GCATTGTTCACGAGCGTCAA	BRT1 dC primer FW for sequencing
BRT1-dC	AACCCTGTCCAGTCTTGAGC	BRT1 dC primer RV for sequencing
BRT1-null	GAAACCACCACTCACACGAC	BRT1 null primer FW for sequencing
BRT1-null	TGGTACGATCCCATGAAGCC	BRT1 null primer RV for sequencing
OsMAIL1	ACCCCATCGTGCTGTGAAT	FW ISH OsMAIL1 LOC_Os07g32406
OsMAIL1	**TAATACGACTCACTATAGG**GAGAAGTACCAGAGCTCTTCGACC	RV ISH OsMAIL1 LOC_Os07g32407 + **T7 promoter**
OsIAA2	GCAGGAAGAGGGCAGCAG	FW ISH OsIAA2 LOC_Os01g09450
OsIAA2	**TAATACGACTCACTATAGG**GCCCGATAATCCCTAGGTCC	RV ISH OsIAA2 LOC_Os01g09450 + **T7 promoter**
MATE-efflux	AGAGTGACGACAGAGTTGCC	FW ISH MATE-EFFLUX LOC_Os04g48290
MATE-efflux	**TAATACGACTCACTATAGG**CCCGCCGAAATTTGGAAAGA	RV ISH MATE EFFLUX LOC_Os04g48290 + **T7 promoter**

Bibliography

Abe M, Kobayashi Y, Yamamoto S, Daimon Y, Yamaguchi A, Ikeda Y, Ichinoki H, Notaguchi M, Goto K, Araki T. **2005**. FD, a bZIP protein mediating signals from the floral pathway integrator FT at the shoot apex. *Science* **309**: 1052–1056.

Abe K, Suge H. **1993**. Role of gravitropic response in the dry matter production of rice (Oryza sativa L.): An experiment with a line having lazy gene. *Journal of Plant Research* **106**: 337–343.

Abe K, TakAhashi H, Suge H. **1994**. Graviresponding sites in shoots of normal and'lazy'rice seedlings. *Physiologia Plantarum* **92**: 371–374.

Ahn JH, Miller D, Winter VJ, Banfield MJ, Jeong HL, So YY, Henz SR, Brady RL, Weigel D. **2006a**. A divergent external loop confers antagonistic activity on floral regulators FT and TFL1. *The EMBO Journal* **25**: 605–614.

Ahn JH, Miller D, Winter VJ, Banfield MJ, Lee JH, Yoo SY, Henz SR, Brady RL, Weigel D. **2006b**. A divergent external loop confers antagonistic activity on floral regulators FT and TFL1. *The EMBO Journal* **25**: 605–614.

Azeez A, Miskolczi P, Tylewicz S, Bhalerao RP. **2014**. A tree ortholog of APETALA1 mediates photoperiodic control of seasonal growth. *Current Biology* **24**: 717–724.

Bernier I, Jollés P. **1984**. Purification and characterization of a basic 23 kDa cytosolic protein from bovine brain. *Biochimica et Biophysica Acta (BBA) - Protein Structure and Molecular Enzymology* **790**: 174–181.

Bernier I, Tresca JP, Jollès P. **1986**. Ligand-binding studies with a 23 kDa protein purified from bovine brain cytosol. *Biochimica et Biophysica Acta (BBA) - Protein Structure and Molecular Enzymology* **871**: 19–23.

Böhlenius H, Huang T, Charbonnel-Campaa L, Brunner AM, Jansson S, Strauss SH, Nilsson O. **2006**. CO/FT regulatory module controls timing of flowering and seasonal growth cessation in trees. *Science* **312**: 1040–1043.

Bradley D, Carpenter R, Copsey L, Vincent C, Rothstein S, Coen E. **1996**. Control of inflorescence architecture in Antirrhinum. *Nature* **379**: 791–797.

Bradley D, Ratcliffe O, Vincent C, Carpenter R, Coen E. **1997**. Inflorescence commitment and architecture in Arabidopsis. *Science* **275**: 80–83.

Brambilla V, Martignago D, Goretti D, Cerise M, Somssich M, De Rosa M, Galbiati F, Shrestha R, Lazzaro F, Simon R, *et al.* 2017. Antagonistic transcription factor complexes modulate the floral transition in rice. *Plant Cell* **29**: 2801–2816.

Cerise M, Giaume F, Galli M, Khahani B, Lucas J, Podico F, Tavakol E, Parcy F, Gallavotti A, Brambilla V, *et al.* 2021. OsFD4 promotes the rice floral transition via florigen activation complex formation in the shoot apical meristem. *New Phytologist* **229**: 429–443.

Chae E, Tan QKG, Hill TA, Irish VF. **2008**. An Arabidopsis F-box protein acts as a transcriptional co-factor to regulate floral development. *Development* **135**: 1235–1245.

Chang B, Partha S, Hofmann K, Lei M, Goebl M, Harper JW, Elledge SJ. **1996**. SKP1 connects cell cycle regulators to the ubiquitin proteolysis machinery through a novel motif, the F-box. *Cell* **86**: 263–274.

Chen Q, Payyavula RS, Chen L, Zhang J, Zhang C, Turgeon R. **2018**. FLOWERING LOCUS T mRNA is synthesized in specialized companion cells in Arabidopsis and Maryland Mammoth tobacco leaf

veins. *Proceedings of the National Academy of Sciences of the United States of America* **115**: 2830–2835.

Chen R, Rosen E, Masson PH. **1999**. Gravitropism in Higher Plants. *Plant Physiology* **120**: 343–350.

Choi JY, Platts AE, Fuller DQ, Hsing YI, Wing RA, Purugganan MD, Kim Y. **2017**. The rice paradox: Multiple origins but single domestication in Asian Rice. *Molecular Biology and Evolution* **34**: 969–979.

Conti L, Bradley D. **2007**. TERMINAL FLOWER1 Is a Mobile Signal Controlling Arabidopsis Architecture. *The Plant Cell* **19**: 767–778.

Dobin A, Davis CA, Schlesinger F, Drenkow J, Zaleski C, Jha S, Batut P, Chaisson M, Gingeras TR. **2013**. STAR: ultrafast universal RNA-seq aligner. *Bioinformatics (Oxford, England)* **29**: 15–21.

Doi K, Izawa T, Fuse T, Yamanouchi U, Kubo T, Shimatani Z, Yano M, Yoshimura A. **2004**. Ehd1, a B-type response regulator in rice, confers short-day promotion of flowering and controls FT-like gene expression independently of Hd1. *Genes and Development* **18**: 926–936.

Dong J, Han L, Wang Y, Huang J, Wu J. **2017**. Transcript expression bias of phosphatidylethanolamine binding protein gene in bumblebee, Bombus lantschouensis (Hymenoptera: Apidae). *Gene* **627**: 290–297.

Dong H, Zhao H, Xie W, Han Z, Li G, Yao W, Bai X, Hu Y, Guo Z, Lu K, *et al.* 2016. A Novel Tiller Angle Gene, TAC3, together with TAC1 and D2 Largely Determine the Natural Variation of Tiller Angle in Rice Cultivars. *PLoS Genetics* **12**: e1006412.

Du A, Tian W, Wei M, Yan W, He H, Zhou D, Huang X, Li S, Ouyang X, A D, *et al.* 2017. The DTH8-Hd1 Module Mediates Day-Length-Dependent Regulation of Rice Flowering. **10**: 948–961.

Fornara F, Pařenicová L, Falasca G, Pelucchi N, Masiero S, Ciannamea S, Lopez-Dee Z, Altamura MM, Colombo L, Kater MM. **2004**. Functional Characterization of OsMADS18, a Member of the AP1/SQUA Subfamily of MADS Box Genes. *Plant Physiology* **135**: 2207–2219.

GARNER WW, ALLARD HA. **1920**. EFFECT OF THE RELATIVE LENGTH OF DAY AND NIGHT AND OTHER FACTORS OF THE ENVIRONMENT ON GROWTH AND REPRODUCTION IN PLANTS. *Monthly Weather Review* **48**: 415.

Geng F, Wenzel S, Tansey WP. **2012**. Ubiquitin and Proteasomes in Transcription. *https://doi.org/10.1146/annurev-biochem-052110-120012* **81**: 177–201.

Giaume F, Bono GA, Martignago D, Miao Y, Vicentini G, Toriba T, Wang R, Kong D, Cerise M, Chirivì D, *et al.* 2023. Two florigens and a florigen-like protein form a triple regulatory module at the shoot apical meristem to promote reproductive transitions in rice. *Nature Plants 2023*: 1–10.

Godbolé R, Takahashi H, Hertel R. **1999**. The Lazy Mutation in Rice Affects a Step between Statoliths and Gravity-Induced Lateral Auxin Transport. *Plant Biology* **1**: 379–381.

Gómez-Ariza J, Brambilla V, Vicentini G, Landini M, Cerise M, Carrera E, Shrestha R, Chiozzotto R, Galbiati F, Caporali E, *et al.* 2019. A transcription factor coordinating internode elongation and photoperiodic signals in rice. *Nature Plants* **5**: 358–362.

Gopi M, Arambakkam Janardhanam V. **2017**. Asiaticoside: Attenuation of rotenone induced oxidative burden in a rat model of hemiparkinsonism by maintaining the phosphoinositide-mediated synaptic integrity. *Pharmacology Biochemistry and Behavior* **155**: 1–15.

Gutaker RM, Groen SC, Bellis ES, Choi JY, Pires IS, Bocinsky RK, Slayton ER, Wilkins O, Castillo CC, Negrão S, *et al.* 2020. Genomic history and ecology of the geographic spread of rice. *Nature Plants* **6**: 492–502.

Gyllenstrand N, Clapham D, Källman T, Lagercrantz U. **2007**. A Norway Spruce FLOWERING LOCUS T Homolog Is Implicated in Control of Growth Rhythm in Conifers. *Plant Physiology* **144**: 248–257.

Hanzawa Y, Money T, Bradley D. **2005**. A single amino acid converts a repressor to an activator of flowering. *Proceedings of the National Academy of Sciences of the United States of America* **102**: 7748–7753.

Hedman H, Källman T, Lagercrantz U. **2009**. Early evolution of the MFT-like gene family in plants. *Plant Molecular Biology* **70**: 359–369.

Hershko A, Ciechanover A. **1998**. The ubiquitin system. *Annual review of biochemistry* **67**: 425–479.

Hershko A, Ciechanover A, Varshavsky A. **2000**. The ubiquitin system. *Nature Medicine 2000 6:10* **6**: 1073–1081.

Ho WWH, Weigel D. **2014**. Structural Features Determining Flower-Promoting Activity of Arabidopsis FLOWERING LOCUS T. *The Plant Cell* **26**: 552–564.

Hoshikawa K. **1989**. *The Growing Rice Plant: An Anatomical Monograph*. Nosan Gyosan Bunka Kyokai (Nobunko).

Hsu CY, Adams JP, Kim H, No K, Ma C, Strauss SH, Drnevich J, Vandervelde L, Ellis JD, Rice BM, *et al.* 2011. FLOWERING LOCUS T duplication coordinates reproductive and vegetative growth in perennial poplar. *Proceedings of the National Academy of Sciences of the United States of America* **108**: 10756–10761.

Hsu CY, Liu Y, Luthe DS, Yuceer C. **2006**. Poplar FT2 shortens the juvenile phase and promotes seasonal flowering. *Plant Cell* **18**: 1856–1861.

Hu X, Meng X, Liu Q, Li J, Wang K. **2018**. Increasing the efficiency of CRISPR-Cas9-VQR precise genome editing in rice. *Plant Biotechnology Journal* **16**: 292–297.

Huang X, Kurata N, Wei X, Wang ZX, Wang A, Zhao Q, Zhao Y, Liu K, Lu H, Li W, *et al.* 2012. A map of rice genome variation reveals the origin of cultivated rice. *Nature* **490**: 497–501.

Ikeda Y, Pélissier T, Bourguet P, Becker C, Pouch-Pélissier MN, Pogorelcnik R, Weingartner M, Weigel D, Deragon JM, Mathieu O. **2017**. Arabidopsis proteins with a transposon-related domain act in gene silencing. *Nature Communications* **8**: 1–10.

Imaizumi T, Schultz TF, Harmon FG, Ho LA, Kay SA. **2005**. Plant science: FKF1 F-box protein mediates cyclic degradation of a repressor of CONSTANS in Arabidopsis. *Science* **309**: 293–297.

Ishikawa R, Aoki M, Kurotani KI, Yokoi S, Shinomura T, Takano M, Shimamoto K. **2011**. Phytochrome B regulates Heading date 1 (Hd1)-mediated expression of rice florigen Hd3a and critical day length in rice. *Molecular genetics and genomics : MGG* **285**: 461–470.

Ishikawa S, Maekawa M, Arite T, Onishi K, Takamure I, Kyozuka J. **2005**. Suppression of Tiller Bud Activity in Tillering Dwarf Mutants of Rice. *Plant and Cell Physiology* **46**: 79–86.

Itoh H, Nonoue Y, Yano M, Izawa T. **2010**. A pair of floral regulators sets critical day length for Hd3a florigen expression in rice. *Nature Genetics* **42**: 635–638.

Izawa T, Oikawa T, Sugiyama N, Tanisaka T, Yano M, Shimamoto K. **2002**. Phytochrome mediates the external light signal to repress FT orthologs in photoperiodic flowering of rice. *Genes and Development* **16**: 2006–2020.

Jain M, Nijhawan A, Arora R, Agarwal P, Ray S, Sharma P, Kapoor S, Tyagi AK, Khurana JP. **2007**. F-Box proteins in rice. Genome-wide analysis, classification, temporal and spatial gene expression during panicle and seed development, and regulation by light and abiotic stress. *Plant Physiology*

143: 1467–1483.

Jeon JS, Lee S, Jung KH, Yang WS, Yi GH, Oh BG, An G. **2000**. Production of transgenic rice plants showing reduced heading date and plant height by ectopic expression of rice MADS-box genes. *Molecular Breeding* **6**: 581–592.

Jiang J, Tan L, Zhu Z, Fu Y, Liu F, Cai H, Sun C. **2012**. Molecular Evolution of the TAC1 Gene from Rice (Oryza sativa L.). *Journal of Genetics and Genomics* **39**: 551–560.

Jin J, Huang W, Gao JP, Yang J, Shi M, Zhu MZ, Luo D, Lin HX. **2008**. Genetic control of rice plant architecture under domestication. *Nature Genetics* **40**: 1365–1369.

Jones JW, Adair CR. **1938**. A 'lazy' mutation in rice. *Journal of Heredity* **29**: 315–318.

Jumper J, Evans R, Pritzel A, Green T, Figurnov M, Ronneberger O, Tunyasuvunakool K, Bates R, Žídek A, Potapenko A, *et al.* 2021. Highly accurate protein structure prediction with AlphaFold. *Nature* **596**: 583.

Kaneko-Suzuki M, Kurihara-Ishikawa R, Okushita-Terakawa C, Kojima C, Nagano-Fujiwara M, Ohki I, Tsuji H, Shimamoto K, Taoka K-I. **2018**. TFL1-Like Proteins in Rice Antagonize Rice FT-Like Protein in Inflorescence Development by Competition for Complex Formation with 14-3-3 and FD. *Plant and Cell Physiology* **59**: 458–468.

Kardailsky I, Shukla VK, Ahn JH, Dagenais N, Christensen SK, Nguyen JT, Chory J, Harrison MJ, Weigel D. **1999**. Activation tagging of the floral inducer FT. *Science* **286**: 1962–1965.

Karlgren A, Gyllenstrand N, Källman T, Sundström JF, Moore D, Lascoux M, Lagercrantz U. **2011**. Evolution of the PEBP gene family in plants: Functional diversification in seed plant evolution. *Plant Physiology* **156**: 1967–1977.

Kendrick RE, Spruit CJP. **1977**. PHOTOTRANSFORMATIONS OF PHYTOCHROME. *Photochemistry and Photobiology* **26**: 201–214.

Kobayashi Y, Kaya H, Goto K, Iwabuchi M, Araki T. **1999**. A pair of related genes with antagonistic roles in mediating flowering signals. *Science* **286**: 1960–1962.

Kobayashi K, Yasuno N, Sato Y, Yoda M, Yamazaki R, Kimizu M, Yoshida H, Nagamura Y, Kyozuka J. **2012**. Inflorescence meristem identity in rice is specified by overlapping functions of three AP1/FUL-like MADS box genes and PAP2, a SEPALLATA MADS box gene. *The Plant Cell* **24**: 1848–1859.

Kojima S, Takahashi Y, Kobayashi Y, Monna L, Sasaki T, Araki T, Yano M. **2002**. Hd3a, a rice ortholog of the Arabidopsis FT gene, promotes transition to flowering downstream of Hd1 under short-day conditions. *Plant and Cell Physiology* **43**: 1096–1105.

Komander D, Rape M. **2012**. The ubiquitin code. *Annual Review of Biochemistry* **81**: 203–229.

Komiya R, Ikegami A, Tamaki S, Yokoi S, Shimamoto K. **2008a**. Hd3a and RFT1 are essential for flowering in rice. *Development* **135**: 767–774.

Komiya R, Ikegami A, Tamaki S, Yokoi S, Shimamoto K. **2008b**. Hd3a and RFT1 are essential for flowering in rice. *Development* **135**: 767–774.

Komiya R, Yokoi S, Shimamoto K. **2009**. A gene network for long-day flowering activates RFT1 encoding a mobile flowering signal in rice. *Development* **136**: 3443–3450.

Lechner E, Achard P, Vansiri A, Potuschak T, Genschik P. **2006**. F-box proteins everywhere. *Current Opinion in Plant Biology* **9**: 631–638.

Lee YS, Jeong DH, Lee DY, Yi J, Ryu CH, Kim SL, Jeong HJ, Choi SC, Jin P, Yang J, *et al.* 2010. OsCOL4 is

a constitutive flowering repressor upstream of Ehd1 and downstream of OsphyB. *The Plant Journal* **63**: 18–30.

Levin J 2, Meyerowitz' EM. **1995**. UFO: An Arabidopsis Gene lnvolved in Both Floral Meristem and Floral Organ Development. *The Plant Cell* **7**: 529–548.

Li Z, Liang Y, Yuan Y, Wang L, Meng X, Xiong G, Zhou J, Cai Y, Han N, Hua L, *et al.* 2019. OsBRXL4 Regulates Shoot Gravitropism and Rice Tiller Angle through Affecting LAZY1 Nuclear Localization. *Molecular Plant* **12**: 1143–1156.

Li P, Wang Y, Qian Q, Fu Z, Wang M, Zeng D, Li B, Wang X, Li J. **2007**. LAZY1 controls rice shoot gravitropism through regulating polar auxin transport. *Cell Research 2007 17:5* **17**: 402–410.

Liu C, Teo ZWN, Bi Y, Song S, Xi W, Yang X, Yin Z, Yu H. **2013**. A Conserved Genetic Pathway Determines Inflorescence Architecture in Arabidopsis and Rice. *Developmental Cell* **24**: 612–622.

Londo JP, Chiang YC, Hung KH, Chiang TY, Schaal BA. **2006**. Phylogeography of Asian wild rice, Oryza rufipogon, reveals multiple independent domestications of cultivated rice, Oryza sativa. *Proceedings of the National Academy of Sciences of the United States of America* **103**: 9578–9583.

Love MI, Huber W, Anders S. **2014**. Moderated estimation of fold change and dispersion for RNA-seq data with DESeq2. *Genome Biology* **15**: 1–21.

de Luxán-Hernández C, Lohmann J, Hellmeyer W, Seanpong S, Wöltje K, Magyar Z, Pettkó-Szandtner A, Pélissier T, De Jaeger G, Hoth S, *et al.* 2020. PP7L is essential for MAIL1-mediated transposable element silencing and primary root growth. *The Plant Journal* **102**: 703–717.

Más P, Kim WY, Somers DE, Kay SA. **2003**. Targeted degradation of TOC1 by ZTL modulates circadian function in Arabidopsis thaliana. *Nature 2004 426:6966* **426**: 567–570.

Miao J, Guo D, Zhang J, Huang Q, Qin G, Zhang X, Wan J, Gu H, Qu LJ. **2013**. Targeted mutagenesis in rice using CRISPR-Cas system. *Cell Research* **23**: 1233–1236.

Miskolczi P, Singh RK, Tylewicz S, Azeez A, Maurya JP, Tarkowská D, Novák O, Jonsson K, Bhalerao RP. **2019**. Long-range mobile signals mediate seasonal control of shoot growth. *Proceedings of the National Academy of Sciences of the United States of America* **166**: 10852–10857.

Nakagawa M, Shimamoto K, Kyozuka J. **2002**. Overexpression of RCN1 and RCN2, rice TERMINAL FLOWER 1/CENTRORADIALIS homologs, confers delay of phase transition and altered panicle morphology in rice. *The Plant Journal* **29**: 743–750.

Nakamura Y, Lin YC, Watanabe S, Liu Y chi, Katsuyama K, Kanehara K, Inaba K. **2019a**. High-Resolution Crystal Structure of Arabidopsis FLOWERING LOCUS T Illuminates Its Phospholipid-Binding Site in Flowering. *iScience* **21**: 577–586.

Nakamura Y, Lin YC, Watanabe S, Liu Y chi, Katsuyama K, Kanehara K, Inaba K. **2019b**. High-Resolution Crystal Structure of Arabidopsis FLOWERING LOCUS T Illuminates Its Phospholipid-Binding Site in Flowering. *iScience* **21**: 577–586.

Navarro C, Abelenda JA, Cruz-Oró E, Cuéllar CA, Tamaki S, Silva J, Shimamoto K, Prat S. **2011**. Control of flowering and storage organ formation in potato by FLOWERING LOCUS T. *Nature* **478**: 119–122.

Nornile D. **1997**. Yangtze seen as earliest rice site. *Science* **275**: 309.

Nuñez FDB, Yamada T. **2017**. Molecular Regulation of Flowering Time in Grasses. *Agronomy* **7**.

O'Connor DL, Runions A, Sluis A, Bragg J, Vogel JP, Prusinkiewicz P, Hake S. **2014**. A Division in PIN-Mediated Auxin Patterning during Organ Initiation in Grasses. *PLOS Computational Biology* **10**:

e1003447.

Peng LT, Shi ZY, Li L, Shen GZ, Zhang JL. **2007**. Ectopic expression of OsLFL1 in rice represses Ehd1 by binding on its promoter. *Biochemical and biophysical research communications* **360**: 251–256.

Pin PA, Nilsson O. **2012**. The multifaceted roles of FLOWERING LOCUS T in plant development. *Plant, Cell & Environment* **35**: 1742–1755.

Pnueli L, Gutfinger T, Hareven D, Ben-Naim O, Ron N, Adir N, Lifschitz E. **2001a**. Tomato SP-interacting proteins define a conserved signaling system that regulates shoot architecture and flowering. *The Plant cell* **13**: 2687–2702.

Pnueli L, Gutfinger T, Hareven D, Ben-Naim O, Ron N, Adir N, Lifschitz E. **2001b**. Tomato SP-Interacting Proteins Define a Conserved Signaling System That Regulates Shoot Architecture and Flowering. *The Plant Cell* **13**: 2687–2702.

Price CTD, Abu Kwaik Y. **2010**. Exploitation of Host Polyubiquitination Machinery through Molecular Mimicry by Eukaryotic-Like Bacterial F-Box Effectors. *Frontiers in Microbiology* **1**.

Putri GH, Anders S, Pyl PT, Pimanda JE, Zanini F. **2022**. Analysing high-throughput sequencing data in Python with HTSeq 2.0. *Bioinformatics* **38**: 2943–2945.

Quail PH. **2002**. Phytochrome photosensory signalling networks. *Nature Reviews Molecular Cell Biology* **3**: 85–93.

Rieu P, Turchi L, Thévenon E, Zarkadas E, Nanao M, Chahtane H, Tichtinsky G, Lucas J, Blanc-Mathieu R, Zubieta C, *et al.* 2023. The F-box protein UFO controls flower development by redirecting the master transcription factor LEAFY to new cis-elements. *Nature Plants* **9**: 315–329.

Ryu CH, Lee S, Cho LH, Kim SL, Lee YS, Choi SC, Jeong HJ, Yi J, Park SJ, Han CD, *et al.* 2009. OsMADS50 and OsMADS56 function antagonistically in regulating long day (LD)-dependent flowering in rice. *Plant, Cell and Environment* **32**: 1412–1427.

Schoentgen F, Jollès P. **1995**. From structure to function: possible biological roles of a new widespread protein family binding hydrophobic ligands and displaying a nucleotide binding site. *FEBS Letters* **369**: 22–26.

Serre L, Vallée B, Bureaud N, Schoentgen F, Zelwer C. **1998**. Crystal structure of the phosphatidylethanolamine-binding protein from bovine brain: a novel structural class of phospholipid-binding proteins. *Structure* **6**: 1255–1265.

Shannon S, Ry Meeks-Wagner' O. **1991**. A Mutation in the Arabidopsis TFL1 Gene Affects Inf lorescence Meristem Development. *The Plant Cell* **3**: 877–892.

Shenouda S, Bosso M, Ahmad R, Al-Mulla F. **2020**. The role of Raf kinase inhibitory protein in inflammation. *Prognostic and Therapeutic Applications of RKIP in Cancer*: 297–322.

Smith H. **2000**. Phytochromes and light signal perception by plants - An emerging synthesis. *Nature* **407**: 585–591.

Somers DE, Schultz TF, Milnamow M, Kay SA. **2000**. ZEITLUPE Encodes a Novel Clock-Associated PAS Protein from Arabidopsis. *Cell* **101**: 319–329.

Song YH, Estrada DA, Johnson RS, Kim SK, Lee SY, MacCoss MJ, Imaizumi T. **2014**. Distinct roles of FKF1, GIGANTEA, and ZEITLUPE proteins in the regulation of constans stability in Arabidopsis photoperiodic flowering. *Proceedings of the National Academy of Sciences of the United States of America* **111**: 17672–17677.

Song S, Y C, L L, Y W, S B, X Z, ZW T, C M, Y G, H Y, *et al.* 2017. OsFTIP1-Mediated Regulation of

Florigen Transport in Rice Is Negatively Regulated by the Ubiquitin-Like Domain Kinase OsUbDKγ4. *The Plant cell* **29**: 491–507.

Sun K, Huang M, Zong W, Xiao D, Lei C, Luo Y, Song Y, Li S, Hao Y, Luo W, *et al.* 2022. Hd1, Ghd7, and DTH8 synergistically determine the rice heading date and yield-related agronomic traits. *Journal of Genetics and Genomics* **49**: 437–447.

Susila H, Jurić S, Liu L, Gawarecka K, Chung KS, Jin S, Kim SJ, Nasim Z, Youn G, Suh MC, *et al.* 2021. Florigen sequestration in cellular membranes modulates temperature-responsive flowering. *Science* **373**: 1137–1142.

Tamaki S, Matsuo S, Hann LW, Yokoi S, Shimamoto K. **2007a**. Hd3a protein is a mobile flowering signal in rice. *Science* **316**: 1033–1036.

Tamaki S, Matsuo S, Hann LW, Yokoi S, Shimamoto K. **2007b**. Hd3a protein is a mobile flowering signal in rice. *Science* **316**: 1033–1036.

Tamaki S, Tsuji H, Matsumoto A, Fujita A, Shimatani Z, Terada R, Sakamoto T, Kurata T, Shimamoto K, Robert LF. **2015**. FT-like proteins induce transposon silencing in the shoot apex during floral induction in rice. *Proceedings of the National Academy of Sciences of the United States of America* **112**: E901–E910.

Tan L, Li X, Liu F, Sun X, Li C, Zhu Z, Fu Y, Cai H, Wang X, Xie D, *et al.* 2008. Control of a key transition from prostrate to erect growth in rice domestication. *Nature Genetics 2008 40:11* **40**: 1360–1364.

Taoka KI, Ohki I, Tsuji H, Furuita K, Hayashi K, Yanase T, Yamaguchi M, Nakashima C, Purwestri YA, Tamaki S, *et al.* 2011a. 14-3-3 proteins act as intracellular receptors for rice Hd3a florigen. *Nature 2011 476:7360* **476**: 332–335.

Taoka KI, Ohki I, Tsuji H, Furuita K, Hayashi K, Yanase T, Yamaguchi M, Nakashima C, Purwestri YA, Tamaki S, *et al.* 2011b. 14-3-3 proteins act as intracellular receptors for rice Hd3a florigen. *Nature* **476**: 332–335.

Tsuji H, Nakamura H, Taoka KI, Shimamoto K. **2013**. Functional diversification of FD transcription factors in rice, components of florigen activation complexes. *Plant and Cell Physiology* **54**: 385–397.

Tsuji H, Tachibana C, Tamaki S, Taoka KI, Kyozuka J, Shimamoto K. **2015a**. Hd3a promotes lateral branching in rice. *Plant Journal* **82**: 256–266.

Tsuji H, Tachibana C, Tamaki S, Taoka KI, Kyozuka J, Shimamoto K. **2015b**. Hd3a promotes lateral branching in rice. *Plant Journal* **82**: 256–266.

Tylewicz S, Tsuji H, Miskolczi P, Petterle A, Azeez A, Jonsson K, Shimamoto K, Bhalerao RP. **2015**. Dual role of tree florigen activation complex component FD in photoperiodic growth control and adaptive response pathways. *Proceedings of the National Academy of Sciences of the United States of America* **112**: 3140–3145.

Ühlken C, Horvath B, Stadler R, Sauer N, Weingartner M. **2014**. MAIN-LIKE1 is a crucial factor for correct cell division and differentiation in Arabidopsis thaliana. *The Plant journal : for cell and molecular biology* **78**: 107–120.

Valverde F, Mouradov A, Soppe W, Ravenscroft D, Samach A, Coupland G. **2004**. Photoreceptor Regulation of CONSTANS Protein in Photoperiodic Flowering. *Science* **303**: 1003–1006.

Wang W, Gao H, Liang Y, Li J, Wang Y. **2022**. Molecular basis underlying rice tiller angle: Current progress and future perspectives. *Molecular Plant* **15**: 125–137.

Wang Y, Li J. **2008**. Molecular Basis of Plant Architecture.

https://doi.org/10.1146/annurev.arplant.59.032607.092902 **59**: 253–279.

Wang L, Ming L, Liao K, Xia C, Sun S, Chang Y, Wang H, Fu D, Xu C, Wang Z, *et al.* 2021. Bract suppression regulated by the miR156/529-SPLs-NL1-PLA1 module is required for the transition from vegetative to reproductive branching in rice. *Molecular Plant* **14**: 1168–1184.

Wenig U, Meyer S, Stadler R, Fischer S, Werner D, Lauter A, Melzer M, Hoth S, Weingartner M, Sauer N. **2013**. Identification of MAIN, a factor involved in genome stability in the meristems of Arabidopsis thaliana. *Plant Journal* **75**: 469–483.

Wigge PA, Kim MC, Jaeger KE, Busch W, Schmid M, Lohmann JU, Weigel D. **2005**. Integration of spatial and temporal information during floral induction in Arabidopsis. *Science* **309**: 1056–1059.

Wu X, Tang D, Li M, Wang K, Cheng Z. **2013**. Loose Plant Architecture1, an INDETERMINATE DOMAIN protein involved in SHOOT GRAVITROPISM, regulates plant architecture in rice. *Plant Physiology* **161**: 317–329.

Xiao W, Jang JC. **2000**. F-box proteins in Arabidopsis. *Trends in Plant Science* **5**: 454–457.

Xu G, Ma H, Nei M, Kong H. **2009**. Evolution of F-box genes in plants: different modes of sequence divergence and their relationships with functional diversification. *Proceedings of the National Academy of Sciences of the United States of America* **106**: 835–40.

Yano M, Katayose Y, Ashikari M, Yamanouchi U, Monna L, Fuse T, Baba T, Yamamoto K, Umehara Y, Nagamura Y, *et al.* 2000. Hd1, a major photoperiod sensitivity quantitative trait locus in rice, is closely related to the Arabidopsis flowering time gene CONSTANS. *Plant Cell* **12**: 2473–2483.

Yoshida H, Nagato Y. **2011**. Flower development in rice. *Journal of Experimental Botany* **62**: 4719–4730.

Yoshihara T, Iino M. **2007**. Identification of the Gravitropism-Related Rice Gene LAZY1 and Elucidation of LAZY1-Dependent and -Independent Gravity Signaling Pathways. *Plant and Cell Physiology* **48**: 678–688.

Yu B, Lin Z, Li H, Li X, Li J, Wang Y, Zhang X, Zhu Z, Zhai W, Wang X, *et al.* 2007a. TAC1, a major quantitative trait locus controlling tiller angle in rice. *Plant Journal* **52**: 891–898.

Yu B, Lin Z, Li H, Li X, Li J, Wang Y, Zhang X, Zhu Z, Zhai W, Wang X, *et al.* 2007b. TAC1, a major quantitative trait locus controlling tiller angle in rice. *The Plant Journal* **52**: 891–898.

Zhang S, Hu W, Wang L, Lin C, Cong B, Sun C, Luo D. **2005**. TFL1/CEN-like genes control intercalary meristem activity and phase transition in rice. *Plant Science* **168**: 1393–1408.

Zhang H, Li X, Sang D, Huang L, Song Y, Du M, Cao J, Wang W. **2022**. PROG1 acts upstream of LAZY1 to regulate rice tiller angle as a repressor. *The Crop Journal*.

Zhang N, Yu H, Yu H, Cai Y, Huang L, Xu C, Xiong G, Meng X, Wang J, Chen H, *et al.* 2018. A core regulatory pathway controlling rice tiller angle mediated by the LAZY1-dependent asymmetric distribution of auxin. *Plant Cell* **30**: 1461–1475.

Zhou F, Lin Q, Zhu L, Ren Y, Zhou K, Shabek N, Wu F, Mao H, Dong W, Gan L, *et al.* 2013. D14–SCFD3-dependent degradation of D53 regulates strigolactone signalling. *Nature 2013 504:7480* **504**: 406–410.

Zhu C, Box MS, Thiruppathi D, Hu H, Yu Y, Martin C, Doust AN, McSteen P, Kellogg EA. **2022a**. Pleiotropic and nonredundant effects of an auxin importer in Setaria and maize. *Plant Physiology* **189**: 715–734.

Zhu W, Yang L, Wu D, Meng Q, Deng X, Huang G, Zhang J, Chen X, Ferrándiz C, Liang W, *et al.*

2022b. Rice SEPALLATA genes OsMADS5 and OsMADS34 cooperate to limit inflorescence branching by repressing the TERMINAL FLOWER1-like gene RCN4. *New Phytologist* **233**: 1682–1700.

Zong W, Ren D, Huang M, Sun K, Feng J, Zhao J, Xiao D, Xie W, Liu S, Zhang H, *et al.* 2021. Strong photoperiod sensitivity is controlled by cooperation and competition among Hd1, Ghd7 and DTH8 in rice heading. *New Phytologist* **229**: 1635–1649.

Appendices

(ACCEPTED)

Rice florigens control a common set of genes at the shoot apical meristem including the F-BOX BROADER TILLER ANGLE 1 that regulates tiller angle and spikelet development

Lorenzo Mineri[2], Martina Cerise[2,3], Francesca Giaume[1,2], Giulio Vicentini[1], Damiano Martignago[2], Matteo Chiara[2], Francesca Galbiati[2], Alberto Spada[1], David Horner[2], Fabio Fornara[2] and Vittoria Brambilla[1].

1. Department of Agricultural and Environmental Sciences, University of Milan, via Celoria 2, 20133 Milan, Italy
2. Department of Biosciences, University of Milan, via Celoria 26, 20133 Milan, Italy
3. Present address: Max Planck Institute for Plant Breeding Research, Carl Von Linne Weg 10, 50829 Cologne, Germany

SUMMARY

Rice flowering is triggered by transcriptional reprogramming at the shoot apical meristem (SAM) mediated by florigenic proteins produced in leaves in response to changes in photoperiod. Florigens are more rapidly expressed under short days (SDs) compared to long days (LDs) and include the HEADING DATE 3a (Hd3a) and RICE FLOWERING LOCUS T1 (RFT1) Phosphatidyl Ethanolamine Binding Proteins. Hd3a and RFT1 are largely redundant at converting the SAM into an inflorescence, but whether they activate the same target genes and convey all photoperiodic information that modifies gene expression at the SAM is currently unclear.

We uncoupled the contribution of Hd3a and RFT1 to transcriptome reprogramming at the SAM by RNA-sequencing of dexamethasone-inducible over-expressors of single florigens and wild type plants exposed to photoperiodic induction.

Fifteen highly differentially expressed genes common to Hd3a, RFT1 and SDs were retrieved, ten of which still uncharacterized. Detailed functional studies on some candidates revealed a role for LOC_Os04g13150 in determining tiller angle and spiklet development and the gene was renamed *BROADER TILLER ANGLE 1* (*BRT1*).

We identified a core set of genes controlled by florigenic-mediated photoperiodic induction and defined the function of a novel florigen target controlling tiller angle and spikelet development.

Environmental Control of Rice Flowering Time, Plant communications, 2023

Giulio Vicentini[2,4], Marco Biancucci[1,4], Lorenzo Mineri[1], Daniele Chirivì[1], Francesca Giaume[2], Yiling Miao[3], Junko Kyozuka[3], Vittoria Brambilla[2], Camilla Betti[1] and Fabio Fornara[1,*]

1. Department of Biosciences, University of Milan, via Celoria 26, 20133 Milan, Italy
2. Department of Agricultural and Environmental Sciences, University of Milan, via Celoria 2, 20133 Milan, Italy
3. Graduate School of Life Sciences, Tohoku University, Sendai, Japan
4. These authors contributed equally

Abstract

Correct measurement of environmental parameters is fundamental for plant fitness and survival, as well as for timing developmental transitions, including the switch from vegetative to reproductive growth. An important parameter affecting flowering time is day length (photoperiod). Its response pathway has been best described in Arabidopsis, that currently offers a detailed conceptual framework, that serves as term of comparison also for other species. Rice, the focus of this review, also possesses a photoperiodic flowering pathway, but 150M years of divergent evolution in very different environments have diversified its molecular architecture. The conservation of some regulatory genes has established the idea that part of the pathway is shared across flowering plants. However, when observing network topologies rather than single genes, it is evident that the rice flowering network is centered on *EARLY HEADING DATE 1*, a rice-specific transcriptional regulator. Here, we summarize the most important features of the rice photoperiodic flowering network, with an emphasis on its uniqueness, and discuss its connections with other pathways, including hormonal and stress ones.